Impact of Small-Scale Structure on the Stochastic Gravitational Wave Background Generated by Cosmic Strings

Teresa Oliveira Miranda
Master in Physics
Department of Physics and Astronomy
Faculty of Sciences of the University of Porto
2024

U.PORTO
FACULDADE DE CIÊNCIAS
UNIVERSIDADE DO PORTO

MSc

Impact of Small-Scale Structure on the Stochastic Gravitational Wave Background Generated by Cosmic Strings

Teresa Oliveira Miranda
Dissertation carried out as part of the Master in Physics
Department of Physics and Astronomy
2024

Supervisor
Lara Sousa, Researcher, Instituto de Astrofísica e Ciências do Espaço

“ It’s a moo point. It’s like a cow’s opinion: it doesn’t matter. It’s moo. ”

Joey Tribbiani

To Egas and Charlie.

Acknowledgements

First, I have to thank my supervisor, Dr. Lara Sousa, for all the guidance and support throughout this past year. I found that my first experience with a research project, although sometimes stressful, was overall very enjoyable, and I credit it all to your great supervision. I am also very thankful for the financial support provided through the research fellowship CIAAUP-26/2023-BI-M under the R&D project 2022.03495.PTDC - *Uncovering the nature of cosmic strings*, funded by Fundação para a Ciência e Tecnologia.

Secondly, to all my friends, for the endless support during all exam seasons and for all the great memories created during this past six years, that I shall always carry with me. A special thank you to Duarte, for not once doubting that I could do it, even when I did not believed in it myself.

Lastly, I have to thank my family for all the support throughout all my academic journey: to my mother, for teaching me the best life motto: "*O que importa é ter saúde*"; to my sister, for being my personal slide design consultant; to Fred, for not once sitting on my keyboard while I wrote this dissertation; and to my father, for being my first ever physics teacher.

Resumo

As cordas cósmicas são objetos topológicos, hipotéticos, previstos por diversas Teorias da Grande Unificação, que terão sido formadas no Universo primordial como resultado de uma transição de fase. Durante a sua evolução as cordas cósmicas interagem levando à criação de descontinuidades na tangente da corda, chamadas de *kinks*, e à formação de *loops* de cordas cósmicas. É esperado que as redes de cordas sobrevivam ao longo da história do Universo deixando marcas observacionais, tais como o Fundo Gravitacional Estocástico (FGE). Quando um *loop* se forma, separa-se da rede, oscila relativistacamente sob o efeito da sua própria tensão e eventualmente decai, emitindo Ondas Gravitacionais (OGs). A sobreposição de todas estas emissões gera o FGE. Também se espera que os *kinks* decaiam, emitindo OGs, mas a sua contribuição é normalmente desprezada em computações do espetro. Para além disso, a presença desta estrutura de pequena escala deverá também ter um impacto na produção de *loops* e por conseguinte deverá impactar o FGE por eles gerado. No entanto, tal efeito nunca foi estudado, o que poderá estar a resultar numa atual sobreestimação da amplitude do espetro do FGE gerado por *loops*.

Nesta dissertação começamos por extender e adaptar modelos existentes na literatura que descrevem a evolução de uma rede de cordas, com o propósito de desenvolver um modelo efetivo que descreva a evolução da estrutura de pequena escala. Este modelo é depois utilizado para estudar a evolução de uma rede de cordas cósmicas com *kinks*, com o objetivo de perceber como é que a presença desta estrutura de pequena escala afeta a produção de *loops*, para que, posteriormente, possamos então estudar de que modo o espetro do FGE que estes geram é afetado.

Observamos que ignorar a presença da estrutura de pequena escala na rede de cordas leva a uma sobreestimação da produção de *loops*, como previsto, e portanto a uma sobreestimação da amplitude do espetro. É então essencial ter em conta a existência de *kinks* na rede para a derivação de limites observacionais e/ou para serem feitas previsões realistas sobre a forma e a amplitude do espetro. Verificamos também que, em geral, a contribuição dos *kinks* para o espetro é subdominante, com a exceção do caso em que os *loops* são consideravalmente pequenos, o que faz com que gerem um espetro com menor amplitude, tornando a contribuição dos *kinks* mais relevante. No entanto, é possível que o espetro produzido por *kinks* domine na gama de baixas frequências do espetro, levando ao aparecimento de um segundo pico, cuja forma não pode ser conhecida, visto ser ainda desconhecido o impacto do decaimento na forma dos *kinks*.

Palavras-chave: cosmologia, universo primordial, ondas gravitacionais, cordas cósmicas

Abstract

Cosmic strings are hypothetical topological objects predicted by many Grand Unified Theories to have been produced as a result of a phase transition in the early Universe. During their evolution, cosmic strings interact, leading to the creation of discontinuities on the string tangent, known as kinks, and to the formation of cosmic strings loops. Cosmic strings networks are expected to survive throughout the cosmic history, leaving behind observational imprints, such as the Stochastic Gravitational Wave Background (SGWB). When a loop is formed, it detaches from the network, oscillates relativistically under its own tension, and eventually decays, emitting Gravitational Waves (GWs). The superposition of all loop emissions generates a SGWB. Kinks, are also expected to decay, by emitting GWs, but their contribution to the spectrum is usually neglected in computations. Moreover, these small-scale structure must also have an impact on loop production, which, as a consequence, must impact the SGWB generated by loops. Such effect has not been yet studied and can possibly be resulting in an overestimation of the spectrum's amplitude.

In this dissertation we begin by developing an effective model to describe the evolution of small-scale structure, by extending and adapting existent models that describe the evolution of a cosmic string network. This model will then be used to study the evolution of a kinky cosmic string network in order to understand how the presence of kinks affects loop production, so that afterwards, we are able to study how the spectrum of SGWB generated by loops is impacted by the existence of kinks.

We observed that ignoring the existence of small-scale structure leads to an overestimation of loop production, and, as a consequence, to an overestimation of the spectrum's amplitude, as expected. It is then essential to consider the presence of kinks on the cosmic string network in order to derive observational limits and/or to make realistic predictions. We have also verified that, in general, kink's contribution to the SGWB is subdominant. However, if loops are considerably small, the spectrum that they generate has a lower amplitude and kink's contribution is more relevant. The spectrum generated by kinks may, however, dominate in the lower frequency range, thus leading to a second peak in the spectrum, whose form cannot be known until the effects of the gravitational backreaction are well studied.

Keywords: cosmology, early universe, gravitational waves, cosmic strings

Table of Contents

List of Figures

Notation and Conventions

Throughout this dissertation, we use the metric signature $(+,-,-,-)$ and natural units, where $c = \hbar = k_B = 1$.

The subscript 0 is used to indicate when a certain quantity is being evaluated at the present time.

Greek indices run over 0,1,2,3.

$A_{\mu,\nu} \equiv \frac{\partial A_\mu}{\partial x^\nu}$ expresses a partial derivative and $A^\mu_{;\nu} \equiv \nabla_\nu A^\mu$ a covariant derivative.

List of Abbreviations

GW Gravitational Wave

SGWB Stochastic Gravitational Wave Background

VOS Velocity-dependent One-Scale

RMS Root-mean-squared

CMB Cosmic Microwave Background

1. Introduction

In 1917, Einstein published a paper entitled *Cosmological Considerations in the General Theory of Relativity* [1], which marks the beginning of the history of Modern Cosmology. In it, he proposed an homogeneous, isotropic and static Universe as a solution for his field equations.

Years later, in 1929, Edwin Hubble found that the Universe was, in fact, not static, but expanding, by analyzing the shift in the spectral lines of several galaxies [2]. Hubble showed that, not only were those galaxies receding from us, but also that there was a linear relationship between their distance from Earth, and the velocity with which they were retreating, expressed by the well known *Hubble Law*.

The idea that our Universe is isotropic, homogeneous and expanding is what sustains the *Standard Cosmological Model*, currently the most widely accepted physical description of the evolution of our Universe. Also known as the Hot Big Bang Model, this model states that our Universe started in a hot dense state, and that it has been expanding and cooling ever since. The assumption of isotropy and homogeneity of the Universe, which is known as the *Cosmological Principle*, is supported by several galaxy surveys showing that, in distances greater that $\sim 3 \times 10^8$ lightyears, the distribution of galaxies is homogeneous [3] and by the discovery of the Cosmic Microwave Background (CMB) by Arno Penzias and Robert Wilson in 1965 [4], a background of microwave radiation almost perfectly isotropic. In fact, the most accurate determination of the temperature of the CMB gives $T_{CMB} \approx 2.72548 \pm 0.00057$K [5], with small fluctuations of order 10^{-5}. It is therefore important to make a small correction to our previous formulation of the Cosmological Principle: the Universe is homogeneous and isotropic *on sufficient large scales*.

In 1916, a year after the publication of the field equations that provide the foundation for General Relativity, Einstein predicted the existence of Gravitational Waves (GWs), by showing that the linearized weak-field equations had wave-like solutions [6]. These are caused by accelerating massive objects, which disrupt space-time, creating waves that travel in all directions away from its source, with little to no interaction with matter*. For

*They can, however, suffer *gravitational lensing*, similarly to what happens to electromagnetic waves. Gravitational lensing occurs when the GW passes nearby an object massive enough to cause a significant curvature in spacetime (for example, a galaxy or a star), bending the path of the wave. This changes the amplitude of the wave, but has no effect on its frequency [7].

this reason, detecting and studying GWs makes it possible to extract relevant information about the sources that generated them.

One potential source of GWs are cosmic strings. Cosmic strings are hypothetical topological objects, thought to be produced in the early Universe, as a result of symmetry breaking phase transitions, in many Grand Unified Theories and other theories Beyond the Standard Model of particle physics [8, 9]. Throughout all their evolution, cosmic strings are expected to emit GWs. The superposition of all these emissions generates the Stochastic Gravitational Wave Background (SGWB).

In this chapter, we begin by briefly introducing the Standard Cosmological Model, by deriving the necessary equations to fully describe the evolution of the Universe from the Einstein field equations (section 1.1). We then briefly explain how the wave-like solutions occur in the Einstein Field Equations in section 1.2 and finally, in section 1.3, we show how cosmic strings are formed.

1.1. Standard Cosmological Model

1.1.1 The Expansion of the Universe - Hubble Law

An uniformly expanding Universe makes it possible to define a set of comoving coordinates, **x**, which move along with the expansion of the background. Thse are related to the physical coordinates, **r**, as follows:

$$\mathbf{r} = a(t)\mathbf{x} \,, \tag{1.1}$$

where $a(t)$ is the scale factor, and is set to be 1 at the present time. Physical coordinates are nothing more than a simply rescaling by $a(t)$ of the comoving coordinates, which depends on time (see Fig. 1.1).

We can also write the physical velocity, **v**, in terms of the comoving coordinates:

$$\begin{aligned} \mathbf{v} = \dot{\mathbf{r}} &= \dot{a}\mathbf{x} + a\dot{\mathbf{x}} \\ &= H\mathbf{r} + \mathbf{v}_{pec} \,. \end{aligned} \tag{1.2}$$

The first term in Eq. (1.2) describes the impact of the expansion of the Universe on the physical velocity. H is the Hubble Parameter, and it is defined as:

$$H = \frac{\dot{a}}{a} \,. \tag{1.3}$$

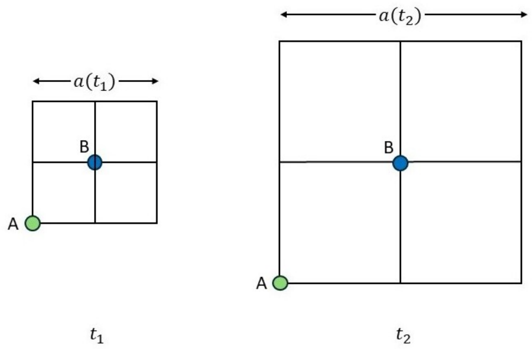

Figure 1.1: Visual representation of the definition of the scale factor, a. t_2 is an instant in time posterior to t_1. The distance between points A and B only changes as a consequence of the change in scale.

On the second term, we have defined a peculiar velocity $\mathbf{v}_{pec}$, which describes the inherent motion of the observers (or objects) relative to the cosmological frame. Neglecting the impact of peculiar velocities, Eq. (1.2) becomes:

$$\mathbf{v}(t) = H(t)\mathbf{r}(t) , \tag{1.4}$$

which is known as the Hubble Law.

The present value of the Hubble Parameter, known as the Hubble Constant, is [10]:

$$H_0 = 100h \quad km\ s^{-1}\mathrm{Mpc} \text{ with } h = 0.678 . \tag{1.5}$$

It is straightforward to see that H_0 has dimensions of the inverse of time. The unusual set of units used has the purpose of emphasizing its meaning: if we consider a galaxy that is $1\mathrm{Mpc}$ away from us, we will see it moving away with a velocity equal to $100h\ km\ s^{-1}$.

The Hubble Parameter allows us to define a characteristic timescale for the expansion of the Universe, known as the Hubble time:

$$t_H = H^{-1} . \tag{1.6}$$

During an interval of time equal to t_H, radiation traveling at the speed of light will reach the Hubble radius:

$$r_H = H^{-1} . \tag{1.7}$$

1.1.2 The Dynamics of the Universe

An homogeneous and isotropic expanding Universe is described by the Friedmann - Lemaître - Robertson - Walker (FLRW) metric:

$$ds^2 = a^2(t)\left(d\tau^2 - \frac{dr^2}{1-Kr^2} - r^2(d\theta^2 + \sin^2\theta d\phi^2)\right) , \tag{1.8}$$

where r, θ and ϕ are comoving coordinates, K is the curvature of the 3-dimensional space and τ is the conformal time, defined as:

$$\tau = \int \frac{dt}{a(t)} . \tag{1.9}$$

The curvature parameter, K defines the geometry of space-time. If:

- $K > 0$, the Universe is closed and has a spherical topology;
- $K = 0$, the Universe is flat, and has an euclidean geometry;
- $K < 0$, the Universe is open, with an hyperbolic topology.

An open or flat Universe will expand forever as opposed to a closed Universe, that will eventually collapse.

The dynamics of the expansion of the Universe is assumed to be governed by the Einstein Field Equations:

$$G_{\mu\nu} = R_{\mu\nu} - \frac{1}{2}g_{\mu\nu}R = 8\pi G T_{\mu\nu} , \tag{1.10}$$

where $g_{\mu\nu}$ is the metric tensor,

$$R_{\mu\nu} = R^{\sigma}_{\mu\sigma\nu} = \Gamma^{\lambda}_{\mu\nu;\lambda} - \Gamma^{\lambda}_{\mu\lambda;\nu} + \Gamma^{\lambda}_{\rho\lambda}\Gamma^{\rho}_{\mu\nu} - \Gamma^{\lambda}_{\rho\nu}\Gamma^{\rho}_{\mu\lambda} \tag{1.11}$$

is the Ricci tensor, $R = R^{\mu}_{\mu}$ is the Ricci Scalar, $\Gamma^{\mu}_{\lambda\sigma}$ are the Christoffel symbols, defined as:

$$\Gamma^{\mu}_{\lambda\sigma} = \frac{1}{2}g^{\mu\nu}(g_{\mu\nu,\sigma} + g_{\sigma\mu,\lambda} - g_{\lambda\sigma,\nu}) . \tag{1.12}$$

and $T_{\mu\nu}$ is the stress-energy tensor. It is reasonable to assume that the background behaves as a perfect fluid, since isotropy implies the absence of heat conduction and of viscosity forces. Therefore, $T_{\mu\nu}$ may be expressed as:

$$T_{\mu\nu} = [p_b(t) + \rho_b(t)]u_\mu u_\nu - p_b(t)g_{\mu\nu} , \tag{1.13}$$

where $u_\mu = dx^\mu/dt$ is the 4-velocity of the fluid, ρ_b is the energy density of the background fluid and p_b is its pressure. In the comoving frame, the fluid is at rest relative to the expansion, and so, $u_0 = 1$ and $u_i = 0$. Let us assume a linear equation of state:

$$p_b = \omega \rho_b \ , \tag{1.14}$$

where ω is the equation-of-state parameter and is determined by the constituents of the Universe. Local conservation of energy-momentum, $T^{\mu\nu}_{;\mu} = 0$, defines a continuity equation:

$$\frac{d\rho_b}{dt} + 3H(\rho_b + p_b) = 0 \ . \tag{1.15}$$

The temporal components of Eqs. (1.10) and (1.13) allow us to write the Friedmann equation:

$$H^2 = \frac{8\pi G\rho}{3} - \frac{K}{a^2} \ , \tag{1.16}$$

which, together with Eqs. (1.14) - (1.15), provides a full description of the evolution of the Universe in terms of its components and curvature.

1.1.3 Components of the Universe

Currently observational data shows that the Universe is spatially flat, and that it contains radiation, matter and a cosmological constant [10]. The cosmological constant, usually represented by the greek letter Λ, was first introduced by Einstein to assure that his field equations described a static Universe [1], modifying them to be:

$$G_{\mu\nu} = R_{\mu\nu} - \frac{1}{2} g_{\mu\nu} R = 8\pi G T_{\mu\nu} + \Lambda g_{\mu\nu} \ . \tag{1.17}$$

In the vacuum (in other words, assuming that there are no other components in the Universe), Eq. (1.17) is:

$$R_{\mu\nu} - \frac{1}{2} g_{\mu\nu} R = \Lambda g_{\mu\nu} \ , \tag{1.18}$$

which shows that the cosmological constant describes the energy of empty space and can be interpreted as a perfect fluid with negative pressure. However, it is known, since 1929, that the Universe is not static, but actually expanding, which raises the question: why is the cosmological constant a part of the Standard Cosmological Model? In 1998, the measure of the luminosity distances of supernovae, showed that the expansion of the Universe is, contrary to initial expectations, accelerating [11]. This acceleration is driven by an exotic component of the energy density that provides a negative pressure, whose origin is unknown and is generally known as *dark energy**. The cosmological constant is the

*Although the cosmological constant can be thought as the vacuum energy, the observationally measured value differs of around 120 orders of magnitude from the theoretical predictions, which has yet to be explained, and, therefore, there is still no explanation for the nature of dark energy [12].

simplest way to describe this accelerated expansion within Einstein Equations. Planck's observational data [10] are perfectly consistent with the existence of a cosmological constant.

Throughout this dissertation, we will assume that the Universe has the following components: radiation, matter and a cosmological constant. This is known as the ΛCDM model. As we shall see, the Universe first underwent a radiation-dominated era, then a matter-dominated era, and is currently in a transition period, entering an era dominated by the cosmological constant*.

It is useful to define a dimensionless density parameter,

$$\Omega_{i0} = \frac{\rho_i}{\rho_{c0}} \,, \tag{1.19}$$

with

$$\sum_i \Omega_{i0} = 1 \,, \tag{1.20}$$

where $i = r, m, \Lambda$ and the subscripts label radiation, matter and a cosmological constant (respectively). Here, $\rho_{c0} = 3H_0^2/(8\pi G)$ is the critical density at the present time and it is defined as the density for $K = 0$. The critical density is a quantity of interest, since it defines a threshold, above which, the Universe would be closed. Let us also write the equation of state for each of the components of the Universe, and make use of Eq. (1.15) to study how their energy density evolves with time.

- For a fluid of relativistic particles (radiation), $\omega = 1/3$, and so,

$$\rho_r \propto a^{-4} \,; \tag{1.21}$$

- For matter, $\omega = 0$ and

$$\rho_m \propto a^{-3} \,; \tag{1.22}$$

- The cosmological constant is, by definition, constant, and so:

$$\rho_\Lambda = \text{constant} \,. \tag{1.23}$$

Fig. 1.2 shows the evolution of the density parameters for each of these components. It becomes evident that it is possible to divide the history of the Universe into three eras,

*Before the radiation dominated era, it is thought that the Universe underwent a period of accelerated expansion, named inflation. Inflation is currently the easier explanation for the fact that the Universe is extremely flat and homogeneous at the present time [13].

as we have already mentioned: an early period where radiation dominated the energy budget, followed by a matter dominated era that lasted until approximately the present time, and the Universe is now entering an era dominated by the cosmological constant.

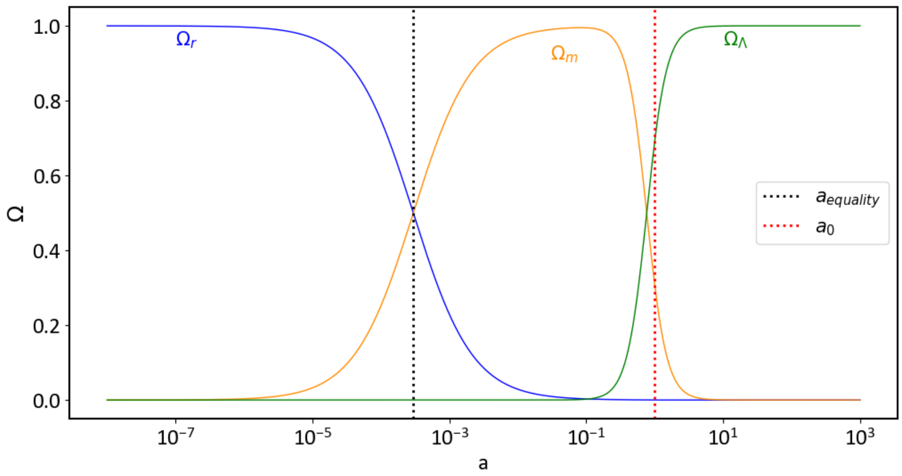

Figure 1.2: Evolution of the energy density for each component of the universe: radiation (Ω_r), matter (Ω_m) and a cosmological constant (Ω_Λ). $a_{equality} = \Omega_r/\Omega_m$ is the time of radiation and matter equality, and $a_0 = 1$ is the scale factor at present time.

It is then useful to rewrite the Friedmann equation in terms of these density parameters:

$$H^2 = H_0^2[\Omega_{m0}a^{-3} + \Omega_{r0}a^{-4} + \Omega_{\Lambda 0}] \, . \tag{1.24}$$

Observational data shows that [10]:

$$\Omega_{r0} = 9.1476 \times 10^{-5} \tag{1.25}$$

$$\Omega_{m0} = 0.308 \tag{1.26}$$

$$\Omega_{\Lambda 0} = 1 - \Omega_{r0} - \Omega_{m0} \, . \tag{1.27}$$

Eq. (1.24) allows us to notice that deep into the radiation and matter dominated eras, the evolution of the Universe is ruled by a power law of the form:

$$a \propto t^{\beta} \, , \text{ with constant } 0 < \beta < 1 \, . \tag{1.28}$$

This can easily be verified by approximating Eq. (1.24) to:

$$H = H_0\sqrt{\Omega_{i0}}a^{j/2} \, , \tag{1.29}$$

where $i = r, m$ corresponding, respectively, to $j = -4, -3$ and solving the differential equation to obtain the relationship between the scale factor and time. Solving Eq. (1.29) for both eras, we obtain the power law solution in Eq. (1.28), with $\beta = 1/2$ in the radiation dominated era, and $\beta = 2/3$ in the matter dominated era.

In the period dominated by a cosmological constant, Eq. (1.24) can be written approximately as:

$$H = H_0\sqrt{\Omega_{\Lambda 0}}\ , \tag{1.30}$$

which has the following solution:

$$a \propto e^{H_0\sqrt{\Omega_{\Lambda 0}}t}\ , \tag{1.31}$$

that represents, as expected, an accelerated expansion rate.

1.2. Gravitational Waves

1.2.1 Weak-Field Einstein Equations

We will now provide a brief derivation of the wave-like solutions of the Einstein Field Equations. Spacetime is flat in the absence of gravity, and so, it is fair to assume that the presence of a weak gravitational field will make it "nearly flat". In other words, its metric may be written as:

$$g_{\mu\nu} = \eta_{\mu\nu} + h_{\mu\nu}\ , \tag{1.32}$$

where $\eta_{\mu\nu} = (+1, -1, -1, -1)$ is the Minkowski metric and $|h_{\mu\nu}| \ll 1$ is a small perturbation. This is a linear expansion, and therefore, terms of order h^2 or higher are being neglected. Coordinates in which the metric may be expressed in this form are called *nearly Lorentz coordinates*.

A Lorentz boost with velocity v along x direction in Special Relativity is defined by:

$$\Lambda^{\bar{\mu}}_{\nu} = \begin{pmatrix} \gamma & -v\gamma & 0 & 0 \\ -v\gamma & \gamma & 0 & 0 \\ 0 & 0 & 1 & 0 \\ 0 & 0 & 0 & 1 \end{pmatrix} \quad , \quad \text{with } \gamma = \frac{1}{\sqrt{1-v^2}}\ . \tag{1.33}$$

For a weak gravitational field, we define a *background Lorentz transformation*, $x^{\bar{\mu}} = \Lambda^{\bar{\mu}}_{\nu}x^{\nu}$, where $\Lambda^{\bar{\mu}}_{\nu}$ is identical to the matrix in Eq. (1.33), but with matrix elements that are constant everywhere. Applying this transformation to Eq. (1.32), we see that $h_{\mu\nu}$ transforms as if it were a tensor* in Special Relativity:

$$h_{\bar{\mu}\bar{\nu}} = \Lambda^{\mu}_{\bar{\mu}}\Lambda^{\nu}_{\bar{\nu}}h_{\mu\nu}\ , \tag{1.34}$$

*Note that, as pointed by B. Schutz, $h_{\mu\nu}$ is not a tensor, but instead *part* of one, since it is a "piece" of $g_{\mu\nu}$ [14].

making it possible to rewrite the Ricci tensor in terms of $h_{\mu\nu}$, and to think of the nearly flat spacetime, as a flat one, where it is possible to define a "tensor" $h_{\mu\nu}$.

Substituting Eq. (1.32) into Eq. (1.10), and keeping only the terms that are linear in $h_{\mu\nu}$, we can write the Weak-Field Einstein Equations, in the Lorentz gauge, as [14]:

$$\Box \bar{h}^{\mu\nu} = -16\pi T^{\mu\nu} \,, \tag{1.35}$$

where $\bar{h}^{\mu\nu}$ is called the trace reverse of $h^{\mu\nu}$, defined by $\bar{h} \equiv \bar{h}^{\alpha}_{\alpha} = -h$, and the operator $\Box = \frac{\partial^2}{\partial t^2} - \nabla^2$ is the *D'Alembertian*.

1.2.2 Wave-Like Solutions of the Einstein Field Equations

The simplest solution we can find corresponds to solving the Weak-Field Einstein Equations in the vacuum, (or far from the source of the field) by setting $T^{\mu\nu} = 0$. Eq. (1.35) then becomes:

$$\left(\frac{\partial^2}{\partial t^2} + \nabla^2\right) \bar{h}^{\mu\nu} = \eta^{\alpha\beta} \bar{h}^{\mu\nu}_{,\alpha\beta} = 0 \,. \tag{1.36}$$

Eq. (1.36) is a 3-dimensional wave equation, which has plane wave solutions of the form:

$$\bar{h}^{\mu\nu} = A^{\mu\nu} e^{ik_\mu x^\mu} \,, \tag{1.37}$$

where k_μ is the wave vector and $A^{\mu\nu}$ represent the amplitude of the wave. This is a Gravitational Wave! Substituting the above expression into Eq. (1.36), we obtain:

$$\eta^{\alpha\beta} k_\alpha k_\beta = k^\beta k_\beta = 0 \,, \tag{1.38}$$

which is only true if k^β is a null four-vector, i.e., if it is tangent to the world line of a photon. If we picture a photon traveling in the direction of the null-vector **k**, it will travel alongside the GW with the same phase as it forever, which can be interpreted as the GW itself traveling at the speed of light.

1.3. Cosmic Strings

1.3.1 Cosmic Strings Formation

As mentioned before, the Standard Cosmological Model predicts that the Universe started in an extremely hot and dense state, cooling down as it expands. Grand-Unified Theories and other Beyond the Standard Model of particle of physics scenarios for the early Universe predict that, as the temperature decreases, several symmetry-breaking phase transitions may occur. As a consequence, topological defects may be formed [15]. In particular, cosmic strings arise when a $U(1)$ symmetry is broken. In Condensed Matter Physics, spontaneous symmetry breaking is a well studied topic, with a common example being the appearance of discrete magnetic dipole orientations in a ferromagnet, in systems both in and out of thermal equilibrium.

In Cosmology, symmetry breaking is often described in terms of the Higgs Mechanism*, the process by which gauge bosons acquire mass. The simplest theory in which cosmic strings arise is the Goldstone Model [16] with a complex scalar field, described by the Lagrangian density:

$$\mathcal{L} = (\partial_\mu \bar{\phi})(\partial^\mu \phi) - V(\phi) \,, \tag{1.39}$$

where:

$$V(\phi) = \mu^2(\bar{\phi}\phi) + \lambda(\bar{\phi}\phi)^2 \,. \tag{1.40}$$

The Lagrangian density in Eq. (1.39) is invariant under the group $U(1)$ of global phase transformations:

$$\phi(x) \to e^{i\alpha}\phi(x) \,. \tag{1.41}$$

In order for the potential to have a finite minimum we should have that $\lambda > 0$. However, there is no such restriction for μ^2. Let us consider the cases in which μ^2 is larger and smaller than zero, which are represented in Fig. 1.3.

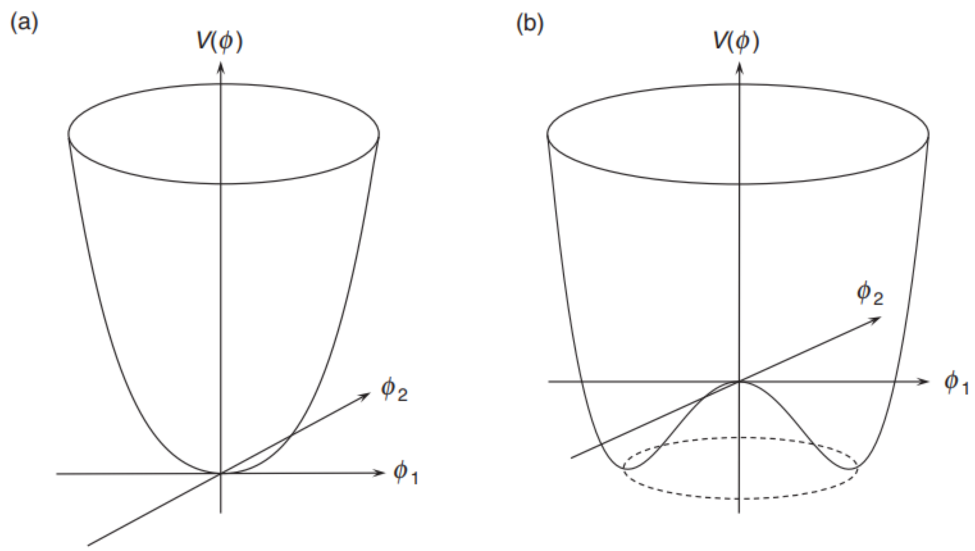

Figure 1.3: Goldstone Model potential in the case where: a) $\mu^2 > 0$ and there is no symmetry breaking; b) $\mu^2 < 0$ and there is a spontaneous symmetry breaking. Figure originally published in [17].

*There are other symmetry breaking processes, but for this specific situation, where we are studying the formation of cosmic strings, we will focus on the Higgs Mechanism.

- $\mu^2 > 0$

  In this case, the potential only has one minima, at $\phi = 0$. The vacuum state corresponds to the case where the field is zero and the Lagrangian represents a scalar particle with mass μ with a self interaction term proportional to the fourth power of ϕ. The global $U(1)$ symmetry is preserved.

- $\mu^2 < 0$

  In this case, the potential has a set of minima that satisfy $|\phi| = \pm\sqrt{-\mu^2/\lambda} = \pm\eta$. The system can now choose between several vacuum states, leading to a spontaneous symmetry breaking: let us consider an arbitrary vacuum state, $\phi_0 = \eta e^{i\theta}$ and let us apply the phase transformation in Eq. (1.41):

$$\phi_0 = \eta e^{i\theta} \to \phi_0' = \eta e^{i(\theta+\alpha)} \ . \tag{1.42}$$

  ϕ_0 and ϕ_0' represent two distinct states and therefore the system no longer has a $U(1)$ symmetry once it acquires a vacuum expectation value. However, they both lie in the circle of minima, $|\phi| = \eta$. We can then write the field as:

$$\phi = \frac{1}{\sqrt{2}}(\phi_1 + i\phi_2) \ , \tag{1.43}$$

  and consider perturbations around the vacuum state:

$$\phi = \frac{1}{\sqrt{2}}(\phi_1 + i\phi_2) + \delta \ . \tag{1.44}$$

  Introducing this expression in Eq. (1.39), we obtain:

$$\mathcal{L} = \frac{1}{2}(\partial\phi_1)^2 - \frac{1}{2}\lambda\delta^2\phi_1^2 + \frac{1}{2}(\partial\phi_2)^2 + \mathcal{L}_{int} \ , \tag{1.45}$$

  where the last term includes cubic and higher order terms in ϕ_1 and ϕ_2. This Lagrangian Density represents a scalar field ϕ_1 with mass $m_{\phi_1} = \delta\sqrt{\lambda}$ and a massless scalar field ϕ_2. The excitations of ϕ_1 happen in the direction where the potential is, in first order, quartic. They are radial oscillations around a point in the circle of minima.

  Moreover, ϕ_2 corresponds to excitations in the direction where the potential does not change. This massless scalar particle is known as a Goldstone Boson. Goldstone bosons are a signature of the spontaneous breaking of a global symmetry.

The second situation in the example above, may occur, in certain models, when the Universe cools down below a certain critical temperature, T_C. The Higgs field, ϕ will take on different vacuum expectation values in different regions of the Universe that are casually disconnected (and therefore, cannot communicate). Since ϕ must vary continuously, in the boundaries between these regions, there may be points in space where the field cannot relax to a vacuum state, leading to a non-trivial configuration of the field, known as a topological defect. In this particular case, this leads to a vortex-like configuration that is known as a cosmic string. This mechanism for defect formation was first proposed by Kibble in 1976 [15] and is known as the Kibble Mechanism.

To make this concept more clear, let us consider a curve, S, (see Fig. 1.4) that encloses the circle of minima. As ϕ goes along that path, it spans the whole vacuum manifold. Doing so, its phase varies by 2π and the field will take the approximate form, $\phi \approx \eta e^{i\theta}$. The number of times it takes for the field to go around the circle and return to the initial point is called the winding number, and it is a conserved topological charge. If we start making the path smaller it will eventually reduce to a point and the winding number becomes 0, which breaks the conservation of charge.

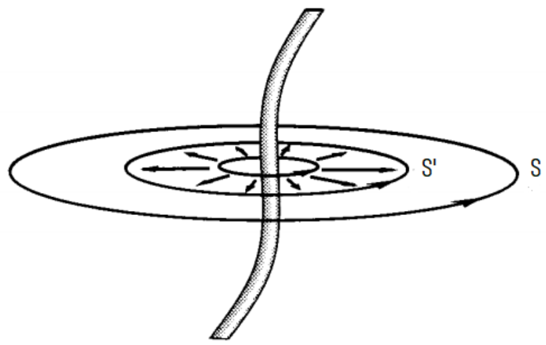

Figure 1.4: Visual representation of the formation of a global string. Figure adapted from [9].

Continuity then implies that there must be a point inside the curve where ϕ vanishes, which means that there is a non-vanishing energy density at that point, an indicator that a cosmic string was formed. Because these strings are associated with the breaking of a $U(1)$ global symmetry, they are known as global strings. These global strings have a divergent mass per unit length, μ, since their energy is not localized within a small region around the core.

This divergence does not arise in strings that originate from the breaking of a local $U(1)$ symmetry, $\phi(x) \rightarrow e^{i\alpha(x)}\phi(x)$, where α now depends on the spacetime coordinates, x. The simplest model with local string solutions is the Abelian-Higgs model, with a Lagrangian density of the form:

$$\mathcal{L} = (D_\mu\bar{\phi})(D^\mu\phi) - \frac{1}{4}F^{\mu\nu}F_{\mu\nu} - \mu^2\bar{\phi}\phi - \lambda(\bar{\phi}\phi)^2 \ , \tag{1.46}$$

where the covariant derivative is given by $D_\mu = \partial_\mu - ieA_\mu$, with A_μ being the gauge vector field, e the gauge coupling and $F^{\mu\nu} = \partial^\mu A^\nu - \partial^\nu A^\mu$ the antisymmetric tensor. In the Lorentz gauge, $\partial_\mu A^\mu = 0$ and the Higgs field takes the same form as the global strings at large distances from the core: $\phi \approx \eta e^{in\theta}$, where n is the winding number. The gauge field will then, at large distances from the core, asymptotically approach [9]:

$$A_\mu \approx \frac{1}{ie}\partial_\mu ln(\phi) \ . \tag{1.47}$$

These asymptotic forms lead to $D_\mu\phi \approx 0$ and $F_{\mu\nu} \approx 0$ far from the string core. The energy density will then vanish rapidly away from the core, and the mass per unit length of the string is now finite and given by $\mu \sim \eta^2$.

In this dissertation, we will consider local strings, as it is expected that they are formed in several relevant theories in cosmology.

1.4. Goal and Structure

It is predicted by several particle physics scenarios, that a cosmic string network is formed in the early stages of the Universe. Such a network is generally expected to survive throughout the cosmological history, potentially leaving behind observational imprints, such as the SGWB. The SGWB is currently the most promising observational signature to detect cosmic strings, or to derive observational constraints in models that predict their formation. The *Laser Interferometer Space Antenna* (LISA), will be the first GW observatory in space, and will be able to probe cosmic strings with much lower tensions than its currently possible [18]. Detecting cosmic strings would allow for a more complete understanding of the physics of the primordial Universe, since it would either validate an existent model, or constrain it observationally.

In their cosmological evolution, cosmic strings often collide and interact with each other, leading to the formation of closed loops of strings (or simply loops), and of small-scale structure (or kinks), which are discontinuities in the derivative of the tangent vector along the string. If two strings meet, they break at the point of contact, exchange partners and reconnect, leading to the formation of two kinky strings (see Fig. 1.5 a)). If a string self intersects, or if two curved strings intersect in more than one point, a closed loop of string is formed (Figs. 1.5 b) and c) respectively). After creation, loops detach from the network, and eventually decay. Cosmic strings networks can then be thought as having two constituents: long strings, which are larger than the horizon (but also closed), and loops, which are usually subhorizon, and as a result, barely feel the effect of Hubble expansion.

When a cosmic string loop is formed, it detaches from the network, oscillates relativistically under its own tension and decays, emitting GWs in different directions. The superposition of the emissions of the large number of loops that exist at any time, generates the SGWB. Kinks, however, travel along the cosmic strings at the speed of light, and are expected to collide quite often. As a result, they are generally expected to also decay, mainly by emitting GWs. This radiation should also contribute to the SGWB, but is generally neglected in computations of this spectrum. It should also affect loop production and have an impact on the contribution of loops. Including the impact of small-scale structure on the evolution of cosmic strings and on their gravitational emission may, therefore, be essential to make accurate predictions of their SGWB.

The main goal of this dissertation is then to study the impact of kinks on the contribution of loops to the SGWB. Additionally, we would also like to make an estimation of the contribution of kinks to the spectrum.

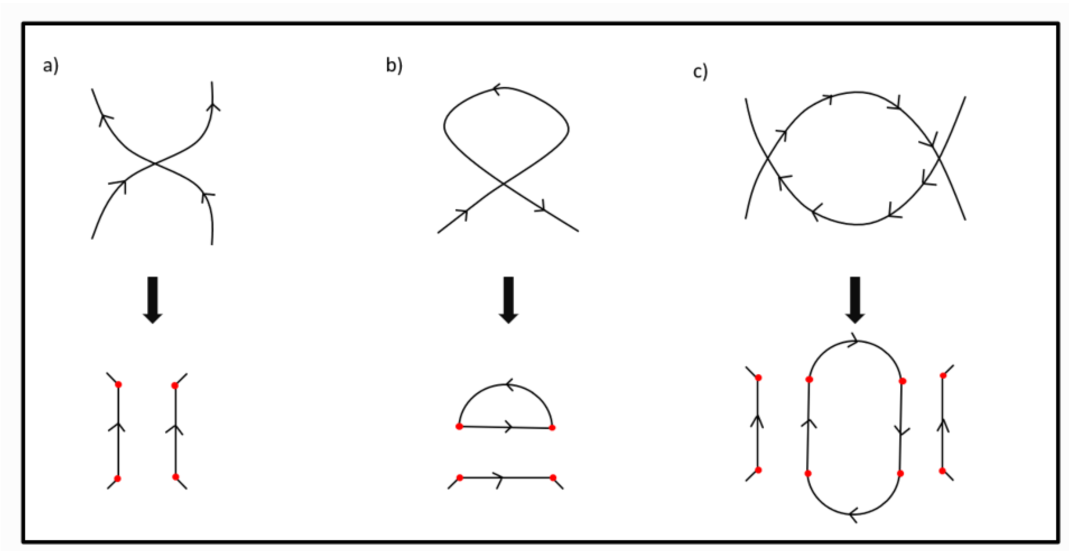

Figure 1.5: Possible interactions of cosmic strings (red dots represent kinks): a) Two strings interact in one point, generating two kinky strings (intercommutation); b) A string self interacts, leading to the formation of a loop and a kinky string; c) Two strings interact in two different points, forming a loop and two kinky strings.

To achieve this, we will begin, in Chapter 2, by providing an overview of the VOS Model. In Chapter 3, we will develop, using different models proposed in the literature, an effective model to describe the evolution of small-scale structure, and afterwards, in Chapter 4, we extend the VOS Model to include the impact of small-scale structure, so that we can study how the existence of kinks affects the evolution of the long string network. Finally, in Chapter 5, we will study the SGWB spectrum with our new Modified VOS Model, and compare the results with the ones obtained with the predictions in the literature that neglect small-scale structure to verify if this structure has a significant impact on the spectrum.

2. Cosmological Evolution of a Cosmic String Network

First attempts to describe the dynamics of a cosmic string network assumed that only a dynamical variable was needed: the characteristic lengthscale of the network, which represents the average distance between two neighboring strings. This description is known as the One-Scale Model, and was first proposed by Kibble [19] in 1985. This model assumes that the cosmic string network will eventually achieve a linear scaling regime, in which the energy density of the network remains constant relative to the background energy density. The first numerical simulations [20] confirmed the existence and stability of such regime. However, subsequent simulations showed the existence of important physical phenomena at small scales that cannot be explained by this One-Scale model, and that can have a very relevant impact on their observational signatures [21]. In 1991, Allen and Caldwell constructed an analytic model to describe the evolution of the small-scale structure on the cosmic string network, by effectively adding a second lengthscale to the One-Scale Model [22] to describe the distance between kinks. On the same year, Quashnock and Piran propose a model with two scales (the characteristic lengthscale and the mean inter-kink distance) [23], where the gravitational back-reaction plays a significant role on the evolution of small-scale structure. Later, Kibble and Copeland [24], motivated by numerical simulations [25], also developed an analytical model with two characteristic lengthscales – the interstring distance and the persistence length – later extended by the same authors, alongside Austin, to include a third lengthscale, describing small-scale structure [26]. This Three-Scale Model confirms the predictions of the One-Scale model for the large-scale properties of the network. It also suggests, that in order for the third lenghtscale to achieve a linear scaling regime as well, the effects of the gravitational back-reaction must be taken into account. Although this model seems to provide a fairly complete description of the evolution of the network, it has an excessive number of unspecified parameters, which makes it quite unappealing. A more recent model, known as the Velocity-dependent One-Scale (VOS) Model, describes the dynamics of the network by also only one characteristic lenghtscale, but in addition, it includes the root-mean-squared (RMS) velocity as a dynamical variable [27]. The VOS model allows for a description of the evolution of the network throughout the cosmological history, including the effects of friction forces, which are relevant very early on. At first, it did not include the effects of the small-scale structure. However, it was later extended by the authors to include a phenomenological parameter, $k(\bar{v})$, attempting, to some extent, to describe its effects [28].

2.1. String Dynamics in an Expanding Universe

Let us assume that the radius of curvature of the cosmic string is much larger than its thickness and that the string does not have internal degrees of freedom, so that we can treat it as a 1-dimensional object. Its world-history can be represented by a $1+1$- dimensional worldsheet, $x^\mu = x^\mu(\zeta^a)$ (where $a = 0, 1$), which obeys the Nambu-Goto action:

$$S = -\mu \int \sqrt{-\gamma} d^2\zeta \,, \tag{2.1}$$

where ζ^0 and ζ^1 are a time-like and a space-like worldsheet parameter, respectively, and γ is the determinant of the worldsheet metric, $\gamma_{\sigma\lambda}$, which is related to the 4-dimensional metric $g_{\mu\nu}$ by $\gamma_{\sigma\lambda} = g_{\mu\nu} x^\mu_{,\sigma} x^\nu_{,\lambda}$.

By varying the action in Eq. (2.1) with respect to x^μ, we obtain the following equation of motion:

$$\frac{1}{\sqrt{-\gamma}} \partial_\sigma (\sqrt{-\gamma} \gamma^{\sigma\lambda} x^\mu_{,\lambda}) + \Gamma^\mu_{\nu\delta} \gamma^{\sigma\lambda} x^\nu_{,\sigma} x^\delta_{,\lambda} = 0 \,. \tag{2.2}$$

Let us consider a flat FLRW Universe, whose line element is given by:

$$ds^2 = a^2(\tau)(d^2\tau - d\mathbf{y} \cdot d\mathbf{y}) \,, \tag{2.3}$$

where t and τ are the physical and conformal times, respectively and $\mathbf{y}$ is a 3-vector whose components are comoving cartesian coordinates. Since the action in Eq. (2.1) is invariant under worldsheet reparametrizations, in this background it is common to impose the following temporal-transverse gauge conditions: $\zeta_0 = \tau$ and $\dot{\mathbf{x}} \cdot \mathbf{x}' = 0$, where $\mathbf{x}(\tau, \zeta_1)$ is the 3-vector that represents the string trajectory. Here, dots and primes represent, respectively, derivatives with respect to τ and ζ_1. We can then rewrite Eq.(2.2) as:

$$\ddot{\mathbf{x}} + 2\mathcal{H}(1 - \dot{\mathbf{x}}^2)\dot{\mathbf{y}} = \epsilon^{-1}(\epsilon^{-1}\mathbf{x}')' \tag{2.4}$$

$$\dot{\epsilon} = -2\mathcal{H}\epsilon\dot{\mathbf{x}}^2 \,, \tag{2.5}$$

where $\epsilon = [\mathbf{x}'^2/(1 - \dot{\mathbf{x}}^2)]^{1/2}$ is the coordinate length per unit length, ζ^1, related to the total string energy by:

$$E = \mu a(\tau) \int \epsilon d\zeta^1 \,, \tag{2.6}$$

and $\mathcal{H} = aH$, where H is the Hubble parameter, defined in Eq. (1.3).

2.2. Cosmic String Network Dynamic

The work in this dissertation will be based on the VOS Model, which we intend to extend to include an effective description of small-scale structure. The VOS Model assumes that the cosmic string network is also homogeneous and isotropic on sufficient large scales, and, therefore, its dynamics can be described macroscopically. To do so, this model makes use of two dynamic variables: the root-mean-squared (RMS) velocity, $\bar{v}$, and the characteristic lenghtscale, L, which can be interpreted as the mean distance between two neighboring strings, or as their typical curvature radius. In an average sense and on sufficient large scales, we can think of the network as a collection of string segments, each with length L and in a volume L^3.

Evolution equations for these macroscopic variables may be obtained by averaging the Nambu-Goto equations of motion (Eqs. (2.4) and (2.5)) over the whole network. There are, however, two important aspects to take into account before doing so.

Strings interact with each other. Depending on the type of interaction that occurs, there can be some energy loss. When two strings simply exchange partners and reconnect, there is no immediate energy loss by the network. However, when a loop is formed, it detaches from the network, evolving separately, and decays, emitting radiation in the process, therefore resulting in an energy loss. This energy loss must then be taken into account when describing the dynamics of the string network. The rate of loop production has been estimated by Kibble in [15]. The probability of a segment with length ℓ, moving with velocity $\bar{v}$, colliding with other segment within a time δt is approximately:

$$\ell\bar{v}\frac{\delta t}{L^2}\,. \tag{2.7}$$

Keeping the one-scale assumption, the probability of creating a loop with a length between ℓ and $\ell + d\ell$ can be described by a scale-invariant function, $w(\ell/L)$. The rate of energy loss into loops is then given by:

$$\left(\frac{d\rho}{dt}\right)_{loops} = -\rho\frac{\bar{v}}{L}\int w(\ell/L)\frac{\ell}{L}\frac{d\ell}{L} \equiv -\tilde{c}\bar{v}\frac{\rho}{L}\,, \tag{2.8}$$

where we introduced the energy-loss parameter $\tilde{c}$, which is assumed to be a constant. Note that in the context of the One-Scale Model (in which the line of thought above was proposed), $\bar{v}$ was absorbed in the definition of $\tilde{c}$, since it was assumed to remain constant.

The second aspect to consider is that, during their evolution, cosmic strings will scatter off the relativistic particles of the background plasma, resulting in a frictional force per unit length that may lead to additional energy loss and effectively decelerate the strings in the early stages of the Universe.

We can now derive the VOS model equations for the evolution of L and $\bar{v}$. We will first derive them assuming that there are no frictional forces or energy loss into loop productions.

The total string energy density, ρ, scales as E/a^3. By differentiating Eq. (2.6) and using Eq. (2.5), we obtain:

$$\frac{d\rho}{dt} + 2H\rho(1+\bar{v}^2) = 0\,, \tag{2.9}$$

where we have defined:

$$\bar{v}^2 \equiv <\dot{\mathbf{x}}^2> = \frac{\int \dot{\mathbf{x}}^2 \epsilon d\zeta^1}{\int \epsilon d\zeta^1} \tag{2.10}$$

as the RMS velocity of the string. The characteristic length, L, can be defined in terms of the energy density

$$\rho \equiv \frac{\mu L}{L^3} = \frac{\mu}{L^2}\,. \tag{2.11}$$

Introducing this expression into Eq. (2.9), we obtain the following expression for the time evolution of L:

$$\frac{dL}{dt} = HL(1+\bar{v}^2)\,, \tag{2.12}$$

where we may see that the dilution of the network caused by expansion leads to an increase of the characteristic lengthscale. To obtain the evolution equation for the RMS velocity, we average Eq. (2.4) and use Eq. (2.10):

$$\frac{d\bar{v}}{dt} = (1-\bar{v}^2)\left[\frac{k}{\bar{R}} - 2H\right]\,, \tag{2.13}$$

which is exact up to second order terms [27] and where we have assumed that $<\dot{\mathbf{x}}^4> = <\dot{\mathbf{x}}^2>^2$. $\bar{R}$ is the average radius of curvature, defined by:

$$\frac{a(\eta)}{\bar{R}}\hat{\mathbf{u}} = \frac{d^2\mathbf{x}}{ds^2}\,, \tag{2.14}$$

where $\hat{\mathbf{u}}$ is the unitary curvature vector and ds is the physical length along the string. In this context, for a long string network, it is generally assumed that $\bar{R} = L$. However, if there is a considerable amount of small-scale structure, this might not be true. We have also introduced the dimensionless curvature parameter k, which measures the angle between the curvature vector and the velocity of the strings, and is defined as:

$$k \equiv \frac{<(1-\dot{\mathbf{x}}^2)(\dot{\mathbf{x}}\cdot\hat{\mathbf{u}})>}{\bar{v}(1-\bar{v}^2)}\,. \tag{2.15}$$

We may see from Eq. (2.13) that curvature accelerates strings since, as a result of their tension, cosmic strings have a tendency to straighten, while the expansion of the background dampens their movement and slows then down. In [28], the following *ansatz* for $k(\bar{v})$ was proposed:

$$k(\bar{v}) = \frac{2\sqrt{2}}{\pi}(1-\bar{v}^2)(1+2\sqrt{2}\bar{v}^3)\frac{1-8\bar{v}^6}{1+8\bar{v}^6} \,. \tag{2.16}$$

in order to provide a phenomenological description of the effect of small-scale structure on the dynamics. However, as we shall see, introducing other lengthscales may be necessary in order to achieve a more precise description of its effects.

The final step to achieve a complete description of the evolution of the L and the $\bar{v}$ is to add the effects of the loop production and of friction, as mentioned above. From Eq. (2.8), and using the relationship from Eq. (2.11), we find that:

$$\left(\frac{dL}{dt}\right)_{loops} = \frac{1}{2}\tilde{c}\bar{v} \,. \tag{2.17}$$

The impact of friction can be described by adding a characteristic frictional length, $l_f \propto a^3$. Its effect surges in Eqs. (2.4) and (2.5) by replacing the Hubble damping term by $2H + a/l_f$ [29].

The VOS Model equations are then:

$$\frac{dL}{dt} = \left(H + \frac{1}{2}\frac{\bar{v}^2}{l_d}\right)L + \frac{1}{2}\tilde{c}\bar{v} \tag{2.18}$$

$$\frac{d\bar{v}}{dt} = (1-\bar{v}^2)\left[\frac{k(\bar{v})}{L} - \frac{\bar{v}}{l_d}\right] \,, \tag{2.19}$$

where we defined the damping lenghtscale, l_d as $l_d^{-1} = 2H + l_f^{-1}$. Eqs. (2.18) and (2.19) allow us to describe the evolution of the cosmic strings networks throughout the cosmological history. Frictional forces become negligible as the Universe expands and becomes less dense, because $l_f \propto a^3$, and therefore the friction lengthscale grows faster than L. Since it only affects the dynamics of the network very early on, from now on, we will assume that $l_f \to \infty$, and so Eqs. (2.18) and (2.19) can be rewritten as:

$$\frac{dL}{dt} = (1+\bar{v}^2)HL + \frac{1}{2}\tilde{c}\bar{v} \tag{2.20}$$

$$\frac{d\bar{v}}{dt} = (1-\bar{v}^2)\left[\frac{k(\bar{v})}{L} - 2\bar{v}H\right] \,. \tag{2.21}$$

Numerical simulations show that $\tilde{c} = 0.23 \pm 0.04$ is a good fit in both radiation and matter dominated eras [28].

2.2.1 Linear Scaling Regimes

The VOS Model predicts the existence of two transient linear scaling regimes, i.e., two time periods where the energy density of the network remains constant relative to the background energy density. Let us characterize these linear scaling regimes, by looking for solutions of the form:

$$L = \xi t \quad \text{and} \quad \bar{v} = \text{constant}\,, \tag{2.22}$$

and by assuming that the evolution of the Universe is ruled by the power law of the form of Eq. (1.28).

Substituting the above expressions into Eqs. (2.20) and (2.21), we find the following linear attractor solution:

$$\xi = \sqrt{\frac{k(k+\tilde{c})}{4\beta(1-\beta)}} \quad \text{and} \quad \bar{v} = \sqrt{\frac{k(1-\beta)}{(k+\tilde{c})\beta}}\,. \tag{2.23}$$

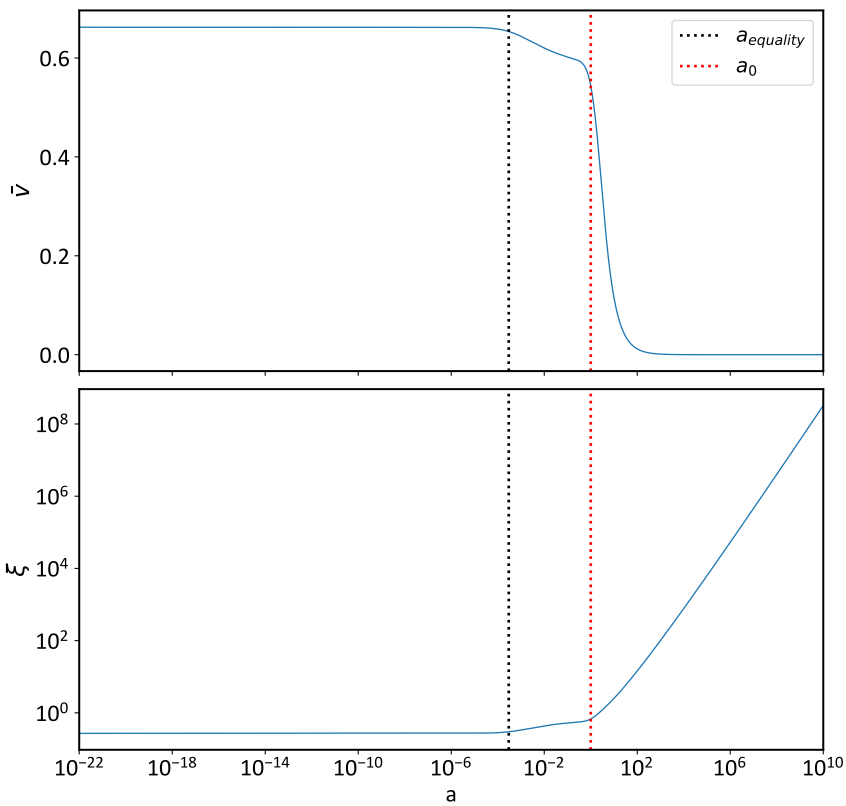

Figure 2.1: Cosmological evolution of $\bar{v}$ (top panel) and $\xi = L/t$ (bottom panel), as predicted by the VOS Model, in a ΛCDM Universe.

It is clear that a linear scaling solution only occurs for a constant value of β, meaning that a linear scaling regime is only attainable either deep into the radiation dominated era or deep into the matter dominated era, breaking off during the radiation-matter transition and once the cosmological constant starts to become relevant to the dynamics of the Universe.

Fig. 2.1 shows the evolution of ξ and $\bar{v}$, in a ΛCDM Universe with an expansion dictated by Eq. (1.24). We can clearly see the scaling regime being achieved during the radiation era. However, it seems that the network never fully achieves a new scaling regime during the matter era. This epoch does not last enough for the network to achieve scaling before the cosmological constant starts dominating the energy density of the Universe.

3. Evolution of Small-Scale Structure on Cosmic Strings

The first step to achieve our end goal is to develop an analytical model that describes the rate at which kinks are created and removed from the network, in order to understand how the linear kink density evolves with time. In this chapter, we will review the work done by Allen and Caldwell [22, 30], Quashnock and Piran [23] and by Kibble and Copeland [31] (and Austin [26]) on modeling analytically the linear kink density. We will study the impact of each of the physical processes that affect the evolution of the linear density of kinks, in order to develop an effective model to describe it, which will be used, in the next Chapter, to develop an extension of the VOS Model, that will allow the study of the cosmological evolution of a cosmic string network with small-scale structure.

Kinks are added to the cosmic string network when intercommutations occur — independently of loops being produced or not — and decay by emitting GWs and due to the stretching caused by the expansion of the Universe. In addition, kinks are also removed from the network when a loop detaches. It is then clear that the loop production rate will play an important role in the development of our model. Throughout this dissertation, we will assume that loops are all created with the same length*. Let n_{loop} be the total number density of loops produced until a time t. The loop production rate is given by:

$$\frac{dn_{loop}}{dt} = \frac{1}{E_{loop}} \left(\frac{d\rho}{dt}\right)_{loops} , \tag{3.1}$$

where $d\rho_{loop}/dt$ is given by Eq. (2.8) and E_{loop} is the energy with which loops are formed (which is determined by their physical length at the moment of creation). In this dissertation we will consider two possibilities for the loop length that have been discussed in the literature:

Case 1: Loops are formed with a physical length, ℓ, that is a fixed fraction of the characteristic lengthscale, that is: $\ell = \alpha L$, where α is a constant between 0 and 1. This is the hypothesis used in studies of the SGWB generated by loops, since it is expected to provide an accurate description of the length of loops being created throughout cosmic history. This hypothesis is supported by the results of numerical simulations of Nambu-Goto strings, where it was shown that large loops are formed with $\alpha \sim 0.34$ [33]. It is,

*Overall, it is not expected for this to be true. However, the results obtained by making this assumption can be used to get results in situations where the length of loops at birth follows some distribution [32].

however, common to find in the literature ℓ written in terms of the time of formation of the loop, t, instead of the characteristic lengthscale at that instant, $L(t)$, since it is usually assumed that the network is in a linear scaling regime. This simply leads to a redefinition of α: $\ell = \alpha L = \alpha\xi t = \alpha' t$, since in this scaling regime, ξ is constant. However, since we want our study to apply to networks both in and out of the linear scaling regimes, we will express ℓ in terms of the characteristic lengthscale, making α a constant in every situation*.

Case 2: Loops are formed with a physical length, ℓ, that is a fixed fraction of the characteristic length of small-scale structure, given by the mean inter-kink distance, l_k, that is: $\ell = \alpha_k l_k$, where $\alpha_k > 0$ is a constant. This case is motivated by the fact that loop production and small-scale structure are intrinsically related, and was first proposed in [30].

Every time a loop detaches from the network, a length of ℓ is removed, alongside $N_r = K\ell$ kinks, where $K = 1/l_k$ is the linear kink density, describing the number of kinks per unit of length of string. Therefore, in **Case 1**, every time a loop detaches, $N_r = \alpha L/l_k$ kinks are removed from the network and, in **Case 2**, the network loses $N_r = \alpha_k$ kinks per loop removed.

We will study the evolution of the linear kink density for both cases separately, according to the following approach:

1. Study the impact of loop production on the number of kinks that are added to the network;
2. Study the impact of non-loop forming intercommutations on the number of kinks added to the network;
3. Study the impact of the kink decay mechanisms.

For each of these steps, we will verify if it is possible – and if it is, under which conditions – for the the lengthscale of small-scale structure, l_k, to reach a linear scaling regime.

Before starting to study each case separately, let us first define how we will model each of these effects.

*Out of scaling, $\xi = \xi(t)$ and we would either need to have a time dependent α — $\alpha = \alpha(t) = \alpha'/\xi(t)$ — or describe the size of loops produced when the network is out of scaling incorrectly.

1. Impact of Loop Production

In [22], the authors propose that the rate of kink creation is proportional to the rate of loop production:

$$\frac{dn_c}{dt} = C\frac{dn_{loop}}{dt} \,, \tag{3.2}$$

where n_c is the number density of kinks created and the proportionality constant, C, is the average number of kinks created on the long string network for each loop formed. Since per intercommutation, each string gains two kinks, and, for a loop to be formed, we need at least one (but probably several) intercommutation, $C \geq 2$.

When a loop detaches, a length of ℓ is removed, and, as a consequence, kinks are carried away. Let n_r be the number density of removed kinks. The rate at which they are removed from the network is then:

$$\frac{dn_r}{dt} = \ell K(t)\frac{dn_{loop}}{dt} \,, \tag{3.3}$$

where $K(t)$ is given by:

$$K(t) = (n_c - n_r)L^2 \,, \tag{3.4}$$

Differentiating Eq. (3.4) with respect to time, we obtain the following differential equation:

$$\frac{d}{dt}[KL^{-2}] = [C - \ell K]\frac{dn_{loop}}{dt} \,. \tag{3.5}$$

In [31], the authors proposed that loop production could be more likely in regions that have a larger density of kinks – since strings are more curved in these regions and move with higher speeds – and, as a result, loops may carry away more kinks. This effect is modeled by introducing a parameter, q, that characterizes the relative "kinkiness" between the loop and the long string. This means that, when a loop detaches from the network, it will remove $qK\ell$ kinks, instead of $K\ell$, and Eq. (3.5) becomes:

$$\frac{d}{dt}[KL^{-2}] = [C - q\ell K]\frac{dn_{loop}}{dt} \,. \tag{3.6}$$

We will verify how the linear kink density, K, is affected by loop production, and study whether a linear scaling regime for l_k can be achieved.

2. Impact of Non-Loop Forming Intercommutations

We mentioned in Chapter 1 that kinks are formed in the network every time strings interact, even when that interaction does not lead to the creation of a loop. So, the next question that arises is: do intercommutations that do not form loops have a significant contribution to the amount of kinks that are created in the network? In other words, what happens to the linear kink density when we vary the parameter C. Let us recall its definition:

$$C = \frac{\text{Number of kinks in the long string}}{\text{One Intercommutation}} \times \frac{\text{Number of Intercommutations}}{\text{One Loop}} \,. \tag{3.7}$$

The first term is equal to 2: When two strings meet, they break at the point of contact, exchange partners and reconnect, leading to the formation of two strings with two kinks each. The second term must be equal to larger than 1, since at least one intercommutation is needed to form a loop. If more than one intercommutation must occur to create a loop (which is likely), then the network should have a higher linear kink density, since there are extra kinks being added to the network that are not being removed when a loop detaches. We will, therefore, verify what the effect of varying C is on the behavior of the linear kink density.

Another way to approach this, is to fix $C = 2$ and add a new term to Eq. (3.5) to characterize these additional intercommutations. In [31] and in [26], the authors model the effect of these non-loop forming intercommutations with a term with the following form:

$$\frac{dn_{int}}{dt} = \frac{\chi(\bar{v})}{L^4} \,, \tag{3.8}$$

where n_{int} is the number density of kinks added to the network by non-loop forming intercommutations, and $\chi(\bar{v}) = 2\bar{v}(1-\bar{v}^2)/\pi$. Eq. (3.2) then has an additional term:

$$\frac{dn_c}{dt} = C\frac{dn_{loop}}{dt} + \frac{dn_{int}}{dt}. \tag{3.9}$$

In the context of the Three-Scale Model, χ is a constant because linear scaling is assumed. However, here we will treat $\bar{v}$ as a dynamical variable, since we intend to develop a model that describes the evolution of small-scale structure throughout cosmic history, so this is no longer true. Adding this term to Eq. (3.6), it becomes:

$$\frac{d}{dt}[KL^{-2}] = [2 - q\ell K]\frac{dn_{loop}}{dt} + \frac{\chi(\bar{v})}{L^4} \,. \tag{3.10}$$

We would then like to answer the following question: *is the inclusion of this term really necessary or can these intercommutations that do not lead to loop formation be described by increasing C*?

3. Impact of Kink Decay

Let n_{GW} and n_H be, respectively, the number density of kinks lost by the network due to the emission of gravitational radiation and by being stretched by the expansion of the background. The rate at which kinks decay by emitting GWs is given by [23, 30]:

$$\frac{dn_{GW}}{dt} = -\Gamma\hat{C}G\mu K^2 L^{-2} = -\hat{\Gamma}G\mu K^2 L^{-2} \,, \tag{3.11}$$

where $\hat{\Gamma} = \Gamma\hat{C}$, Γ describes the efficiency of emission of GWs and $\hat{C} > 1$ was introduced to account for the impact of gravitational backreaction, which should lead to a smoothing of the kinks as they emit GWs and may make their decay more efficient [26]. The larger the value of $\hat{C}$ considered, the faster kinks are expected to be smoothed out, and, therefore, $\hat{\Gamma}$ could be regarded as an effective value for the GW emission efficiency, accounting for the effects of gravitational backreaction.

The rate at which the number density of kinks decreases due to being Hubble stretched is given by [31]:

$$\frac{dn_H}{dt} = -2H(1-2\bar{v}^2)KL^{-2} \,. \tag{3.12}$$

Eq. (3.3) has now two new extra terms:

$$\frac{dn_r}{dt} = \ell K \frac{dn_{loop}}{dt} + \frac{dn_{GW}}{dt} + \frac{dn_H}{dt} \,, \tag{3.13}$$

and so, Eq. (3.6) becomes:

$$\frac{d}{dt}[KL^{-2}] = [C - q\ell K]\frac{dn_{loop}}{dt} + \frac{\chi(\bar{v})}{L^4} - \hat{\Gamma}G\mu K^2 L^{-2} - 2H(1-2\bar{v}^2)KL^{-2} \,. \tag{3.14}$$

We will now see how each of the above mentioned effects impacts the evolution of the linear kink density and its ability to reach a linear scaling regime. Eqs. (3.6), (3.10) and (3.14) can be solved analytically if we assume that the the expansion of the Universe is ruled by the power law in Eq. (1.28), so that the network is in a linear scaling regime, with scaling values given by Eq. (2.23)). We can also solve them numerically, alongside the Friedmann Equation, (1.24), to see how the linear kink density evolves in a ΛCDM Universe.

3.1. Case 1: $\ell = \alpha L$

Let us begin by assuming that loops are formed with a size that is a fixed fraction of the characteristic lengthscale, $\ell = \alpha L$. They each will be formed with energy, $E_{loop} = \mu\alpha L$.

3.1.1 Impact of Loop Production

Setting $q = 1$ for now, the loop production rate per unit volume is [34]:

$$\frac{dn_{loop}}{dt} = \frac{1}{E_{loop}}\left(\frac{d\rho}{dt}\right)_{loops} = \frac{\tilde{c}\bar{v}}{\alpha L^4} \,, \tag{3.15}$$

and the rate at which kinks are removed from the network is:

$$\frac{dn_r}{dt} = \alpha L K \frac{dn_{loop}}{dt} \, . \tag{3.16}$$

When a loop detaches from the network, a length of αL is removed. We can then rewrite Eq. (3.6) as:

$$\frac{d}{dt}[KL^{-2}] = [C - \alpha L K]\frac{\tilde{c}\bar{v}}{\alpha L^4} \, , \tag{3.17}$$

which has the following analytical solution, when assuming linear scaling conditions, and that the network is formed at the instant t_i without kinks (that is, $K(t_i) = 0$):

$$K(t) = \frac{\tilde{c}\bar{v}C}{\alpha\xi^2(3 - \frac{\tilde{c}\bar{v}}{\xi})}\frac{1}{t}\left[\left(\frac{t}{t_i}\right)^{3-\frac{\tilde{c}\bar{v}}{\xi}} - 1\right] \, , \tag{3.18}$$

for $3 - \tilde{c}\bar{v}/\xi \neq 0$. In order for the characteristic lengthscale of small-scale structure to achieve a linear scaling regime, we must have $l_k \propto t$ (or, equivalently, $K(t) \propto 1/t$), which only happens if $3 - \tilde{c}\bar{v}/\xi < 0$. Substituting $\bar{v}$ and ξ by their scaling values given by the expressions in Eq. (2.23), we obtain that:

$$\beta < -\frac{1}{2}\left(1 + \frac{3k(\bar{v})}{\tilde{c}}\right) \, . \tag{3.19}$$

Both $k(\bar{v})$ and $\tilde{c}$ are, by definition, positive*, and therefore, Eq. (3.19) implies $\beta < 0$, which is not possible in an expanding Universe (as is our own). Therefore, $3 - \tilde{c}\bar{v}/\xi$ must be larger than 0, which means that K never stops increasing as time moves forward. More kinks need then to be removed from the network for the small-scale structure lengthscale to reach a linear scaling regime. Let us then consider $q > 1$ and verify if the linear scaling regime is possible if loops remove enough kinks. Rewriting Eq. (3.18) as:

$$K(t) = \frac{\tilde{c}\bar{v}C}{\alpha\xi^2(3 - \frac{\tilde{c}\bar{v}q}{\xi})}\frac{1}{t}\left[\left(\frac{t}{t_i}\right)^{(3-\frac{q\tilde{c}\bar{v}}{\xi})} - 1\right] \, , \tag{3.20}$$

and once again imposing $K \propto t^{-1}$, we now have that $3 - \tilde{c}q\bar{v}/\xi < 0$. The linear kink density will then reach linear scaling if q is higher than a critical value, q_c^1, equal to:

$$q_c^1 = \frac{3\xi}{\tilde{c}\bar{v}} = \frac{3}{2\tilde{c}}\frac{k(\bar{v}) + \tilde{c}}{1 - \beta} \, , \tag{3.21}$$

where, once again, we replaced $\bar{v}$ and ξ by their scaling solutions. Let us consider some arbitrary value of q for which scaling occurs, i.e., $q = q_c^1 + \delta$, $\delta > 0$. Substituting this value

*This is not true for $\bar{v}^2 \geq 1/2$. However, for an expanding Universe, it is not expected for the velocity to have such values.

in Eq. (3.20), we obtain the following linear scaling value for K:

$$K_{\text{scaling}}(t) = \frac{C}{\alpha\xi t\delta} = \frac{C}{\ell\delta}\,, \tag{3.22}$$

which means that the average inter-kink distance in scaling is determined by the physical length of loops:

$$l_k = \frac{\delta}{C}\ell\,. \tag{3.23}$$

For $q < q_c^1$, K never reaches a linear scaling regime and always increases with time. If we now consider $q = q_c^1 - \delta$, for $q_c^1 > \delta > 0$, we have that the linear kink density evolves with time as follows:

$$K_{\text{out of scaling}}(t) = \frac{C}{\delta\ell}\left[\left(\frac{t}{t_i}\right)^{\tilde{c}\bar{v}\delta/\xi} - 1\right]\,. \tag{3.24}$$

This growth is faster for smaller q, since more small-scale structure builds up in the network. Finally, let us see what happens in the critical case.

Solving Eq. (3.17) but this time with $q = q_c^1$, we obtain

$$K_{\text{critical}}(t) = \frac{C\tilde{c}\bar{v}}{\alpha\xi^2}\frac{\log(t/t_i)}{t}\,, \tag{3.25}$$

and linear scaling is also not possible in this situation. There is an initial increase in the linear kink density which then decreases and will tend to zero as time goes on. The value of Kt will grow logarithmically.

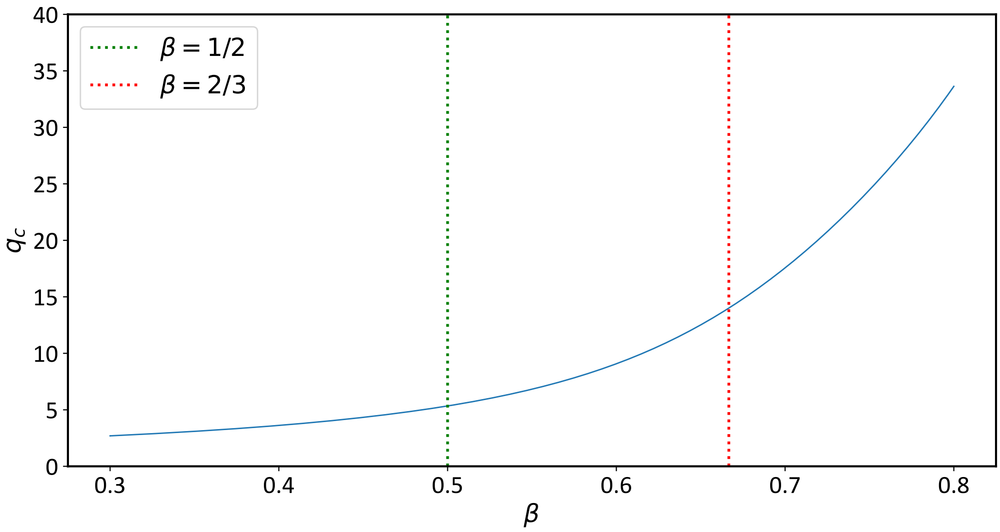

Figure 3.1: Minimum value of q required for the small-scale structure lengthscale to achieve a linear scaling regime, as a function of β. In the radiation dominated era, $\beta = 1/2$ and $q_c^1 \sim 5$. In the matter dominated era, $\beta = 2/3$ and $q_c^1 \sim 15$.

Solving Eq. (3.21) alongside Eqs. (2.23) and (2.16), we may study the dependence of q_c^1 on β. The results are plotted in Fig. 3.1, and therein one may see that $q_c^1 \sim 5$ in the radiation dominated era, while $q_c^1 \sim 15$ in the matter dominated era.

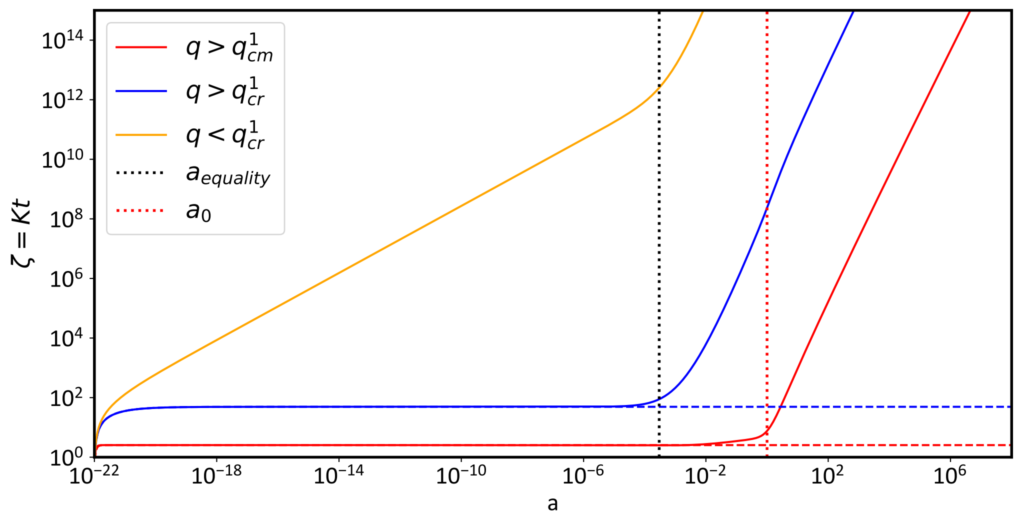

Figure 3.2: Evolution of the linear kink density, $K = \zeta/t$, in a ΛCDM Universe for $q > q_{cr}^1$,q_{cm}^1 and for $q = 1 < q_{cr}^1$, where q_{cr}^1 and q_{cm}^1 are the critical values of q in the radiation and in the matter era, respectively. Solid lines represent the numerical solution, and dashed lines the solution obtained analytically for the radiation era. Dashed and solid lines match during the radiation dominated era for r $q > q_{cr}^1$,q_{cm}^1 (i.e., when the linear kink density is in a linear scaling regime.

Solving now Eq. (3.17) alongside Eqs. (2.18), (2.19) and (1.24), we can see how the linear kink density evolves in a realistic background. The plot in Fig. 3.2 shows the evolution of $\zeta = Kt$ for $q > q_{cr}^1$,q_{cm}^1 and for $q = 1 < q_{cr}^1$, where q_{cr}^1 and q_{cm}^1 are the critical values of q in the radiation and in the matter era, respectively. As expected, the linear scaling regime cannot be achieved for $q = 1$; loops do not remove enough kinks and the linear kink density increases quickly. For a value of $q > q_{cm}^1$, K does reach a linear scaling regime in the radiation era, since $q_{cm}^1 > q_{cr}^1$, but, never reaches it in the matter dominated era. Once again, this epoch does not last long enough for that to happen, and the energy density of the Universe starts being dominated by a cosmological constant. The growth is much smaller during the matter era. Kt is simply evolving towards the new scaling constant until Λ starts dominating. When the Universe enters this Λ-dominated epoch, which is equivalent of having $\beta \longrightarrow 1$, it is not possible for the linear kink density to achieve a linear scaling regime, as in this limit, $q_c^1 \longrightarrow \infty$ (as we can see by looking at Eq. (3.21)).

3.1.2 Impact of Non-Loop Forming Intercommutations

Let us now study the effect of intercommutations that do not form loops on the number density of kinks.

We will begin by comparing the linear kink density for some arbitrary value of $C > 2$, K_C, with the linear kink density for $C = 2$, K_2, in order to verify if these extra intercommutations lead to an increase in the linear kink density. We can assume that $\bar{v}$ and L are in a linear scaling regime, since their scaling values are independent of C, and therefore, so is q_{c1}, which means that varying C also has no impact on the linear scaling condition for K. Let us consider some arbitrary value of q and use the analytical expression in Eq. (3.18) to make the comparison. For a given time instant, and a fixed value of α, we have that:

$$\frac{K_C}{K_2} = \frac{C}{2}\,. \tag{3.26}$$

Let us now see if we can model the effect of these non-loop forming intercommutations by fix $C = 2$, and instead add the term in Eq. (3.8) to Eq. (3.6).

Assuming that $\bar{v}$ and L are in a linear scaling regime, we obtain the same analytical solution as in Eq. (3.20) but with :

$$C \longrightarrow 2\left[1 + \frac{\chi(\bar{v})\alpha}{2\bar{v}\pi\tilde{c}}\right] \sim \begin{cases} 2\,, & \alpha \ll 1 \\ 2\left[1 + \frac{\chi(\bar{v}_\beta)}{2\bar{v}_\beta\pi\tilde{c}}\right]\,, & \alpha \sim 1\,, \end{cases} \tag{3.27}$$

where $\bar{v}_\beta = \bar{v}_r, \bar{v}_m$, for $\beta = 1/2,\ 2/3$, are the scaling values of the RMS velocity for the radiation and the matter dominated eras respectively. Since q_c^1 is independent of C, considering a term of the form of Eq. (3.8) has no impact on the critical value of q. We then have that, if the loops produced are small – and then many loop-forming intercommutations occur –, non-loop forming intercommutations have a negligible impact on the kink number density, and may be approximately described by setting $C = 2$. The maximum effect occurs in the limit where $\alpha \longrightarrow 1$, i.e., when loops are large. This may be seen in the plot in Fig. 3.3: the presence of this term causes the linear kink density to increase by a factor of at most 1.78, and can therefore be described by setting $C \sim 4$. This value depends on β, i.e., depends whether the Universe is in a radiation or in a matter dominated era, but, as we can see in Fig. 3.3, this dependence is weak and does not have a significant impact in the results.

3.1.3 Impact of Kink Decay

Finally, let us add the effects of kink decay, and see how they affect the evolution of the linear kink density and the attainability of the linear scaling regime. Let us solve Eq. (3.14) both analytically, by assuming that $\bar{v}$ and L are in linear scaling regimes, and numerically,

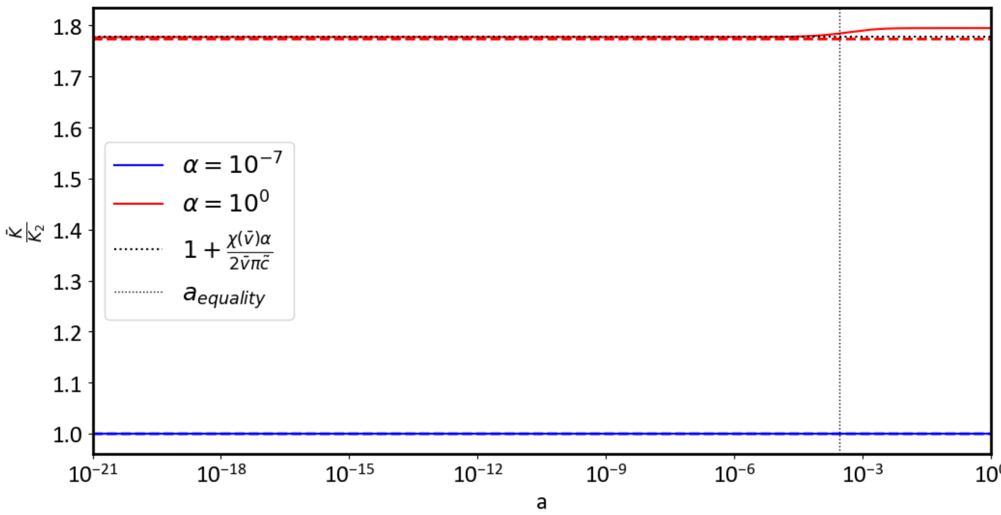

Figure 3.3: Impact of the non-loop forming intercommutations. Solid lines correspond to a value of $q > q^1_{cr}$ and dashed lines correspond to a value of $q < q^1_{cr}$, where q^1_{cr} is the critical value of q in the radiation dominated era. Dashed and solid lines match, for their respective value of α. The black doted line represents the analytical value for the ratio between the linear kink density for $C = 2$ with a non-loop forming intercommutation term, $\bar{K}$, and the linear kink density without a non-loop forming intercommutation term and $C = 2$, K_2 for $\alpha = 1$, in the radiation era. It matches the numerical solutions. $a_{equality} = \Omega_r/\Omega_m$ is the scale factor at the time of radiation-matter equality.

by solving it alongside the VOS Model and Friedmann Equations. This is a Riccati Differential Equation:

$$\frac{dK}{dt} = -\hat{\Gamma}G\mu K^2 - \left[\frac{q\tilde{c}\bar{v}}{\xi} + 2\beta(1-\bar{v}^2)\right]\frac{K}{t} + \frac{C\tilde{c}\bar{v}}{\alpha\xi^2 t^2}\,, \tag{3.28}$$

which can be solved by making the following change of variable, that reduces it to a Cauchy-Euler Differential Equation:

$$u = e^{-\int f(t)K(t)dt}\,,\ \text{where } f(t) = -\hat{\Gamma}G\mu\,. \tag{3.29}$$

We then find the following solution (once again considering that the network is formed at a time t_i without small-scale structure):

$$K(t) = \frac{N(1-M)}{2\hat{\Gamma}G\mu t}\,\frac{\left[1-\left(\frac{t}{t_i}\right)^{NM}\right]}{1+\left(\frac{M-1}{M+1}\right)\left(\frac{t}{t_i}\right)^{NM}}\,, \tag{3.30}$$

for $N \neq 0$, where $N = M_2 + 1$, $M = \sqrt{1 + 4\hat{\Gamma}G\mu M_1/N^2}$ and $M_1 = C\tilde{c}\bar{v}/(\alpha\xi^2)$ and $M_2 = 2 - q\tilde{c}\bar{v}/\xi - 2\beta(1-2\bar{v}^2)$. Once again, it is possible to define a critical value of q, corresponding to having $N = 0$:

$$\bar{q}^1_c = \frac{\xi}{\tilde{c}\bar{v}}[3 - 2\beta(1-2\bar{v}^2)] = \frac{(k(\bar{v})+\tilde{c})(3-2\beta)}{\tilde{c}(1-\beta)} + \frac{2k(\bar{v})}{\tilde{c}}\,. \tag{3.31}$$

There are now two possible situations that lead to a linear scaling regime:

1. $N > 0 \Rightarrow q < \bar{q}_c^1$

   In this case, $K(t) \longrightarrow \frac{N(M+1)}{2\hat{\Gamma}G\mu t}$ as $t \longrightarrow \infty$.

   Considering an arbitrary value of $q = \bar{q}_c^1 - \delta$, with $\bar{q}_c^1 > \delta > 0$, and that $\alpha \gg \hat{\Gamma}G\mu$*, we have that:
$$K(t) \approx \frac{\delta\tilde{c}\bar{v}}{\hat{\Gamma}G\mu L} \longrightarrow l_k(t) \approx \frac{1}{\delta\tilde{c}\bar{v}}\hat{\Gamma}G\mu L \,. \tag{3.32}$$
   In this case, loops alone cannot remove enough kinks to ensure scaling. This regime is maintained mostly by kink decay and the scaling value of the mean inter-kink distance is then determined by the characteristic lengthscale of the gravitational backreaction.

2. $N < 0 \Rightarrow q > \bar{q}_c^1$

   In this case, $K(t) \longrightarrow \frac{N(1-M)}{2\hat{\Gamma}G\mu t}$ as $t \longrightarrow \infty$.

   Considering now a value of $q = \bar{q}_c^1 + \delta$, with $\delta > 0$, we have, to first order in $\hat{\Gamma}G\mu/\alpha$, that:
$$K(t) \approx \frac{C}{\delta\ell} \longrightarrow l_k(t) \approx \frac{\delta}{C}\ell \,. \tag{3.33}$$
   Loop production is now sufficient to guarantee the attainment of the linear scaling regime. The scaling value of the mean-inter kink distance is determined by the physical length of loops, similarly to what happens when there are no decay mechanisms.

Eq. (3.30) is not well defined for $q = \bar{q}_c^1$, since for $N = 0$, we have:
$$M = \sqrt{1 + \frac{4\hat{\Gamma}G\mu M_1}{N^2}} \longrightarrow \sqrt{1 + \frac{4\hat{\Gamma}G\mu M_1}{\infty}} \,. \tag{3.34}$$
To see what happens in this case, let us replace q for $\bar{q}_c^1$ in Eq. (3.14) and try to find an analytical solution. In this critical case, we have that:
$$K_{\text{critical}}(t) = \frac{\sqrt{M_1}}{t}\tanh\left[\sqrt{M_1}\log\left(\frac{t}{t_i}\right)\right] , \tag{3.35}$$
and linear scaling is not possible.

Let us now solve Eq. (3.14) — without the term associated with the non-loop forming intercommutations given the results of the previous section — alongside Eqs. (1.24),

*It is expected for α to always be larger than $\hat{\Gamma}G\mu$, since gravitational backreaction smooths out cosmic strings on scales smaller than this gravitational backreaction.

(2.20) and (2.21) to see how K evolves in a realistic background. The plot on Fig. 3.4 shows the evolution of the linear kink density in a ΛCDM Universe, for $q < \bar{q}^1_{cr}$, $q = \bar{q}^1_{cr}$, $\bar{q}^1_{cm} > q > \bar{q}^1_{cr}$ and for $q > \bar{q}^1_{cm}$, where $\bar{q}^1_{cr}$ and $\bar{q}^1_{cm}$ correspond to the critical value of q in the radiation and in the matter dominated eras, respectively. We also include the two analytically predicted linear scaling situations, for q both smaller and larger than its critical value for the radiation era. We can see that for $q > \bar{q}^1_c$, i.e., when loop production assures scaling, this regime is achieved significantly faster than in the opposite case, since the scaling value of ζ in this case is smaller (because l_k is determined by the length of loops). For a value of q lower than the critical value, this regime, as we have seen, is maintained mostly by kink decay, and so, K takes some time to reach scaling and strings have a large number density of kinks. This is exactly the same behavior found by Allen and Caldwell in ([30]) (although the authors did not take into consideration the effects of expansion). For $q = \bar{q}_{c1r}$, we observe, as expected, that the linear kink density cannot achieve a linear scaling regime. The linear kink density does not reach a linear scaling regime for $q > \bar{q}^1_{cm}$ in the matter era, since, once again, this epoch does not last long enough for that to happen. We also see that for values of q smaller than the critical value in the matter dominated era, in situations where scaling occurs in the radiation era, the linear kink density approaches values close to $\hat{\Gamma}G\mu$ soon after the beginning of the radiation-matter transition. For $q > \bar{q}^1_{cm}$, however, this growth is much slower, because there is a linear scaling regime in the matter era, characterized by a low kink density.

It seems, however, that, as soon as the cosmological constant starts dominating the energy density of the Universe, K enters a new linear scaling regime, independently of the value of q. When Λ starts dominating the energy density of the Universe, $\bar{v} \longrightarrow 0$, and so, we can rewrite Eq. (2.18) as follows:

$$\frac{dL}{dt} = HL \rightarrow L \propto a \ . \tag{3.36}$$

In this limit, where $\bar{v} = 0$ and $L \propto a$, Eq. (3.14) becomes :

$$\frac{d}{dt}[Ka^{-2}] = -\hat{\Gamma}G\mu K^2 a^{-2} - 2HKa^{-2} \rightarrow K \propto \frac{1}{\hat{\Gamma}G\mu t} \ . \tag{3.37}$$

Therefore, as the energy density of the Universe starts being dominated by a cosmological constant, the only decay mechanism that is relevant is gravitational backreaction, and the characteristic lenghtscale of small-scale structure enters a linear scaling regime characterized by a high density of kinks. Once again, when the energy density of the Universe begins to be Λ dominated, (i.e., when $\beta \longrightarrow 1$), $\bar{q}^1_c \longrightarrow \infty$. Therefore, it will always be the scale of the gravitational backreaction to determine the length of the small-scale structure. We have verified numerically that both the red and gray lines in the plot of Fig. 3.4 will evolve towards the regime in Eq. (3.37). However, since they represent situations which during the matter era were in a linear scaling regime with a lower linear kink density (determined by loop size), they take a longer time to reach this new regime.

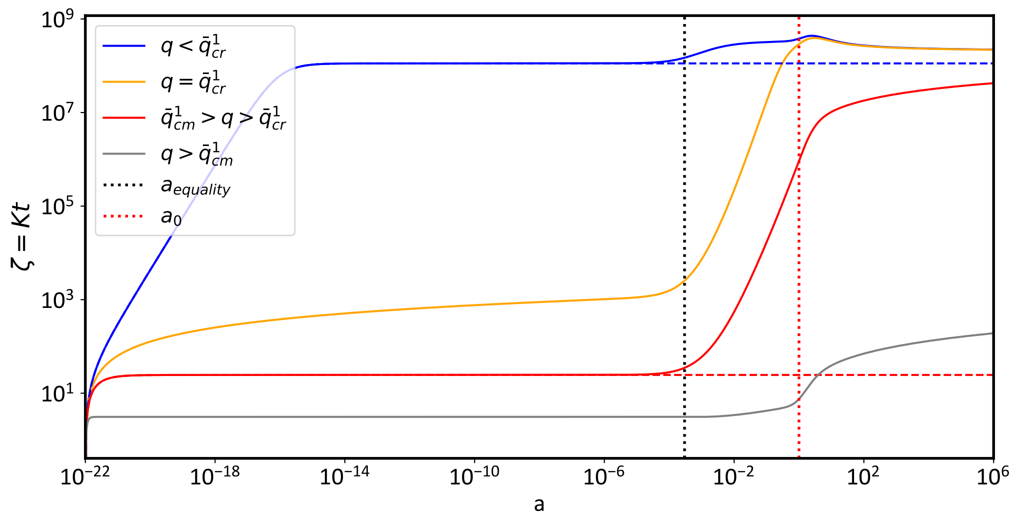

Figure 3.4: **Case 1**: Evolution of the linear kink density, $K = \zeta/t$, in a ΛCDM Universe for $q < \bar{q}^1_{cr}$, $q = \bar{q}^1_{cr}$, $\bar{q}^1_{cm} > q > \bar{q}^1_{cr}$ and for $q > \bar{q}^1_{cm}$, where $\bar{q}^1_{cr}$ and $\bar{q}^1_{cm}$ correspond to the critical value of q in the radiation and in the matter dominated eras, respectively (solid lines). Dashed lines represent the analytical solutions for the first three situations (i.e., for $\beta = 1/2$). Solid and dashed lines match in the radiation dominated era when K reaches scaling. Parameters used: $C = 2$, $\alpha = 0.3$, $\hat{\Gamma} = 50$ and $G\mu = 10^{-10}$. Ω_{i0}, where $i = r, m, \Lambda$ are given by Eqs. (1.25) - (1.27).

The similarity between our results and those in [30], where expansion is not considered, raises the question: *are the effects of expansion negligible?* To answer this question, let us once again solve Eq. (3.14) (alongside Eqs. (1.24), (2.20) and (2.21)), but without its last term, that accounts for the kinks that are lost by the network due to Hubble stretching. By looking at Eq. (3.31), we can see that expansion decreases the value of $\bar{q}^1_c$. It is also safe to assume that the presence of an extra decay mechanism will lead to a lower linear kink density. But is it significant?

The plot in Fig. 3.5 shows the ratio between the linear kink density when both kink decay mechanisms are present and when only gravitational backreaction is considered, for different values of the string tension, $\epsilon = G\mu$, in a ΛCDM Universe. We can see that the Hubble expansion's impact on the linear kink density increases as ϵ decreases, that is, as the gravitational backreaction loses strength. This effect gets more evident on the matter dominated era, where the rate of expansion is faster and we have verified that it increases substantially in an epoch dominated by a cosmological constant, where the expansion is accelerated. Let us also point out, that the linear scaling regime described in Eq. (3.37) is only possible when considering decay by Hubble stretching, since the growth of L balances exactly the decay, and so, only the emission of GWs will be relevant. However, without Hubble stretching as a decay mechanism, the same does not occur, Kt will continue to grow, and there won't be a linear scaling regime. This explains the accentuated differences in the cosmological constant era.

Since values of tension higher than $\epsilon \sim 10^{-7}$ have already been excluded observationally using CMB data [35], scenarios of interest will correspond to situations where the gravitational backreaction is weak enough for the Hubble expansion to be relevant. Throughout this dissertation, we will, therefore, not neglect the expansion of the Universe as a mechanism of kink decay.

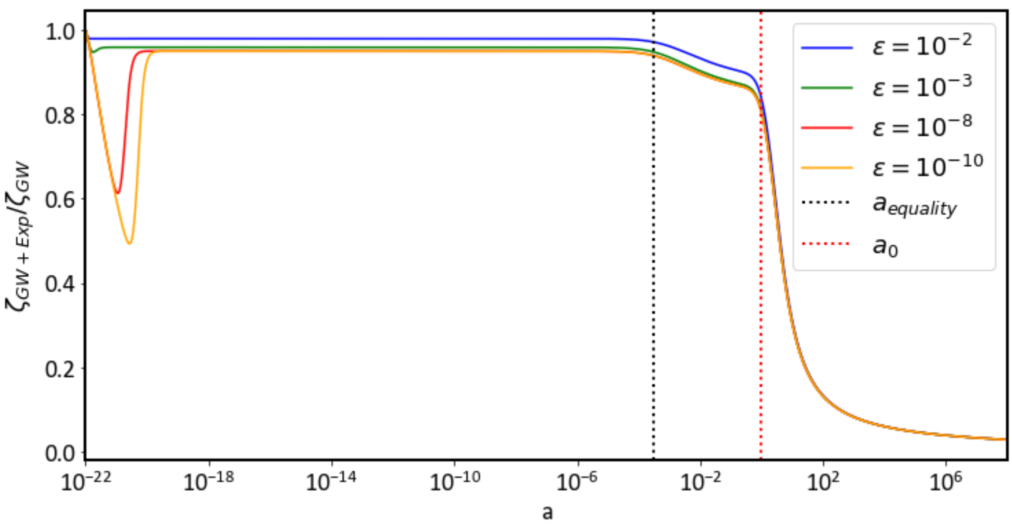

Figure 3.5: **Case 1**: Comparison between the evolution of the linear kink density when both kink decay to GWs and due to Hubble stretching are present, ζ_{GW+Exp} and its evolution when the only mechanism of kink decay considered is the gravitational backreaction, ζ_{GW}, where $\zeta = Kt$, in a ΛCDM Universe. Parameters used: $C = 2$, $\alpha = 0.3$, $q = 1$, $\hat{\Gamma} = 50$. Ω_{i0}, where $i = r, m, \Lambda$ are given by Eqs. (1.25) - (1.27).

3.2. Case 2: $\ell = \alpha_k l_k$

Let us now assume that loops are created with a size that is a fixed fraction of the characteristic lengthscale of small-scale structure, i.e., $\ell = \alpha_k l_k = \alpha_k / K$. Each loop is then formed with energy $E_{loop} = \mu\alpha_k / K$.

3.2.1 Impact of Loop Production

The rate of loop production is now given by:

$$\frac{dn_{loop}}{dt} = \frac{\tilde{c}\bar{v}\rho/L}{\mu\alpha_K/K} = \frac{\tilde{c}\bar{v}K}{\alpha_k L^3}\,, \tag{3.38}$$

and the rate at which kinks are removed from the network is :

$$\frac{dn_r}{dt} = q\alpha_k \frac{dn_{loop}}{dt}\,. \tag{3.39}$$

Eq. (3.6) now becomes:

$$\frac{d}{dt}[KL^{-2}] = [C - q\alpha_k]\frac{\tilde{c}\bar{v}K}{\alpha_k L^3}\,, \tag{3.40}$$

and has the following analytical solution, when considering that both $\bar{v}$ and L are in linear scaling and by assuming that the network is formed at an instant t_i with an initial linear kink density $K_i \equiv K(t_i)$:

$$K(t) = K_i \left(\frac{t}{t_i}\right)^{(C-q\alpha_k)\frac{\tilde{c}\bar{v}}{\alpha_k\xi}+2}\,. \tag{3.41}$$

Unlike the previous case, the network must now be formed with a non-vanishing initial kink number density, K_i, since otherwise loops would be created with an infinite length.

To have $K \propto t^{-1}$, we must have that $(C - q\alpha_k)\tilde{c}\bar{v})/(\alpha_k\xi) + 2 = -1$, which implies that q must be equal to the following critical value, q_c^2:

$$q_c^2 = \frac{C}{\alpha_k} + \frac{3\xi}{\tilde{c}\bar{v}} = \frac{C}{\alpha_k} + \frac{3}{2\tilde{c}}\frac{k(\bar{v}) + \tilde{c}}{1-\beta}\,. \tag{3.42}$$

This critical value is now highly dependent on the values of C and α_k, and similarly to **Case 1**, it is not possible to reach scaling if loops are not created in places which have more kinks than the average in the long string, i.e., if $q = 1$, since that would imply $\beta > 1$. We are, in this case, removing a fixed number of kinks so, scaling is only possible if we remove exactly the needed number of loops to compensate the number of created kinks and the changes in the characteristic lengthscale. If $q < q_c^2$, the linear kink density will always increase with time; if $q > q_c^2$, the strings will eventually lose all the small-scale structure. The plots in Fig. 3.6 show the values that q must take, as a function of loop size (α_k), for several values of C in the radiation dominated era. We observe that increasing the value of C causes q_c^2 to be larger. Increasing C means increasing the number of intercommutations needed to form a loop, therefore, increasing the number of kinks in the long string, and, as a consequence, loops need to remove more kinks for the linear kink density to reach scaling. We also observe that as loop size increases, which is equivalent to say, as $C/\alpha_k \longrightarrow 0$, q_c^2 evolves towards $3\xi/(\tilde{c}\bar{v})$, the same value we have in **Case 1**.

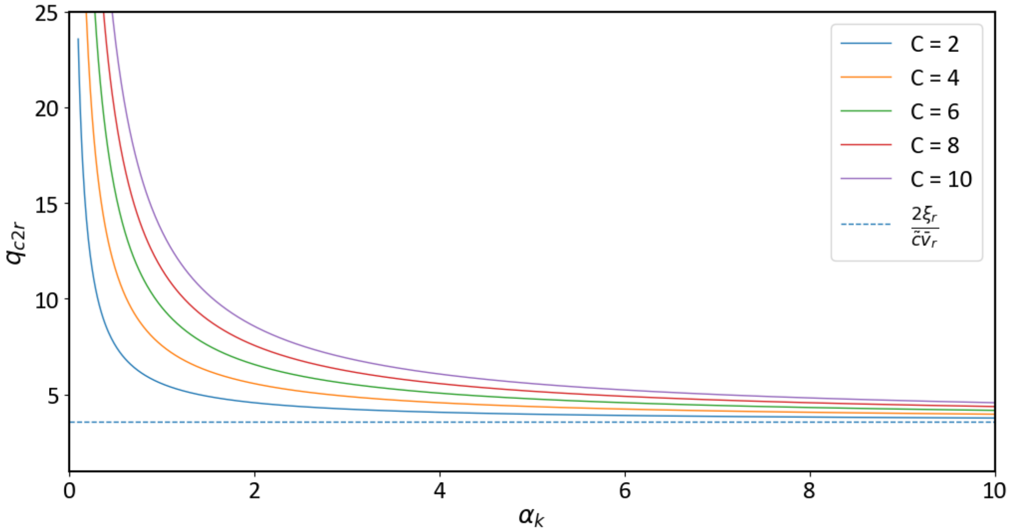

Figure 3.6: Value of q necessary to achieve a linear scaling regime in **Case 2**, as a function of loop size, α_k, for different values of C, in the radiation dominated era. ξ_r and $\bar{v}_r$ are the linear scaling values of the characteristic lengthscale and of the RMS velocity in the radiation dominated era.

3.2.2 Impact of Non-Loop Forming Intercommutations

Let us now see what the effects of varying the parameter C are in the linear kink density. Contrary to **Case 1**, the linear scaling condition is now dependent on the value of C. The linear scaling values of $\bar{v}$ and L are not, and, once again, we can assume that both these dynamical variables are in a linear scaling regime, and look for analytical solutions.

As may be seen from Eq. (3.41),

$$\frac{K_C}{K_2} = 1\,, \tag{3.43}$$

and therefore, the linear kink density has no dependence on the number of intercommutations that are needed to create a loop. However, since increasing C changes the value of q_c^2, this may cause K to no longer achieve scaling.

Let us now set C to be 2 and see if the same happens when we model the effect of non-loop forming intercommutations with the term in Eq. (3.8). When $\bar{v}$ and L are in linear scaling, Eq. (3.10) has the following analytical solution (once again, we assumed that the network was created at the time t_i with a linear kink density of K_i):

$$\bar{K}(t) = \left[K_i + \frac{\chi(\bar{v})}{\xi^2[(2-q\alpha_k)\tilde{c}\bar{v}/(\alpha_k\xi)+3]t_i}\right]\left(\frac{t}{t_i}\right)^{(2-q\alpha_k)\tilde{c}\bar{v}/(\alpha_k\xi)+2} - \frac{\chi(\bar{v})}{\xi^2[(2-q\alpha_k)\tilde{c}\bar{v}/(\alpha_k\xi)+3]}\frac{1}{t} \,. \tag{3.44}$$

The critical value of q is still given by Eq. (3.42), with $C = 2$, but note that Eq. (3.44) is not defined for $q = q_c^2$. Let us see what happens when q is either larger or smaller than its critical value:

1. $q > q_c^2$

   Let us consider some arbitrary value of $q = q_c^2 + \delta$, where $\delta > 0$. We then have that:

   $$\bar{K}(t) \longrightarrow \frac{\chi(\bar{v})}{\xi\tilde{c}\bar{v}\delta}\frac{1}{t} \Rightarrow l_k \longrightarrow \frac{\tilde{c}\bar{v}\delta}{\chi(\bar{v})}L \,. \tag{3.45}$$

   The small-scale structure lengthscale reaches a linear scaling regime and the mean inter-kink distance is determined by the characteristic lengthscale of the network. This is precisely what we have in **Case 1** and, if we compare the above equation with Eq. (3.23), we see that for $\tilde{c}\bar{v}/(\chi(\bar{v})) = \alpha/C$, we recover exactly the result in Eq.(3.8).

2. $q < q_c^2$

   Let us now consider some arbitrary value of $q = q_c^2 - \delta$, where $q_c^2 > \delta > 0$. We now have that:

   $$\bar{K}(t) = \frac{\chi(\bar{v})}{\tilde{c}\bar{v}\xi\delta t}\left[\left(\frac{t}{t_i}\right)^{\tilde{c}\bar{v}\delta/\xi-1} - 1\right] + K_i\left(\frac{t}{t_i}\right)^{\tilde{c}\bar{v}\delta/\xi} , \tag{3.46}$$

   and, therefore, the linear kink density will always increase with time, and it will never reach a linear scaling regime.

For the case where q is equal to its critical value, Eq. (3.10), has the following analytical solution when we set $q = q_c^2$:

$$\bar{K}_{critical}(t) = \frac{\chi(\bar{v})}{\xi^2 t}\log\left(\frac{t}{t_i}\right) + K_i t_i \,, \tag{3.47}$$

and therefore, the linear kink density does not reach a linear scaling regime in this case either.

It seems that modeling non-loop forming intercommutations by varying C or by adding an additional term and fixing $C = 2$ does not represent the same physical situation. While simply varying the value of C does not seem to cause a significant impact on the linear kink density, the presence of the term in Eq. (3.8) does, which indicates that in **Case 2**, this term is necessary. We will then keep it for the remaining of this chapter. It is also interesting to point out that including this term in **Case 2** makes it qualitatively (although not quantitatively) identical to **Case 1**, and both describe a very similar physical situation.

3.2.3 Impact of Kink Decay

Finally, let us add the effects of the kink decay mechanisms.

Considering once again that the network is in a linear scaling regime and that it is created at a time t_i, with $K(t_i) = K_i$, we have a differential equation with the same form as Eq. (3.28), which has the same solution, given by Eq. (3.30), but with the following redefinition of the constants:

$$M_1 \longrightarrow \frac{\chi(\bar{v})}{\xi^2} \tag{3.48}$$

$$M_2 \longrightarrow \frac{\tilde{c}\bar{v}(C-\alpha_k)}{\xi\alpha_k} - 2\beta(1-2\bar{v}^2) + 2 \tag{3.49}$$

The critical value of q is now given by:

$$\bar{q}_c^2 = \frac{C}{\alpha_k} + \frac{\xi}{\tilde{c}\bar{v}}[3 - 2\beta(1-2\bar{v}^2)] = \frac{C}{\alpha_k} + \bar{q}_c^1 \,, \tag{3.50}$$

where $\bar{q}_c^1$ is given by Eq. (3.31). So, if $C/\alpha_k \longrightarrow 0$, both **Case 1** and **Case 2** represent the same physical situation. Let us what happens for both q larger and smaller than $\bar{q}_c^2$:

1. $q > \bar{q}_c^2$

   Let us consider some arbitrary value of $q = \bar{q}_c^2 + \delta$, with $\delta > 0$. When $t \longrightarrow \infty$, we have that:

$$K(t) \longrightarrow \frac{\tilde{c}\bar{v}\delta}{2\xi\hat{\Gamma}G\mu t}\left[\sqrt{\frac{4\hat{\Gamma}G\mu\chi(\bar{v})\xi}{\tilde{c}^2\bar{v}^2\delta^2}+1}-1\right] \approx \frac{\chi(\bar{v})}{\tilde{c}\bar{v}\delta\xi t} \,, \tag{3.51}$$

   if $4\hat{\Gamma}G\mu\chi(\bar{v})\xi/(\tilde{c}^2\bar{v}^2\delta^2) \ll 1$, which is true provided that δ is not extremely small. Therefore, in the linear scaling regime, the mean inter-kink distance is determined by the characteristic lengthscale:

$$l_k \approx \frac{\tilde{c}\bar{v}\delta}{\chi(\bar{v})} L \,, \tag{3.52}$$

   which is, qualitatively, same behavior found in **Case 1**, when considering kink decay but neglecting the term in Eq. (3.8).

2. $q < \bar{q}_c^2$

   Let us now consider some arbitrary value of $q = \bar{q}_c^2 - \delta$, with $\bar{q}_c^2 > \delta > 0$. We know have that, as $t \longrightarrow \infty$:

$$K(t) \longrightarrow \frac{\tilde{c}\bar{v}\delta}{2\xi\hat{\Gamma}G\mu t}\left[\sqrt{\frac{4\hat{\Gamma}G\mu\chi(\bar{v})\xi}{\tilde{c}^2\bar{v}^2\delta^2}+1}+1\right] \approx \frac{\tilde{c}\bar{v}\delta}{\hat{\Gamma}G\mu\xi t}\,, \tag{3.53}$$

   if, once again, we consider $4\hat{\Gamma}G\mu\chi(\bar{v})\xi/(\tilde{c}^2\bar{v}^2\delta^2) \ll 1$, and the mean inter-kink distance is now determined by the characteristic lengthscale of the gravitational backreaction:

$$l_k \approx \frac{1}{\delta\tilde{c}\bar{v}}\hat{\Gamma}G\mu L\,, \tag{3.54}$$

   which is exactly the same result found in **Case 1**.

Similar to the previous case, when $q = \bar{q}_c^2$, the evolution of K is given by Eq. (3.35), but with the constant M_1 given by Eq. (3.48).

Finally, let us study what happens when the Universe enters an era dominated by Λ, characterized by $\bar{v} \longrightarrow 0$ and $L \propto a$. In this limit, Eq. (3.14) turns into Eq. (3.37), and, therefore, as found in **Case 1**, as soon as the cosmological constant starts dominating the energy density of the Universe, the only decay mechanism that is relevant is the gravitational backreaction and K will enter a linear scaling regime characterized by a high density of kinks.

Solving now Eq. (3.14) alongside Eqs. (1.24), (2.21) and (2.20), we can see how the linear kink density evolves in a realistic background. The plot in Fig. 3.7 shows the evolution of $\zeta = Kt$, for $q = \bar{q}_{cr}^2$, $q < \bar{q}_{cr}^2$, $\bar{q}_{cm}^2 < q < \bar{q}_{cr}^2$ and $q > \bar{q}_{cm}^2$, where $\bar{q}_{cr}^2$ and q_{cm}^2 are the critical values of q in the radiation and in the matter dominated eras, respectively. We observe, as expected, a behavior that is similar to that found in **Case 1**: when $q < \bar{q}_{cr}^2$, the linear scaling regime is determined by the gravitational backreaction, whereas for $\bar{q}_{cm}^2 < q < \bar{q}_{cr}^2$ and for $q > \bar{q}_{cm}^2$ it is the loop production that assures scaling. Soon after the radiation-matter transition, K starts approaching values close to $\hat{\Gamma}G\mu$ in the former case, but has a growth considerably smaller in the latter, because there is still a linear scaling regime determined by the characteristic lengthscale during the matter era. When $q = \bar{q}_{cr}^1$, K never reaches a linear scaling regime. In all cases, when the energy density of the Universe starts being dominated by a cosmological constant, the linear kink density starts again approaching the new linear scaling regime described in the previous paragraph.

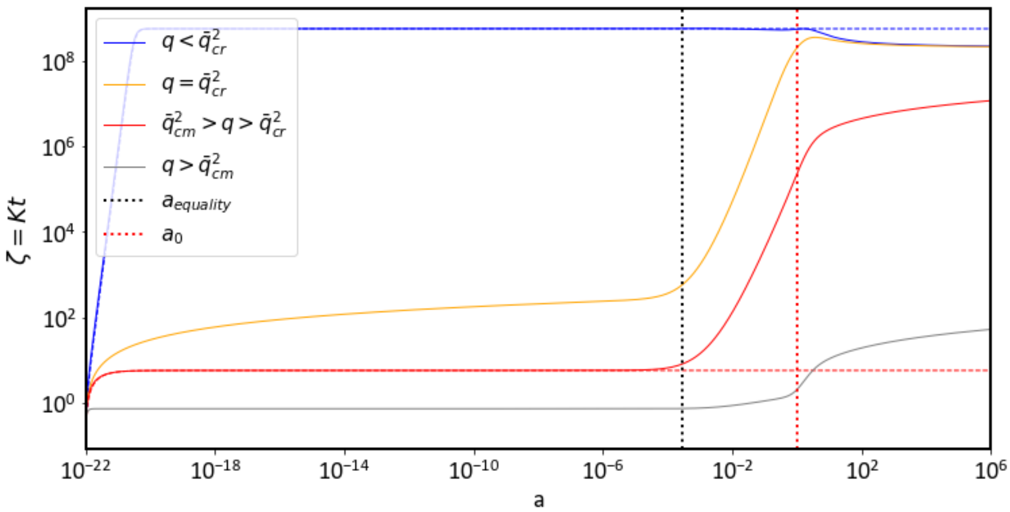

Figure 3.7: **Case 2**: Evolution of the linear kink density, $K = \zeta/t$, in a ΛCDM Universe for $q < \bar{q}^1_{cr}$, $q = \bar{q}^1_{cr}$, $\bar{q}^1_{cm} > q > \bar{q}^1_{cr}$ and for $q > \bar{q}^1_{cm}$, where $\bar{q}^1_{cr}$ and $\bar{q}^1_{cm}$ correspond to the critical value of q in the radiation and in the matter dominated eras, respectively (solid lines). Dashed lines represent the analytical solutions for the first three situations (i.e., for $\beta = 1/2$). Solid and dashed lines match in the radiation dominated era when K reaches scaling. Parameters used: $C = 2$, $\alpha_k = 2$, $\hat{\Gamma} = 50$ and $G\mu = 10^{-10}$. Ω_{i0}, where $i = r, m, \Lambda$ are given by Eqs. (1.25) - (1.27).

Finally, let us once again evaluate the effects of the Hubble expansion on the characteristic lengthscale of small-scale structure. Considering all the above conclusions, one would expect to once again find a similar behavior to **Case 1**. The plot in Fig. 3.8 shows a comparison of the values of K, in a ΛCDM Universe, when both decay mechanisms are present and when only the gravitational backreaction is considered. We can see that, in fact, we observe the same behavior as in Fig. 3.5.

We can then conclude that **Case 2**, with an additional term modeling the effects of non-loop forming intercommutations, is qualitatively identical to **Case 1**. In fact, one may see that:

$$\ell = \alpha_k l_k = \frac{\alpha_k}{K} = \alpha_k \frac{t}{\zeta} = \frac{\alpha_k}{\zeta \xi} L \, , \tag{3.55}$$

which shows that **Case 2** is nothing more than **Case 1**, but with a time-dependent α, equal to $\alpha(t) = \alpha_k/(\zeta\xi)$. In a linear scaling regime, both ζ and ξ are constants, and, therefore, there is no need to study these two cases separately.

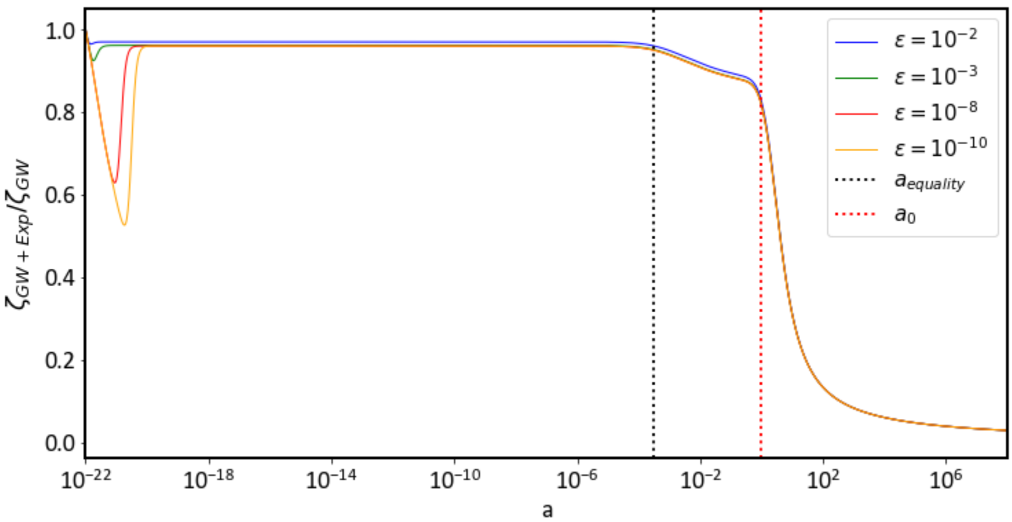

Figure 3.8: **Case 2**: Comparison between the evolution of the linear kink density when both kink decay to GWs and due to Hubble stretching are present, ζ_{GW+Exp} and its evolution when the only mechanism of kink decay considered is the gravitational backreaction, ζ_{GW}, where $\zeta = Kt$, in a ΛCDM Universe. Parameters used: $C = 2$, $\alpha_k = 2$, $q = 1$, $\hat{\Gamma} = 50$. Ω_{i0}, where $i = r, m, \Lambda$ are given by Eqs. (1.25) - (1.27).

3.3. Summary

In this chapter, we adapted and extended analytical models existing in the literature to characterize the evolution of the linear kink density, to describe the evolution in a realistic cosmological background. We studied the impact of loop production, non-loop forming intercommutations, gravitational backreaction and Hubble expansion on the evolution of the small-scale structure lengthscale, to understand which of these physical processes are relevant to accurately describe the small-scale structure lengthscale.

Two possible cases were considered for the physical length with which a loop is formed: **Case 1**, where loops are formed with a size that is a fixed fraction of the characteristic lengthscale, $\ell = \alpha L$; and **Case 2**, where loops are formed with a size that is a fixed fraction of the mean inter-kink distance, $\ell = \alpha_k l_k$.

We began by ignoring the mechanisms of kink decay, and studied the possibility of the small-scale structure lenghtscale achieving a linear scaling regime when only loops remove kinks from the network. We considered that loop production could be more likely in regions with a larger density of small-scale structure, therefore making them carry away more kinks when detaching from the network. We modeled this effect by introducing the parameter q, which characterizes the relative "kinkiness" between the loop and the long string. We observed that the mean inter-kink distance only achieved a linear scaling regime provided that loops are kinky enough and carry away enough kinks to compensate for the kinks that are created in the loop production process and for the impact of the change of the characteristic lengthscale (i.e., if $q > q_{c1}$, given by Eq. (3.21) in **Case 1**). In **Case 2**, the achievement of a linear scaling regime is more difficult, as the number of kinks removed is fixed, thus q has to be exactly equal to the critical value.

The impact of non-loop forming intercommutations on the kink number density was studied in two different ways: by varying the parameter C, which parameterizes how many intercommutations are necessary to form a loop and by fixing $C = 2$ (i.e., fixing the number of intercommutations needed to form a loop to 1) and introducing the term in Eq. (3.8). We observed, that for **Case 1**, the impact of these intercommutations can be modeled by setting $C \sim 4$, without the need to introduce this additional term, while in **Case 2**, varying C has no effect on the evolution of K, but, the term in Eq. (3.8) has, so, we cannot ignore this additional term. Interestingly, however, adding this term makes **Case 2** qualitatively similar to **Case 1**, as it ensures that scaling can be reached for all values of q larger than a critical value.

Finally, we studied the impact of the kink decay mechanisms. We began by including both the gravitational backreaction and the Hubble expansion, and afterwards, verified if the Hubble expansion had a non-negligible effect. We observed, in **Case 1**, that the small-scale structure lengthscale only achieved a linear scaling regime if q was either higher or lower than its critical value, given by Eq. (3.31): when $q > \bar{q}_c^1$, the scaling value of the mean inter-kink density is determined by the physical length of loops, while for $q < \bar{q}_c^1$ is determined by the characteristic lengthscale of the gravitational backreaction. We also observed that once the cosmological constant starts to become relevant to the evolution of the Universe, the linear kink density starts growing towards values of order $\hat{\Gamma} G\mu$. In fact, during this stage, the only decay mechanism that remains relevant is the gravitational backreaction and the characteristic lengthscale of small-scale structure enters a linear scaling regime characterized by a high density of kinks. We studied the importance of Hubble stretching as a decay mechanism, and verified that for values of string tension lower than 10^{-7}, it cannot be neglected, as it has a considerable impact on the evolution of the linear kink density.

Regarding **Case 2**, we found that, keeping the non-loop forming intercommutation term makes it represent the same physical situation as **Case 1** (with different constants), and, therefore, we found the same behaviors for the situations described above. Additionally, we also found that it simply corresponds to having a time-dependent α in **Case 1**: $\alpha(t) = \alpha_k/(\zeta\xi)$. Since in a linear scaling regime, both ζ and ξ are constants, both cases represent the same physical situation.

With all the above considerations in mind, we conclude that we can discard **Case 2**, and model the evolution of the linear kink density effectively, with the following equation:

$$\frac{d}{dt}[KL^{-2}] = [C - q\ell K]\frac{dn_{loop}}{dt} - \hat{\Gamma}G\mu K^2 L^{-2} - 2H(1-2\bar{v}^2)KL^{-2}\,, \tag{3.56}$$

where dn_{loop}/dt is given by Eq. (3.15).

4. Impact of Small-Scale Structure on Cosmic String Network Evolution

So far, we have only studied how the evolution of the long string network affects the linear kink density. However, to provide an accurate description of a cosmic string network with small-scale structure, we must also study the impact of the presence of kinks on the large scale dynamics of the string network as well (which will, as a consequence, also impact the linear kink density). When deriving the VOS equations in Chapter 2, we pointed out two import aspects to take into consideration: that friction forces are relevant early on in the history of the Universe, and that the network loses energy when a loop detaches. A third aspect surges now: the network will also lose energy density when kinks decay by emitting GWs, at a rate given by [23, 36, 37]:

$$\left(\frac{d\rho}{dt}\right)_{kinks} = -\Gamma G\mu\rho K \,. \tag{4.1}$$

Eq. (2.20) then gets an additional term describing the impact of kink decay on the characteristic lengthscale, becoming:

$$\frac{dL}{dt} = (1+\bar{v}^2)HL + \frac{1}{2}\tilde{c}\bar{v} + \frac{1}{2}\Gamma G\mu K L \,, \tag{4.2}$$

and this equation, alongside Eqs. (2.21) and (3.56), provides a description of the cosmological evolution of a cosmic string network with small-scale structure.

We will begin this chapter by studying under which conditions the network can now achieve a linear scaling regime. We concluded, at the end of the previous chapter, that **Case 1** and **Case 2** represent the same physical situations, and, therefore, we only need to consider the first one from this point forward. However, we will not drop **Case 2** for now, for reasons that will soon become apparent.

We will end this chapter by comparing the predictions of the VOS Model with our new Modified VOS Model, to study the impact of the presence of small-scale structure on the cosmological evolution of a cosmic string network .

4.1. Linear Scaling Regimes

Let us then study the conditions necessary for a cosmic string network with small-scale structure to achieve a linear scaling regime. We have verified numerically that there are now two possible linear scaling regimes: a *full linear scaling regime*, where all three dynamical variables reach scaling; a *partial linear scaling regime*, where the small-scale structure lengthscale reaches scaling, but $\bar{v}$ and L do not.

4.1.1 Full Linear Scaling Regime

Starting with the case where the network reaches a full linear scaling regime, let us assume that the expansion of the Universe is governed by the power law in Eq. (1.28), and look for linear scaling solutions of the form:

$$\bar{v} = \text{constant} \quad , \quad L = \xi t \quad \text{and} \quad K = \frac{\zeta}{t} \, , \tag{4.3}$$

with ξ and ζ constants. Only when all these conditions are met, one may say that the network is in a *complete linear scaling regime*. Introducing these expressions into Eqs. (2.19) and (4.2), we obtain the following linear scaling solutions for the RMS velocity and the characteristic lengthscale:

$$\bar{v} = \sqrt{\frac{k(\bar{v})(1-\beta-\frac{1}{2}\Gamma G\mu\zeta)}{\beta[k(\bar{v})+\tilde{c}]}} \tag{4.4}$$

$$\text{and} \quad \xi = \sqrt{\frac{k(\bar{v})[k(\bar{v})+\tilde{c}]}{4\beta(1-\beta-\frac{1}{2}\Gamma G\mu\zeta)}} \, . \tag{4.5}$$

Imposing that $\xi^2 > 0$ (or, equivalently, $\bar{v}^2 > 0$), we obtain the following restriction for the values that ζ can take:

$$\zeta < \frac{2(1-\beta)}{\Gamma G\mu} \, . \tag{4.6}$$

Let us now find the linear scaling solution for ζ for both **Case 1** and **Case 2**.

Introducing Eq. (4.2) into Eq. (3.56), and considering that $\ell = \alpha L$, we obtain the following evolution equation for the linear kink density:

$$\frac{dK}{dt} = \frac{C\tilde{c}\bar{v}}{\alpha L^2} + \tilde{c}(1-q)\frac{K\bar{v}}{L} + 6HK\bar{v}^2 - \hat{\Gamma}' G\mu K^2 \, , \tag{4.7}$$

where $\hat{\Gamma}' = (\hat{C}-1)\Gamma = \hat{\Gamma} - \Gamma$.

Substituting the linear scaling solution for K into this equation, we obtain a rather complicated equation, that cannot be solve analytically.

However, if we now consider **Case 2** and assume that loops are created with a physical length equal to $\ell = \alpha_k l_k$, the evolution equation for K becomes:

$$fracdKdt = \left[\frac{C}{\alpha_k} - q + 1\right]\frac{\tilde{c}\bar{v}K}{L} + 6\bar{v}^2 HK - \hat{\Gamma}' G\mu K^2 \, , \tag{4.8}$$

where once again, $\hat{\Gamma}' = (\hat{C}-1)\Gamma$.

Substituting the third expression in Eq. (4.3) into Eq (4.8), we find the following linear scaling solution for ζ:

$$\zeta = \frac{1}{\Gamma G\mu}\frac{2D(1-\beta)+B}{D+(\hat{C}-1)B}\,, \tag{4.9}$$

where $D = A\tilde{c} + 3k(\bar{v})$, $B = [k(\bar{v}) + \tilde{c}]$ and $A = C/\alpha_k - q + 1$*.

If we now once more impose that ζ must be such that $\xi^2 > 0$, we obtain the following condition that $\hat{C}$ must satisfy to assure complete scaling of the cosmic string network:

$$\hat{C} > \frac{1}{2(1-\beta)} + 1 \tag{4.10}$$

which means that $\hat{C} > 2$ in the radiation era and $\hat{C} > 2.5$ in the matter era. Note that since $\hat{C} - 1 > 0$ for $\beta < 1$, ζ is always well defined. For lower values of $\hat{C}$, the gravitational backreaction cannot remove enough kinks from the network to assure scaling, and Hubble stretching on its own is not enough to do so. Also, let us point out that this condition is independent of q.

This is the reason why we decided not to drop **Case 2** right away. Although both cases represent the same physical situation in a linear scaling regime, the way that **Case 2** is formulated allows us to obtain analytical conditions for linear scaling. From this point forward, we will always assume that loops are formed with a physical length equal to $\ell = \alpha L$, as described by **Case 1**.

If q is large enough so that Eq. (4.9) becomes negative, the condition in Eq. (4.10) no longer needs to be respected for the network to achieve a linear scaling regime. In fact, in such case, the network will always achieve linear scaling, and such regime is now maintained by loop production, and not by the gravitational backreaction. This is exactly the behavior that we found in the previous chapter. If q is smaller than some critical value, q_c, loop production alone cannot guarantee scaling, and gravitational backreaction is necessary to assure it. It is then the characteristic lengthscale of gravitational backreaction that determines l_k in this case. If, on the other hand, q is larger than its critical value, gravitational backreaction is no longer needed for the network to reach linear scaling, and this regime is sustained solely by loop production, that is, if q is sufficiently large, the network can achieve a linear scaling regime, even for $\hat{C} = 1$, i.e. scaling is also possible when gravitational backreaction is not present as a decay mechanism. It is the physical length

*Besides the trivial solution, $\zeta = 0$, where the network has no small-scale structure and its dynamics can be described by the VOS Model.

of loops that now determines the characteristic lengthscale of small-scale structure. This critical value of q is not easily calculated analytically in this situation, unlike the previous Chapter. It is, however, highly dependent on $\hat{C}$: the smaller the efficiency of the gravitational backreaction, the largest q must be in order for loop production to assure linear scaling.

4.1.2 Partial Linear Scaling Regime

The *partial linear scaling regime* occurs when q is small, but $\hat{C}$ does not satisfy Eq. (4.10). In this regime, l_k may still reach linear scaling, but L and $\bar{v}$ do not. This regime is characterized by non-relativistic velocities, $\bar{v} \ll 1$, and so, we can rewrite Eqs. (2.21), (4.2) and (4.7) as follows:

$$\frac{d\bar{v}}{dt} \simeq 0 \Rightarrow \bar{v} \simeq \frac{k(\bar{v})}{2HL} \tag{4.11}$$

$$\frac{dL}{dt} \simeq HL + \frac{1}{2}\Gamma G\mu KL \tag{4.12}$$

$$\frac{dK}{dt} \simeq -(\hat{C}-1)\Gamma G\mu K^2 \,. \tag{4.13}$$

This system of equations admits solutions of the form $L \propto a^{\eta}$, $\bar{v} \propto a^{1/\beta-\eta}$ and $K = \zeta/t$, with

$$\zeta = \frac{1}{(\hat{C}-1)\Gamma G\mu}\,, \tag{4.14}$$

and

$$\eta = 1 + [2\beta(\hat{C}-1)]^{-1} > 0 \,. \tag{4.15}$$

Note that the scaling value of ζ is, in this case, independent of β. The characteristic lengthscale will increase with time, at a rate that is dependent of β, and, since:

$$\frac{1}{\beta} - \eta = -\left(1 + \frac{1-\beta}{\beta(\hat{C}-1)}\right) < 0\,, \tag{4.16}$$

for $\beta < 1$, the RMS velocity will decrease with time. Finally, let us also note that, in this non-relativistic partial linear scaling regime, the number of kinks per string does not remain constant over time:

$$N = KL \propto a^{\eta-1/\beta}\,, \tag{4.17}$$

i.e., it will increase with time. N is only constant when the network is in a full linear scaling regime, described by Eq. (4.3).

4.2. Evolution of a Cosmic String Network With Small-Scale Structure

We can now finally solve Eqs. (2.19), (4.2) and (4.7) numerically, alongside the Friedmann Equation, and see how a cosmic string network with small-scale structure evolves in a ΛCDM Universe. In this section, we shall study how the different parameters — q, $\hat{C}$, $G\mu$, α and C — affect the evolution of the network.

4.2.1 Impact of the Relative "Kinkiness" and of the Gravitational Backreaction

First, let us see how the relative "kinkiness", that is, q, and the gravitational backreaction efficiency, i.e., $\hat{C}$, impact the evolution of the cosmic string network.

The plots in Fig. 4.1 show the evolution of the RMS velocity, of the characteristic lengthscale and of the linear kink density, in a ΛCDM Universe, for small q, that is, in the case where gravitational backreaction is the mechanism that assures linear scaling. We observe both linear scaling regimes mentioned in the previous section: for $\hat{C} < 2$, $\bar{v}$ and L do not reach linear scaling but, the small-scale structure lengthscale does, with a linear scaling value independent of β, i.e., the linear scaling value of ζ remains constant over time, and is given by Eq. (4.14); for $\hat{C} > 2$, there is an initial rapid build-up of small-scale structure, causing an increase in the linear kink density and a decrease in the RMS velocity, comparative to the predictions of the VOS Model. Eventually, gravitational backreaction is able to compensate the rate of kink creation, and the network enters in a full linear scaling regime during the radiation dominated era, given by Eq. (4.3). Once again, it never reaches scaling during the matter dominated era when $\hat{C} > 2.5$, since this epoch does not last long enough, and soon the cosmological constant begins dominating the energy density of the Universe. Regarding the characteristic lengthscale of the network, it would be expected for it to be larger than the one predicted by the VOS Model, since we are now considering that the network does not only lose energy density when loops are removed, but also when kinks decay due to the gravitational backreaction, which is exactly what we observe in Fig. 4.1.

In Fig. 4.2 we can see the evolution of all three dynamical variables of the Modified VOS Model in the case where q is large enough for loop production to assure linear scaling. As expected, we can see that, even for $\hat{C} < 2$, the network always reaches a full linear linear scaling regime in the radiation era.

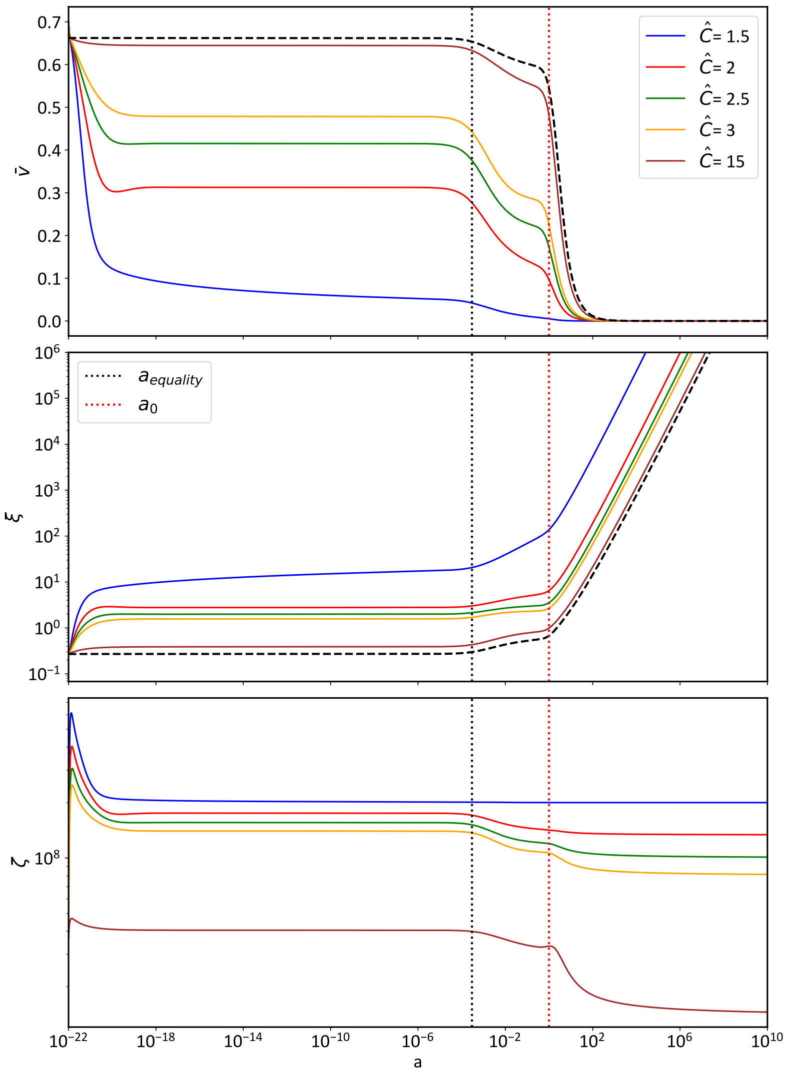

Figure 4.1: Evolution of $\bar{v}$ (top panel), $\xi = L/t$ (middle panel) and $\zeta = Kt$ (bottom panel) in a ΛCDM Universe for $q = 1 < q_c$. Full linear scaling occurs in the radiation dominated era for $\hat{C} > 2$. The blue line represents the situation where the network is in a partial linear scaling regime. The black dashed line in the top and middle panel represents the evolution of the RMS velocity and of the characteristic lengthscale, respectively, as predicted by the VOS Model. We observe that, by increasing $\hat{C}$, we approach the VOS solution. Parameters used: $\alpha = \hat{C}\Gamma G\mu$, $C = 4$ and $\Gamma G\mu = 50 \times 10^{-10}$.

We also verify that increasing $\hat{C}$, i.e., increasing the efficiency of the gravitational backreaction — in both the cases where q is small or large — causes the network to reach a linear scaling regime faster, with a lower scaling value for ζ, comparative to the case where the gravitational backreaction is weaker (as it would be expected). Since instantaneous emissions will always be proportional to K^2, and since increasing $\hat{C}$ causes kinks to decay faster, strings will collide less, causing the network to lose less energy density. Therefore, in the full linear scaling regime, less energy density will be lost due to kink decay by the network, resulting in a lower characteristic lengthscale. Also, both the RMS

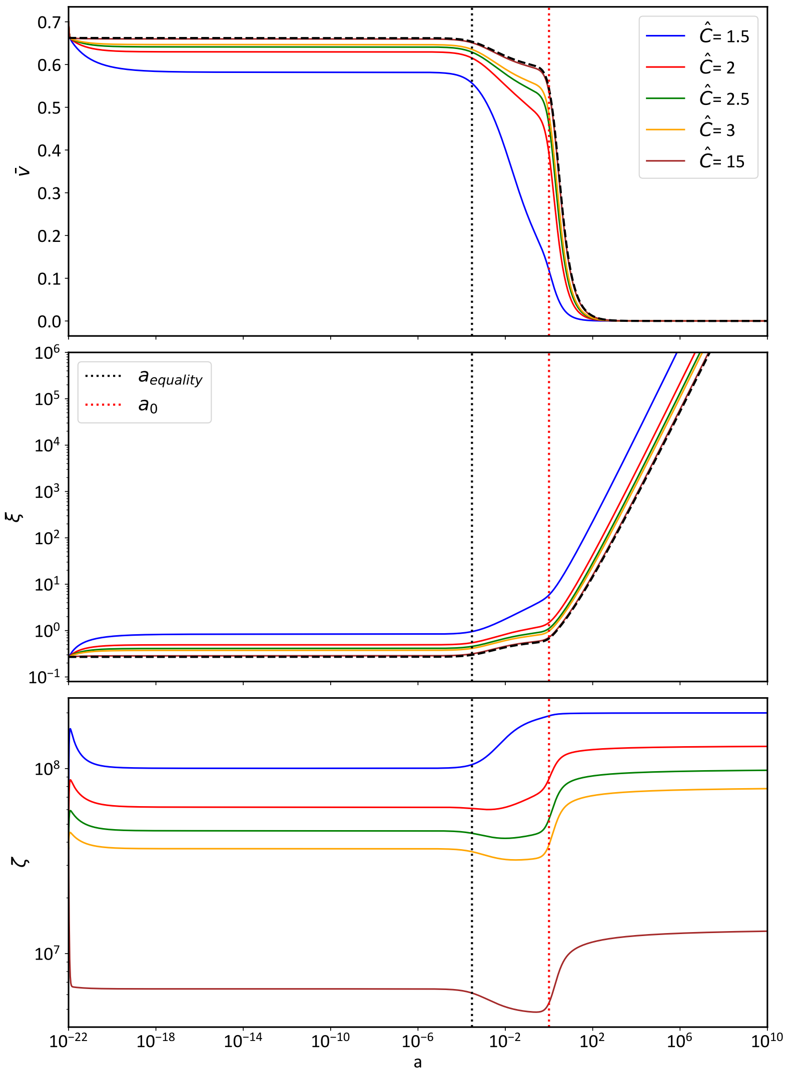

Figure 4.2: Evolution of $\bar{v}$ (top panel), $\xi = L/t$ (middle panel) and $\zeta = Kt$ (bottom panel) in a ΛCDM Universe for $q = 20 > q_c$. All three dynamical variables now reach a full linear scaling regime, for all values of $\hat{C}$. The black dashed line in the top and middle panel represents the evolution of the RMS velocity and of the characteristic lengthscale, respectively, as predicted by the VOS Model. Parameters used: $\alpha = \hat{C}\Gamma G\mu$, $C = 4$ and $\Gamma G\mu = 50 \times 10^{-10}$.

velocity and the characteristic lengthscale start approaching the VOS solution as $\hat{C}$ increases, which happens quicker when q is large. The smallest the linear kink density, the better the dynamics of the network can be described by a model which assumes it to kinkless (as one would expect).

4.2.2 Impact of String Tension

Let us now verify what is the effect of varying the string's tension, $\epsilon = G\mu$, on the evolution of the cosmic string network. The plots in Fig. 4.3 show the evolution of $\bar{v}$, L and K, for different values of ϵ*, for large loops. We observe that varying the string tension has no effect on the linear scaling values of $\bar{v}$ and L, although higher tensions cause the network to reach them faster. Regarding the impact of this parameter on the linear kink density, as one would expect, higher values of ϵ lead to a lower linear kink density, as the network loses more kinks due to GWs emission. We have verified this exactly behavior for small-loops.

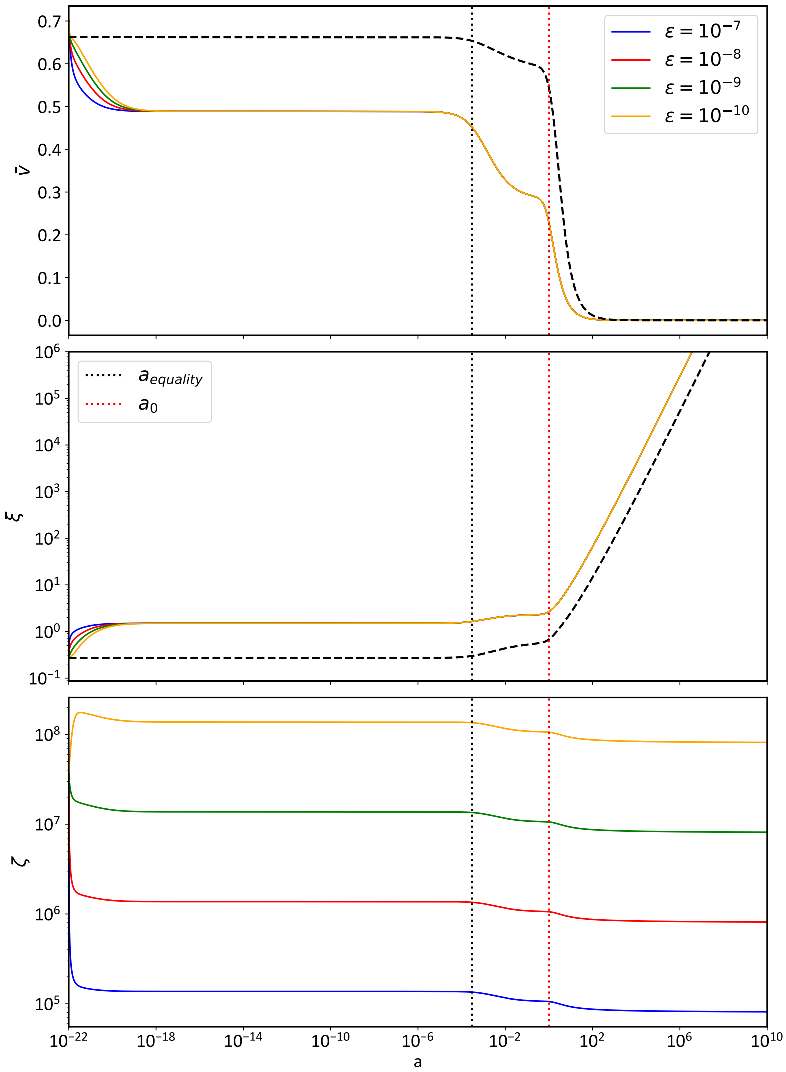

Figure 4.3: Evolution of $\bar{v}$ (top panel), $\xi = L/t$ (middle panel) and $\zeta = Kt$ (bottom panel), for different values of the string tension, $\epsilon = G\mu$. The black dashed lines represent the VOS solution for $\bar{v}$ and $\xi = L/t$ in the top and bottom panels, respectively. Parameters used: $\hat{C} = 3$, $q = 1$, $\alpha = 0.1$ and $\Gamma = 50$.

*We have only used values of $\epsilon \leq 10^{-7}$, because, as we have mentioned in Chapter 3, higher values of string tension have already been excluded observationally.

4.2.3 Impact of Loop Size

The plots in Fig. 4.4 show how the evolution of the network depends on loop size, i.e., on the parameter α. We verify that a loop's physical length starts having some impact on the evolution of the network when α starts approaching the gravitational backreaction scale, i.e., when α gets close to $\hat{C}\Gamma G\mu$. In that case, loops will remove less kinks, and so, the linear kink density is higher, comparative to what occurs when α is larger. Also, since that the loop production rate per unit volume, given by Eq. (3.15) is inversely proportional to α, there are more loops being produced in the small-loop regime, and so, the network loses more energy density due to loops detaching, and the characteristic lengthscale is larger.

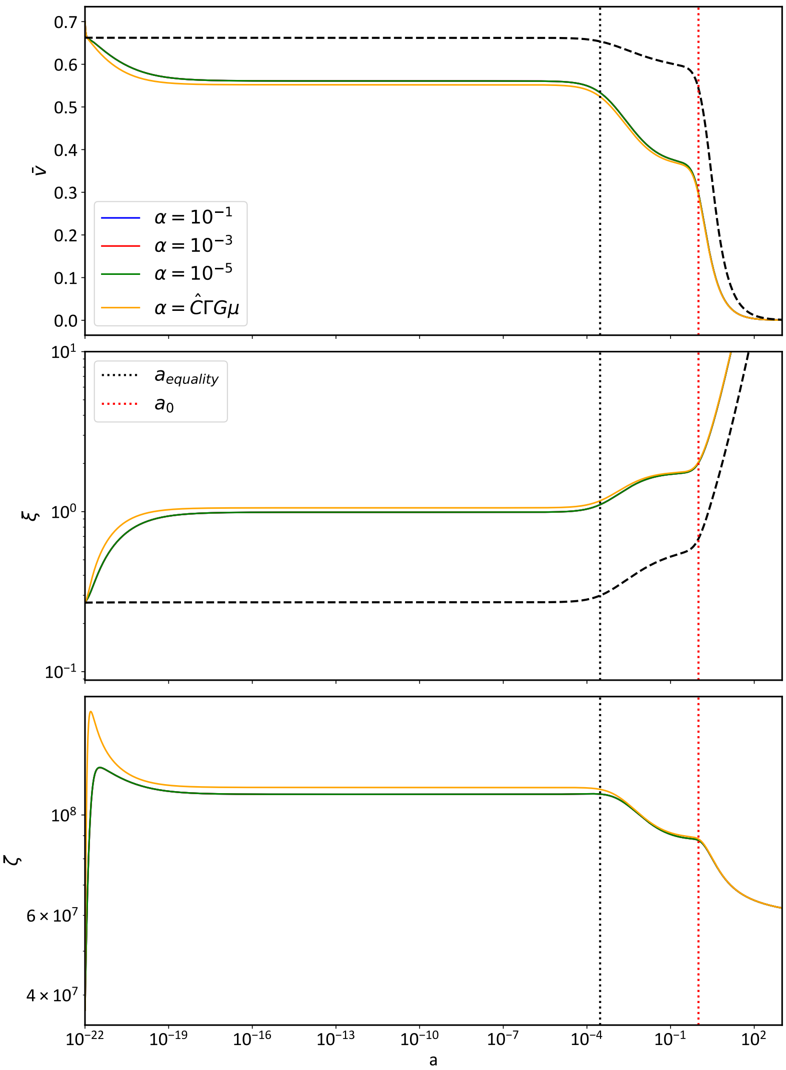

Figure 4.4: Evolution of $\bar{v}$ (top panel), $\xi = L/t$ (middle panel) and $\zeta = Kt$ (bottom panel), for different values of loop size, i.e., α. The black dashed lines represent the VOS solution for $\bar{v}$ and $\xi = L/t$ in the top and bottom panels, respectively. Parameters used: $\hat{C} = 4$, $C = 4$, $\Gamma G\mu = 50 \times 10^{-10}$ and $q = 1$.

4.2.4 Impact of Non-Loop Forming Intercommutations

In Chapter 3, we verified that the effect of non-loop forming intercommutations could be described by setting $C \sim 4$. Let us verify the validity of this statement now. The plots in Figs. 4.5 and 4.6 show the evolution, for large loops, of the RMS velocity, the characteristic lengthscale and of the linear kink density, for $C = 2$ and $C = 4$, for small and large q, respectively. We see that, when q is small, these extra intercommutations seem to have no impact on the evolution of the network. For large q, however, seems that the kinks added to the network due to these intercommutations lead to a slight increase in the linear kink density, but cause no impact on the RMS velocity and on the characteristic lengthscale.

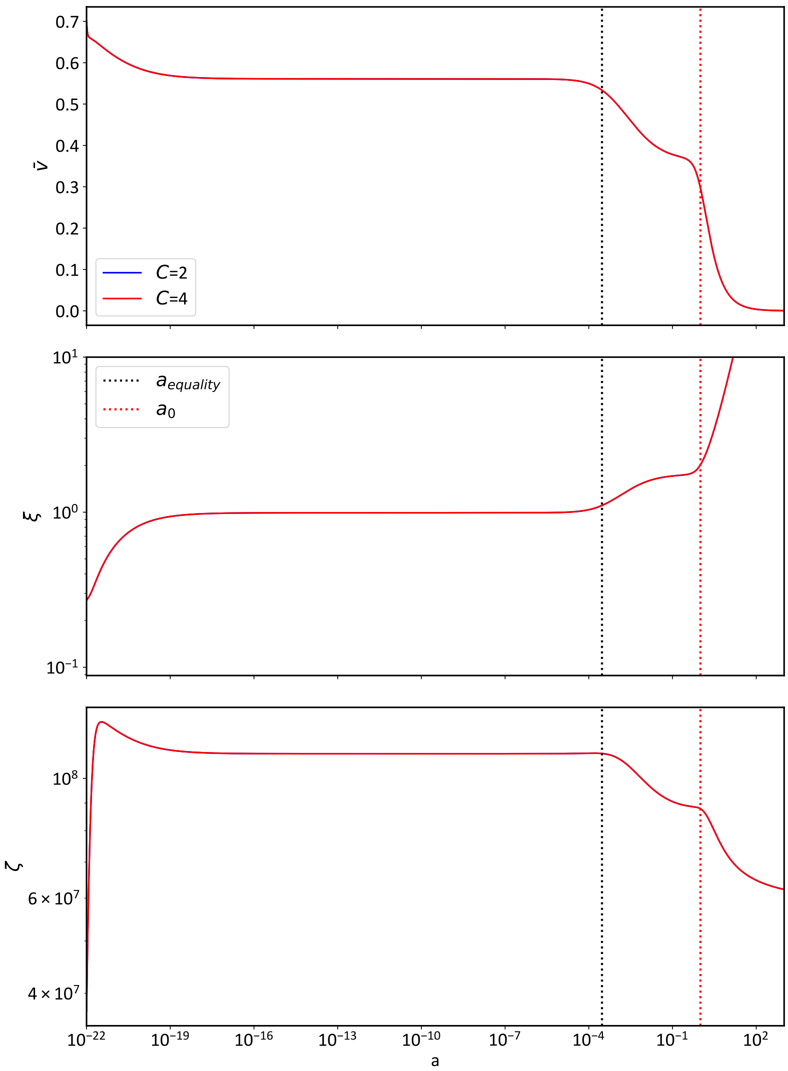

Figure 4.5: Evolution of $\bar{v}$ (top panel), $\xi = L/t$ (middle panel) and $\zeta = Kt$ (bottom panel), for $C = 2$, 4 and for small q. Parameters used: $\hat{C} = 4$, $\alpha = 0.1$, $\Gamma G\mu = 50 \times 10^{-10}$ and $q = 1$.

We have verified, however, that, for small-loops, setting $C = 2$ leads to an underestimation of the linear kink density, and therefore, to accurately describe this extra intercommutations, it is necessary for q to be 4.

Considering that the goal of this dissertation is to study the SGWB, we will, in the following chapters, be interested in the cases where gravitational backreaction is the most relevant decay mechanism, and therefore, we will always consider that q is small. Given that in the large-loop regime, the behavior of the network is independent of C being 2 or 4 for small q, and that in the small-loop regime there is a significant dependence on this parameter, we will keep the conclusions of Chapter 3, and keep $C = 4$ from this point forward.

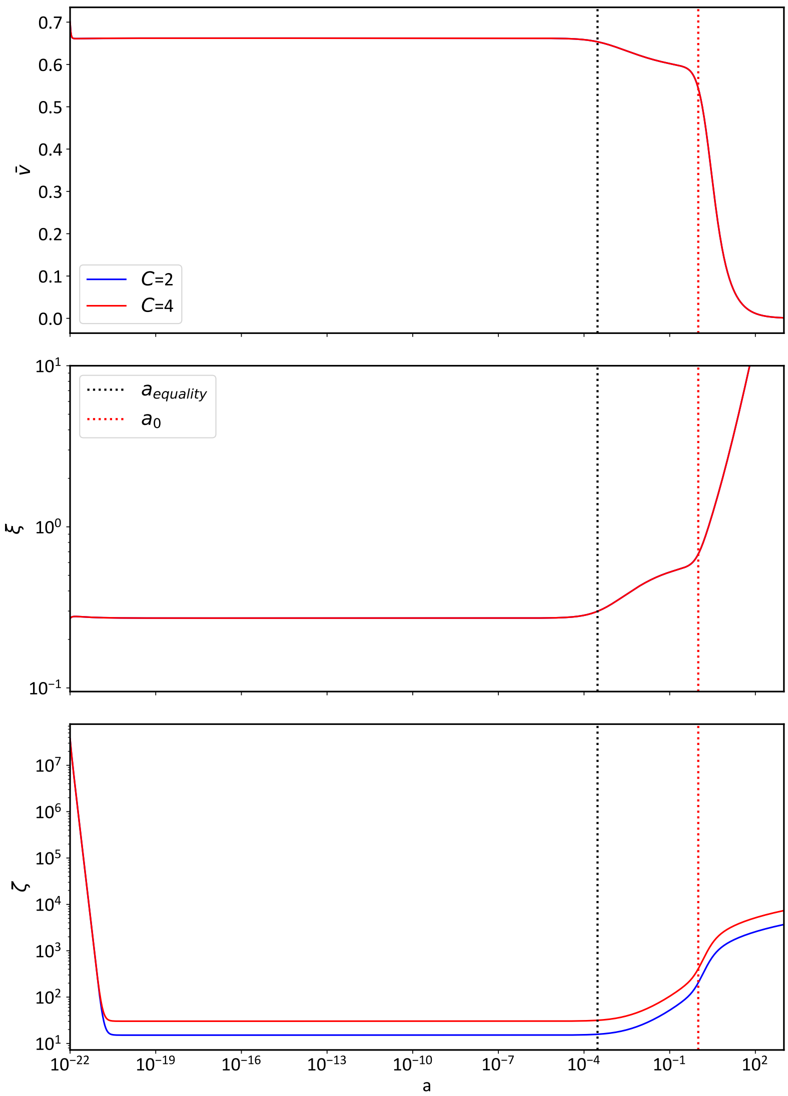

Figure 4.6: Evolution of $\bar{v}$ (top panel), $\xi = L/t$ (middle panel) and $\zeta = Kt$ (bottom panel), for $C = 2$, 4 and for large q. Parameters used: $\hat{C} = 4$, $\alpha = 0.1$, $\Gamma G\mu = 50 \times 10^{-10}$ and $q = 10$.

4.3. Comparison with Existent Models

We mentioned, in Chapter 2, that the Three-Scale Model [26] provided a fairly complete description of the evolution of a cosmic string network with small-scale structure, in a linear scaling regime (since $\bar{v}$ is taken to be constant). This model characterizes the network by three different lengthscales:

- The characteristic lengthscale, ξ, which corresponds to the VOS Model characteristic lengthscale, L;
- The persistence length, $\bar{\xi}$, which gives us roughly the distance below which points on a string are correlated;
- The mean-inter kink distance, ζ, which corresponds to l_k in our extended version of the VOS Model.

This model assumes, in general, that the RMS velocity remains constant and, therefore, does not include an equation for $\hat{v}$.

The plots in Fig. 4.7 show the evolution of all three lengthscales, published originally in Ref. [38]*. We can see that our lengthscales, L and l_k, behave in a similar manner to the correspondent lengthscales of the Three-Scale Model. The persistence length seems to have a very similar behavior to the characteristic lengthscale, therefore, not being strictly necessary. The Three-Scale Model, however, seems to predict a short-lasting transient linear scaling regime on the early stages of the network evolution, which we did not predict. However, for a high enough value of q, we have also verified a slower approach to the linear scaling regime. Finally, the observed differences between the plots in Fig. 4.7 and ours after the radiation-matter equality are explained by the fact that dark energy is not considered by the authors in [38]. So, what is the advantage of the Modified VOS Model compared to the already existent Three-Scale Model?

The Modified VOS Model describes the cosmic string network using only two characteristic lengthscales and 5 unspecified parameters, with very clear physical meanings† — $\tilde{c}$, α, q, $\hat{C}$ and $G\mu$ — only 4 more than the usual VOS Model, one of them being the string tension, which is a fundamental parameter that sets the energy scale. The Three-Scale

*This paper includes a plot for the evolution of the RMS velocity, but does not specify which equations were used to calculate it.

†Γ can also be considered an additional parameter, but it is usually considered to have the same value as for loops.

Model, however, makes use of three lengthscales and has 10 unspecified parameters — $\bar{\alpha}_{nl},\ F,\ \tilde{c},\ G\mu,\ \bar{G},\ \chi,\ \omega,\ I,\ \hat{C}$ and k —, which makes it much harder to understand from the physical point of view, and use, for example, in computations of the SGWB spectrum.

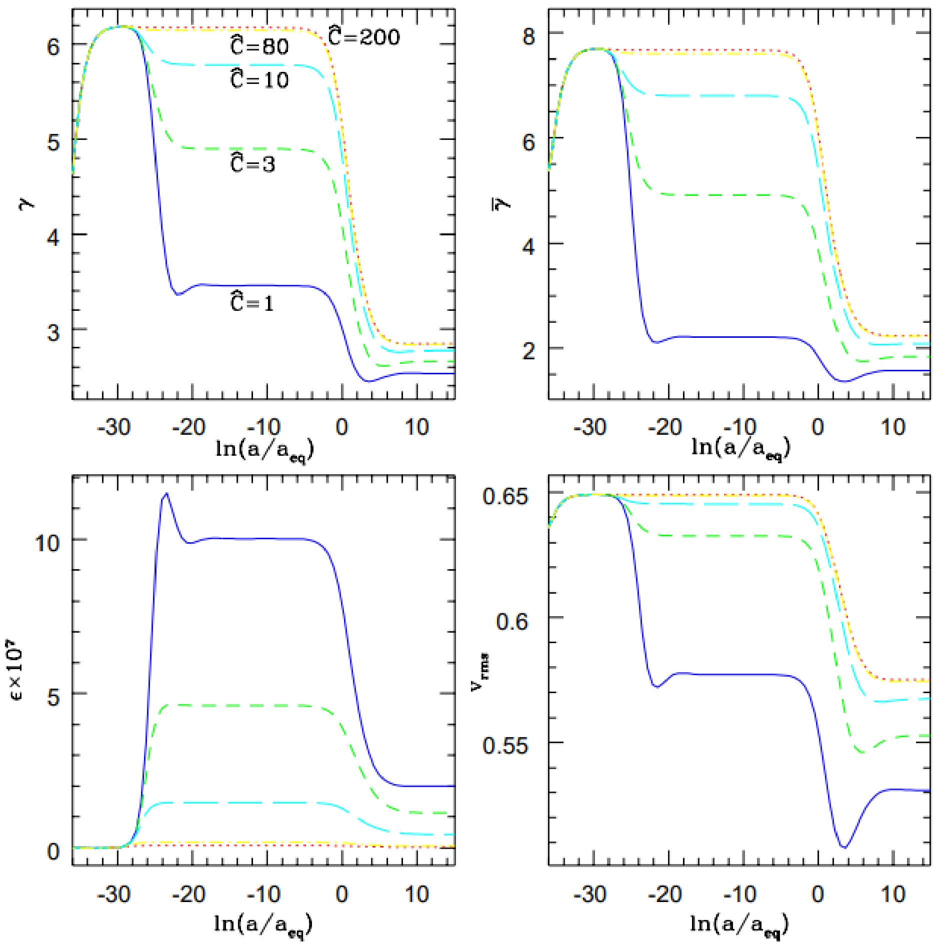

Figure 4.7: Evolution of the characteristic lengthscale $\xi = \gamma t$, the persistence lengthscale $\bar{\xi} = \bar{\gamma} t$ and of the mean inter-kink distance, $\zeta = \epsilon t$, as predicted by the Three-Scale Model, for different values of $\hat{C}$. Parameters used: $\Gamma G\mu = 10^{-8}$ and $\tilde{c} = 0.15$. This figure was originally published in [38].

In [39], the authors proposed that the VOS Model could describe the effects of the gravitational backreaction on the cosmic string network, by adding the following term to Eq. (2.20):

$$\left(\frac{dL}{dt}\right)_{GBR} = 2\Gamma G\mu \bar{v}^6 \ . \tag{4.18}$$

The plots in Fig. 4.8 show the evolution of the RMS velocity and of the characteristic lengthscale as predicted by the VOS Model with and without the additional term in Eq. (4.18), alongside the Modified VOS predictions. We can see that modeling the impact of gravitational backreaction with this term is not sufficient: only for very high values of string tension, completely excluded by observational data — $\epsilon = G\mu \sim 10^{-2}$ — does it have some kind of impact on the network (although very small). Otherwise, it is completely negligible, and does not provide an accurate description of the effects of the gravitational backreaction on the cosmic string network. This may be explained by the fact that this does not take into consideration the accumulation of small-scale structure on cosmic strings and how the gravitational wave emission depends on the number density of kinks.

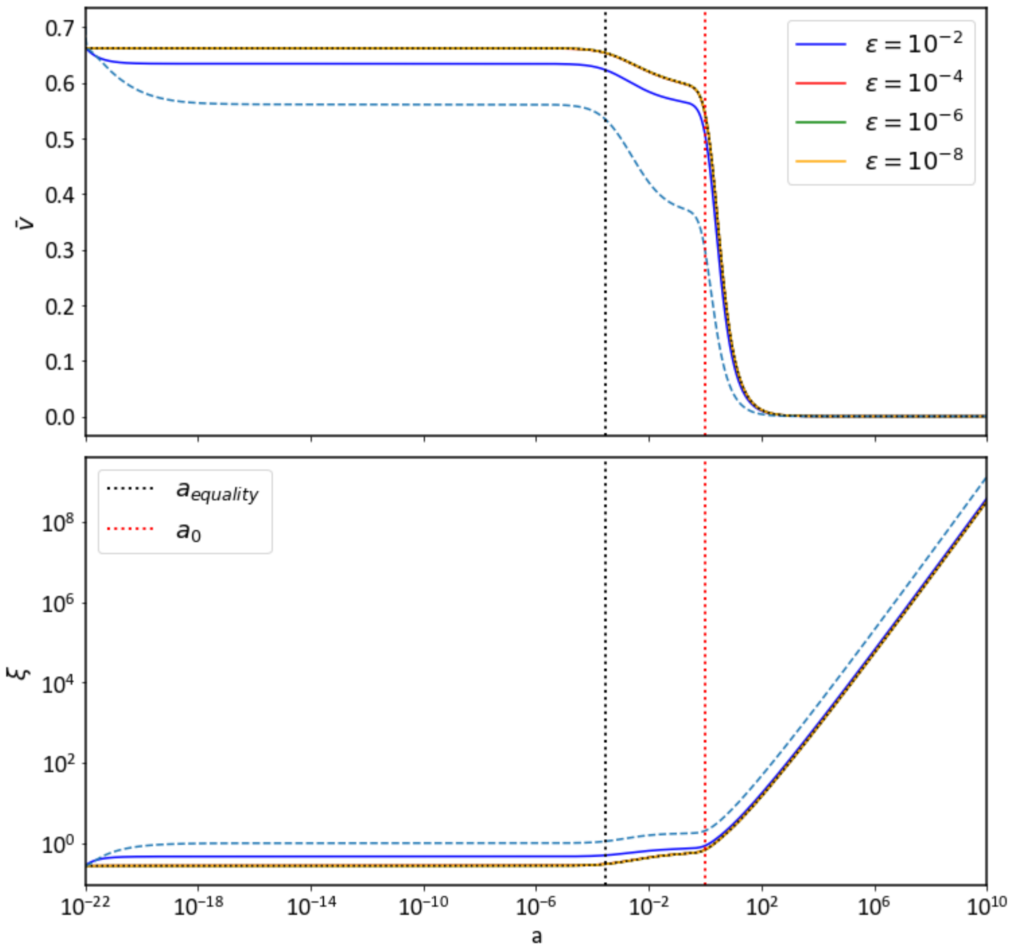

Figure 4.8: Evolution of $\bar{v}$ and $\xi = L/t$ for different values of the string tension, $\epsilon = G\mu$, as predicted by (solid lines) the VOS Model with the additional term in Eq. (4.18) . Blue dashed line represents the results obtained by the Modified VOS Model, with $\hat{C} = 3$ and $\Gamma G\mu = 50 \times 10^{-10}$. The black doted line represents the results obtained by the VOS Model. Solid lines match with the black doted line, for all values of ϵ except for $\epsilon = 10^{-2}$.

4.4. Summary

In this chapter, we studied how the presence of kinks affects the evolution of a cosmic string network, by extending the VOS Model to include an additional lengthscale describing small-scale structure. The resulting Modified VOS Model consists of the following three equations, which dictate the evolution of the RMS velocity ($\bar{v}$), the characteristic lengthscale (L) and the linear kink density (K), respectively:

$$\frac{d\bar{v}}{dt} = (1-\bar{v}^2)\left[\frac{k(\bar{v})}{L} - 2\bar{v}H\right] ,$$
$$\frac{dL}{dt} = (1+\bar{v}^2)HL + \frac{1}{2}\tilde{c}\bar{v} + \frac{1}{2}\Gamma G\mu KL ,$$
$$\frac{dK}{dt} = \frac{4\tilde{c}\bar{v}}{\alpha L^2} + \tilde{c}(1-q)\frac{K\bar{v}}{L} + 6HK\bar{v}^2 - \hat{\Gamma}' G\mu K^2 ,$$

where $\hat{\Gamma}' = (\hat{C}-1)\Gamma$. The Modified VOS Model provides an effective description of the evolution of a kinky cosmic string network in a ΛCDM Universe, predicting that the presence of small-scale structure causes the network to decelerate and the characteristic lengthscale to increase (or, in other words, makes the network significantly less dense). We expect that strings will then collide less often, due to the decrease in the velocity, and, as a consequence, fewer loops will be produced. Therefore, ignoring the presence of small-scale structure may lead to an overestimation of loop production, which can then lead to an overestimation of the amplitude of the SGWB they generate. We will verify this hypothesis in the next Chapter. We also expect that the network will be significantly more affected when loops are less kinky, i.e., when q is small, since in that case, l_k is determined by the characteristic lengthscale of the gravitational backreaction, which, in general, is much larger than L. In that case, the degree of efficiency of the gravitational backreaction in smoothing kinks is essential to determine how affected the network will be. When q is large enough, the effect will be, in general, smaller, and it is even possible for the network to reach full scaling without gravitational backreaction as a decay mechanism.

We saw in the previous chapter that **Case 1** and **Case 2** represent the same physical situation in a linear scaling regime, thus deciding to discard the last one. However, we verified in this chapter that **Case 2** allows us to determinate the linear scaling values of the dynamical variables analytically, and therefore we will use it in future calculations where those values might be necessary.

We have also concluded that setting $C = 4$ accurately describes the impact that non-loop intercommutations have on the linear kink density, in agreement with the previous chapter conclusions, and that the linear scaling values of $\bar{v}$ and L are independent of the string tension, $\epsilon = G\mu$ (although the network takes longer to achieve it for lower values of ϵ).

Finally, we compared our results with the ones from already existent models, and verified that our extended version of the VOS Model not only provides an accurate qualitative description of the cosmic string evolution, but has a lower number of unspecified parameters, making it fairly easy to understand.

5. Stochastic Gravitational Wave Background

Having developed the appropriate framework to characterize the evolution of a cosmic string network with small-scale structure, we are now finally able to study how the presence of kinks will affect loop production, and, as a consequence the SGWB generated by loops. We will additionally estimate the contribution of kinks to the spectrum.

The results of the previous chapter showed that the presence of small-scale structure causes the network to decelerate and become less dense. This leads us to think that strings will collide less, causing a decrease in loop formation. Therefore, we expect to also see a decrease in the amplitude of the spectrum of the SGWB generated by loops.

We will begin this chapter by reviewing the existent formalism to calculate the SGWB generated by loops [18, 40]. Afterwards, we will estimate the spectrum generated by kinks and, in the final section, we will compare the spectrum obtained when assuming that the cosmic string network dynamics is modeled by the VOS and by the Modified VOS Model. We will also study the validity of the existent analytical approximations for the SGWB generated by loops [32] when small-scale structure is included.

5.1. SGWB Generated by Loops

After formation, loops detach from the network, oscillate relativistically under their own tension, and decay, by emitting GWs. While doing so, they lose energy at a constant rate, given by:

$$\frac{dE_{loop}}{dt} = \Gamma G\mu^2 \, . \tag{5.1}$$

Results from several analytical studies and from recent numerical simulations show that $\Gamma \sim 50$ [41–44]. A loop's physical length will then decrease as GWs are emitted. Considering that a loop is created with a size ℓ_b, at the time of birth, t_b, its physical length will evolve in time as follows:

$$\ell(t) = \alpha L(t_b) - \Gamma G\mu(t - t_b) \, . \tag{5.2}$$

Loops emit GWs in a discrete set of frequencies, $f_j = 2j/\ell$, where ℓ is the physical length of the loop at the time of emission, and f_j is the frequency of the j-th harmonic mode. For now, let us assume that loops emit all their energy in a single harmonic mode, i.e., let us set $j = 1$.

The amplitude of the SGWB is usually quantified by the energy density in GWs, ρ_{GW}, per logarithmic frequency, in units of the critical density, ρ_c:

$$\Omega_{GW} = \frac{1}{\rho_c}\frac{d\rho_{GW}}{d\log(f)} , \tag{5.3}$$

where, for $j = 1$ [9]:

$$\frac{d\rho_{GW}}{dfdt} = 2\pi\left(\frac{a(t')}{a(t)}\right)^3 \times \Gamma G\mu^2 \int_0^\ell d\ell n(\ell, t') . \tag{5.4}$$

Here, $n(\ell, t')d\ell$ is the number density of cosmic string loops with lengths between ℓ and $\ell + d\ell$ at time t. In order for loops to emit – in harmonic mode j – GWs that have frequency f at the present time, at each instant t, they must have physical length equal to:

$$\ell_j(t) = \frac{2ja(t)}{fa_0} . \tag{5.5}$$

We therefore have that the amplitude of the SGWB at the present time, t_0, is given by:

$$\Omega^{j=1}_{GW}(f, \ell) = \frac{16\pi\Gamma(G\mu)^2}{3H_0^2 f}\int_{t_i}^{t_0} n(\ell_1(t'), t')\left(\frac{a(t')}{a_0}\right)^5 dt', \tag{5.6}$$

where t_i is the instant in time when loop production becomes significant. To account for the contributions of all the harmonic modes, we have that:

$$\Omega_{GW}(f, p, n_*) = \sum_j^\infty \frac{j^{-p+1}}{\varepsilon}\Omega^j_{GW}(f, \ell_j) , \tag{5.7}$$

where Ω^j_{GW} is the contribution of the j-th harmonic mode of emission to the SGWB, $\varepsilon = \Sigma_m^\infty m^{-p}$, and p is a constant dependent on the shape of the loop. If the emission is dominated by cusps (a point in which the string moves instantaneously at the speed of light), $p = 4/3$; if the emission is dominated by kinks, $p = 5/3$; if it is dominated by collisions between kinks, $p = 2$ [9]. It is also straightforward to show that [45]:

$$\Omega^j_{GM}(jf) = \Omega^1_{GW}(f) , \tag{5.8}$$

and, therefore, it is possible to construct Ω^j_{Gw} for any harmonic mode, once Ω^1_{GW} is computed.

5.1.1 Loop Number Density

The most important step to compute the SGWB spectrum is then to characterize the loop number density, $n(\ell, t)$, at all times, since GWs are emitted throughout the network history. The loop number density can be inferred from numerical simulations [46, 47] or calculated analytically. The first analytical approach to compute $n(\ell, t)$ was proposed by Kibble, in [48] and was later extended by [49–52]. Since we would like to study analytical approximations to the spectrum, and simulations do not include the effect of the gravitational backreaction, we will compute $n(\ell, t)$ semi-analytically, following the approach in [52]. At a given time instant, t, the number density of loops with physical length ℓ, $n(\ell(t), t)$, will have contributions from all preexisting loops with size $\ell(t)$ at time t. We therefore need to find the time, t_b, when such loops were created, since, as we have seen, one may infer the number of loops that are produced from the evolution of the network. Considering that loops are diluted away due to the background expansion, we then have that:

$$n(\ell_j(t'), t') = \sum_i n(\ell_j(t_b^i), t_b^i) \left(\frac{a(t_b^i}{a(t')} \right)^3 , \tag{5.9}$$

where t_b^i are the times of birth of the contributing loops to the loop number density, and:

$$n(\ell_j(t_b^i), t_b^i) = \frac{dn_{loop}}{dt}\Big|_{t=t_b^i} \frac{dt}{d\ell}\Big|_{t=t_b^i} , \tag{5.10}$$

where dn_{loop}/dt is given by Eq. (3.15) and $dt/d\ell$ can be calculated using Eq. (5.2). We then have that:

$$n(\ell_j(t'), t') = \sum_i \frac{1}{\alpha \frac{dL}{dt}\Big|_{t=t_b^i} + \Gamma\epsilon} \frac{\tilde{c}\bar{v}(t_b^i)}{\alpha L^4(t_b^i)} \left(\frac{a(t_b^i)}{a(t')} \right)^3 . \tag{5.11}$$

Loop size at birth will always increase with time, and, therefore, the first frequency each loop created at a time t will emit (i.e., the frequency that corresponds to the physical length at the time of birth ℓ_b) will always be the smallest frequency emitted until that instant. There won't be any emissions from any preexisting loops with that frequency, only from loops that will be created posteriorly can contribute to the SGWB in that range. So, we, in general, may drop the summation over i in Eq. (5.11) in a ΛCDM background. In other words, if a loop has a size αL at the time of its creation, it will radiate, at the present time, GWs with frequencies*:

$$f \geq f_{min} = \frac{2j}{\alpha L} \frac{a(t)}{a_0} . \tag{5.12}$$

The first contribution to a given frequency, f, corresponds to the instant in which there are loops created with $f_{min} = f$, and all the following loops will also contribute to that frequency (see Fig. 5.1).

*Eq. (5.12) shows that f_{min} also has a dependence on the scale factor, a. However, in a ΛCDM Universe, the characteristic lengthscale, L grows faster than a.

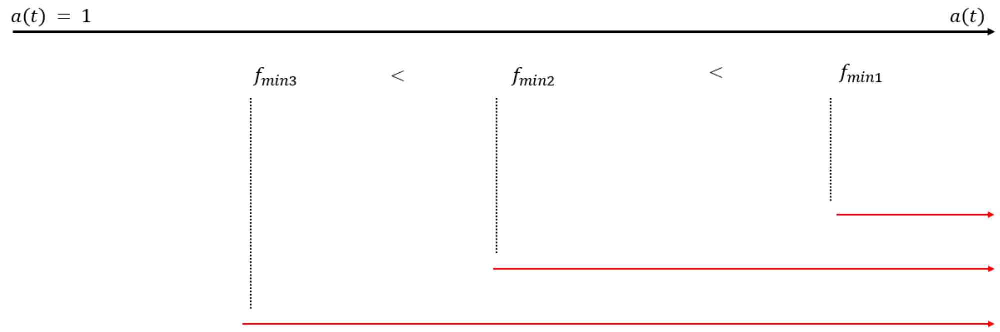

Figure 5.1: Contribution of loops to a given frequency. The first loop to be formed, ℓ_1 is the smallest loop possible. The first frequency it will emit, f_{min1} is the smallest frequency ever emitted at that time. That loop will emit all frequencies $f > f_{min1}$. All the subsequent loops will be formed with increasingly larger physical lengths, and, therefore, their minimum emitted frequency will decrease. Therefore, a loop formed with a size $\ell_2 > \ell_1$, will radiate GWs with frequencies $f > f_{min2}$ and therefore, also larger than f_{min1}.

5.1.2 Small-Loop Regime

In [40], the authors developed an alternative way to compute the spectrum of the SGWB in the small-loop regime, characterized by $\alpha \ll \Gamma G\mu$. In the small-loop regime, loops live less than a Hubble time, t_H, defined in Eq. (1.6), therefore radiating their energy in the form of GWs effectively immediately after being formed. Once again, this energy is not radiated in a single frequency, but the frequency will increase as the loop size decreases, instead. However, in this case this occurs instantaneously in the cosmological timescale. The energy density per frequency per time is given by:

$$\frac{d\rho_{GW}}{dtdf} = \left(\frac{d\rho}{dt}\right)_{loops} p(f) \left(\frac{a(t)}{a_0}\right)^4 , \tag{5.13}$$

where $(d\rho/dt)_{loops}$ is given by Eq. (2.8) and $p(f)$ is the probability distribution function that describes the power radiated by small-loops over different frequencies, and is given by:

$$p(f) \equiv \frac{dE}{df} = p(\ell) \left|\frac{d\ell}{df}\right| \Theta(f - f_{min}) = \frac{f_{min}}{f^2} \Theta(f - f_{min}) , \tag{5.14}$$

and $p(\ell) = dE/d\ell$. Inserting Eq. (5.13) into Eq. (5.3), we have that the SGWB spectrum for a given harmonic mode, j, can be computed as:

$$\Omega^j_{GW} = \frac{16 j \pi G}{3H_0^2} \int_{t_{min}}^{t_0} \left(\frac{d\rho}{dt}\right)_{loops} \frac{a(t)^5}{\alpha f L(t)} dt , \tag{5.15}$$

where t_{min} is the time of creation of loops that have $f_{min} = f$. The full spectrum can be once again obtained by introducing this expression into Eq. (5.7).

5.1.3 Analytical Approximations to the Spectrum

Numerical computations of the spectrum can sometimes be quite slow. It is useful to develop analytical approximations that accurately describe the spectrum to, for instance, enable faster analysis of GW data. This can be done by assuming that the dynamics of the Universe is governed by the power law in Eq. (1.28), so that the cosmic string network is in a linear scaling regime, with $L = \xi_i t$ and $\bar{v} = \bar{v}_i$, with $i = r, m$ for $\beta = 1/2\ ,\ 2/3$ during the radiation and matter eras, respectively. We will follow the work in [32], where the authors developed an analytical approximation for the SGWB, both in the large and small-loop regime.

In a linear scaling regime, we can rewrite Eq. (5.11) as:

$$n(\ell, t) = \frac{A_\beta C_\beta(\alpha)}{t^{3\beta}(\ell + \Gamma G\mu t)^{4-3\beta}}\ , \tag{5.16}$$

with:

$$A_\beta = \frac{\tilde{c}\bar{v}_\beta}{\xi_\beta^3}\ , \tag{5.17}$$

and

$$C_\beta(\alpha) = \frac{(\alpha\xi_\beta + \Gamma G\mu)^{3(\beta-1)}}{\alpha\xi_\beta}\ , \tag{5.18}$$

and Eq. (5.12) as:

$$f \geq f_{min} = \frac{2}{\alpha\xi_\beta t_b}\frac{a(t_b)}{a_0}\ . \tag{5.19}$$

Considering the contributions of loops that are formed in the radiation dominated era and of loops that are formed in the matter dominated era separately, we can solve the integral in Eq. (5.6).

Radiation Dominated Era

For the contributions of the loops produced in the radiation dominated era, we must consider two possible situations: loops that decay during the radiation era, and loops that are created in the radiation era but also decay in the matter era. For the first case, we can obtain the loop number density by simply replacing β with $1/2$ in Eq. (5.16). For the second case, the number density of loops in the matter era that were produced in the radiation era will result from the dilution and decay of the loops that existed at the time of the radiation-matter equality [53]. We therefore have:

$$n_r(\ell,t) = \frac{A_r C_r(\alpha)}{t^{3/2}(\ell+\Gamma G\mu t)^{5/2}} \tag{5.20}$$

$$n_{rm}(\ell,t) = \frac{A_r C_r(\alpha)(2H_0\sqrt{\Omega_r})^{3/2}}{(\ell+\Gamma G\mu t)^{5/2}}\left(\frac{a_0}{a(t)}\right)^3 , \tag{5.21}$$

where $n_r(\ell,t)$ and $n_{rm}(\ell,t)$ are the loop number densities of loops that are created and decay in the radiation dominated era and of loops that are created in the radiation dominated era but that decay in the matter era, respectively.

The dynamics of a radiation dominated Universe is governed by:

$$H = \frac{1}{a}\frac{da}{dt} = H_0\sqrt{\Omega_{ro}}a^{-2} . \tag{5.22}$$

The first loops that contribute to the spectrum are the ones created after*:

$$a^r_{min} = \frac{4H_0\sqrt{\Omega_{r0}}}{\alpha\xi_r f} , \tag{5.23}$$

with $f = f_{min}(t_{min})$. To account for the contributions of the loops that are formed and that decay in the radiation era, we have to consider the time interval [a^r_{min}, a_{eq}]. For the loops that will only decay during the matter era. For the loops that will only decay in the matter era, we must consider [a_{eq},, a_{max}], where a_{max} is the time of decay of the last loops created in the radiation era. Since that, for large enough loops, $a_{max} = a_0$, this value is usually taken in this approximation. When loops are small, this contribution is negligible and should not be included in this approximation [32].

Matter Dominated Era

In the matter dominated era, Eq. (5.16) can be rewritten as:

$$n_m(\ell,t) = \frac{A_m C_m(\alpha)}{t^{1/2}(\ell+\Gamma G\mu t)^2} . \tag{5.24}$$

The dynamics of a matter dominated Universe is governed by:

$$H = \frac{1}{a}\frac{da}{dt} = H_0\sqrt{\Omega_{mo}}a^{-3/2} , \tag{5.25}$$

*Actually, since our approximation assumes scaling, it is only valid when the loop production reaches a linear scaling regime, i.e., when for a given instant t, there are loops in all stages of life, and the lower limit should actually be: $a_{min} = (2H_0\sqrt{\Omega_{r0}(\epsilon_r+1)t_p l})^{1/2}/(G\mu)$, where $\epsilon_r = \alpha\xi_r/(\Gamma G\mu)$ and $t_{pl} = \sqrt{G}$ is Planck time [54].

and so, the first loops that will contribute to the spectrum are formed after:

$$a^m_{min} = \sqrt{\frac{3H_0\Omega_{m0}^{1/2}}{\alpha\xi_m f}} \, . \tag{5.26}$$

Total Spectrum

The total spectrum is then given by:

$$\bar{\Omega}_{GW} = \bar{\Omega}^r_{GW} + \bar{\Omega}^{rm}_{GW} + \bar{\Omega}^m_{GW} \, , \tag{5.27}$$

where:

$$\bar{\Omega}^r_{GM} = \frac{128}{9}\pi A_r\Omega_r\frac{G\mu}{\epsilon_r}\left[\left(\frac{f(1+\epsilon_r)}{Br\Omega_m/\Omega_r+f}\right)^{3/2} - \left(\frac{f(\epsilon_r+1)}{B_i+f}\right)^{3/2}\right] \, , \tag{5.28}$$

with $\epsilon_r = \alpha\xi_r/(\Gamma G\mu)$, $B_r = 4H_0\sqrt{\Omega_r}/(\Gamma G\mu)$ and $B_i = 2[2H_0\sqrt{\Omega_r}/(t_{pl}(\epsilon_r+1))]^{1/2}/\Gamma$,

$$\bar{\Omega}^{rm}_{GW} = 32\sqrt{3}\pi(\Omega_r\Omega_m)^{3/4}H_0\frac{A_r(\epsilon_r+1)^{3/2}}{\Gamma f^{1/2}\epsilon_r}\left\{\frac{(\Omega_m/\Omega_r)^{1/4}}{(B_m(\Omega_m/\Omega_r)^{1/2}+f)^{1/2}}\times\right.$$

$$\left.\left[2+\frac{f}{B_m(\Omega_m/\Omega_r)^{1/2}+f}-\frac{2+f/(B_m+f)}{(B_m+f)^{1/2}}\right]\right\} \, , \tag{5.29}$$

where $B_m = 3H_0\sqrt{\Omega_m}/(\Gamma G\mu)$, and

$$\begin{aligned}\bar{\Omega}^m_{GM} = {} & 54\pi H_0\Omega_m^{3/2}\frac{A_m(\epsilon_m+1)B_m}{\Gamma\epsilon_m f}\times \\ & \left\{\frac{2B_m+f}{B_m(B_m+f)} - \frac{2\epsilon_m+1}{f\epsilon_m(\epsilon_m+1)} + \frac{2}{f}\log\left(\frac{B_m(\epsilon_m+1)}{\epsilon_m(B_m+f)}\right)\right\} \, ,\end{aligned} \tag{5.30}$$

where $\epsilon_m = \alpha\xi_m/(\Gamma G\mu)$.

Small-Loop Regime

In the small-loop regime, since loops decay almost immediately after formation, we can use the above approximation and simply ignore the term $\bar{\Omega}^{rm}$ in Eq. (5.27). However, as we have seen in the previous section, the fact that small-loops decay almost immediately after formation allows for a simplification in how the spectrum is calculated, therefore also leading to a simplified expression of the analytical approximation [32]:

$$\bar{\Omega}_{small-loops}(f) = \frac{64\pi G\mu\Omega_r}{3}A_r + 54\pi\frac{H_0\Omega_m^{3/2}}{\epsilon_m\Gamma}\frac{A_m}{f}\left[1 - \frac{B_m}{\epsilon_m f}\right] \, . \tag{5.31}$$

5.1.4 Impact of Small-Scale Structure on the SGWB Generated by Loops

We are now finally able to study the impact that the presence of small-scale structure has on the SGWB generated by loops. We will consider the following to situations, that have been discusses in Chapter 4: the network reaches a full linear scaling regime, i.e., all three dynamical variables reach scaling; the network reaches a partial linear scaling regime, that is, only the small-scale structure lengthscale, l_k achieves scaling. We will also take $q = 1$, as we are interested, as mentioned at the beginning of this Chapter, in the case where the impact of the presence of small-scale structure is the highest.

Full Linear Scaling Regime

Let us start by considering that the network reaches a full linear scaling regime. The plots in Fig. 5.2 show the spectrum of the SGWB generated by large and small-loops, as predicted by the VOS and the Modified VOS Model, calculated both numerically and by using the analytical approximations developed in the previous section (but using the scaling values of $\bar{v}$ and ξ obtained with the Modified VOS), for different values of $\hat{C}$ (larger than 2.5, to assure full scaling both in the radiation and in the matter dominated eras). This spectrum is characterized by a high frequency plateau, which corresponds to the contributions of loops produced in the radiation dominated era, – as we would expect, since the analytical approximations mentioned in the previous section show that the SGWB spectrum during the radiation era is independent of f – followed by a peak in the lower frequencies.

It seems that our initial expectation was correct: ignoring the presence of kinks on the long string network does in fact leads to an overestimation of loop production, and, therefore, to an overestimation of the spectrum's amplitude, which gets more significant for smaller values of $\hat{C}$, i.e., when the gravitational backreaction is weaker, and so the linear kink density is higher. We also observe that, as we increase $\hat{C}$, the amplitude of the spectrum starts approaching the VOS solution: the gravitational backreaction is more efficient in removing kinks, leading to a lower linear kink density. The shape of the spectrum, however, is not significantly affected.

In Fig. 5.3, we can see the ratio between the radiation era plateau predicted by the VOS Model and the Modified VOS Model for different loop sizes. We see that the impact of kinks

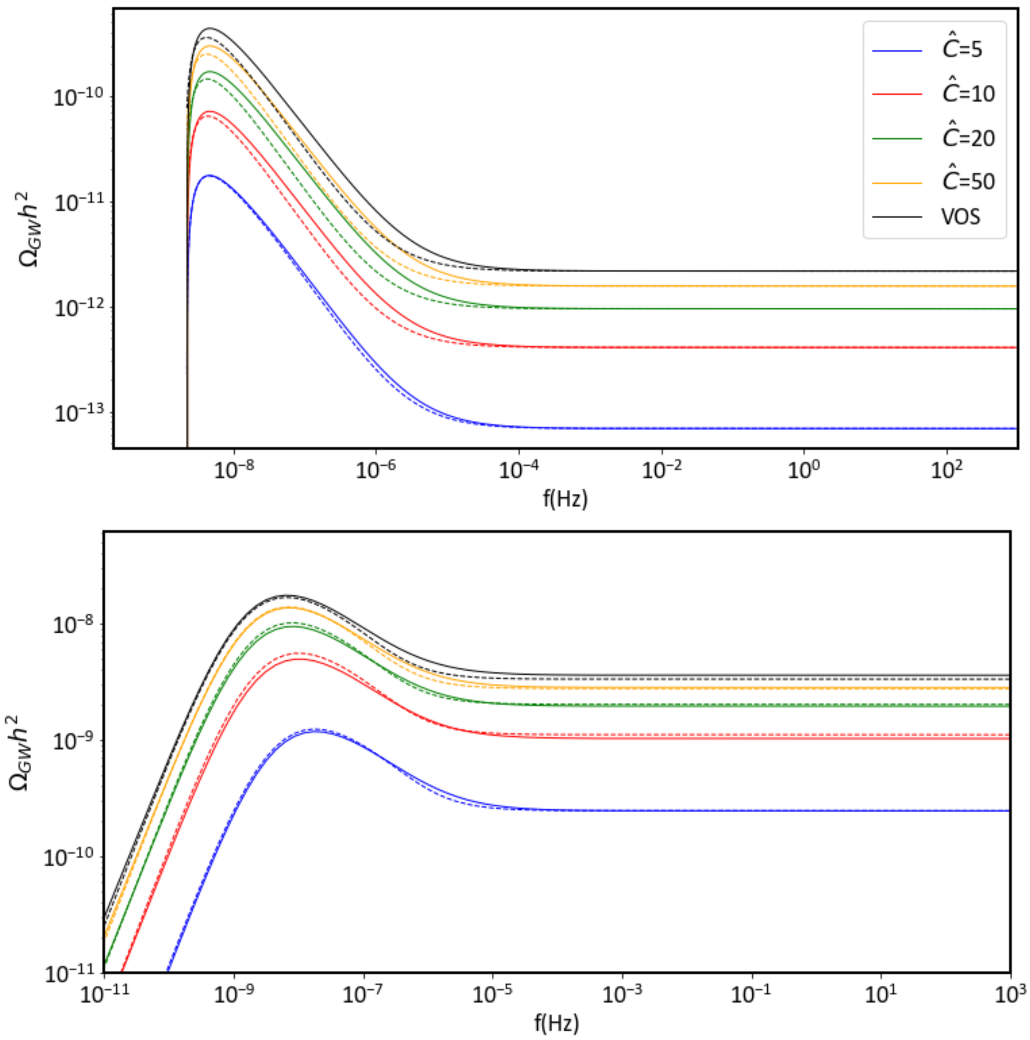

Figure 5.2: SGWB generated by small loops (upper panel) and large loops (lower panel), as predicted by the VOS Model (black line) and the Modified VOS Model (colored lines), for different values of the gravitational backreaction efficiency parameter, $\hat{C}$. Solid lines represent the spectrum obtained numerically and dashed lines represent the analytical approximations. Dashed and solid lines coincide in the radiation dominated era. Parameters used: $\Gamma = 50$, $G\mu = 10^{-10}$ and $\alpha = 0.1$ for the large loop spectrum and $\alpha = \hat{C}\Gamma G\mu$ for the small loop spectrum.

on the spectrum's amplitude is more significant in the small-loop regime: in this regime, there are more loops being formed, which, as a consequence, leads to a higher linear kink density, and, therefore, the network will also lose more energy due to the emission of GWs.

The plot in Fig. 5.4 shows the dependence of the spectrum on the string tension, $\epsilon = G\mu$. We observe that, as it would be expected, the more efficient the gravitational backreaction, the higher the amplitude of the spectrum generated by loops, since the network is less kinky. The ratio between the plateau predicted by the VOS Model, and the plateau predicted by the Modified VOS Model, is however, independent of ϵ. We found the same

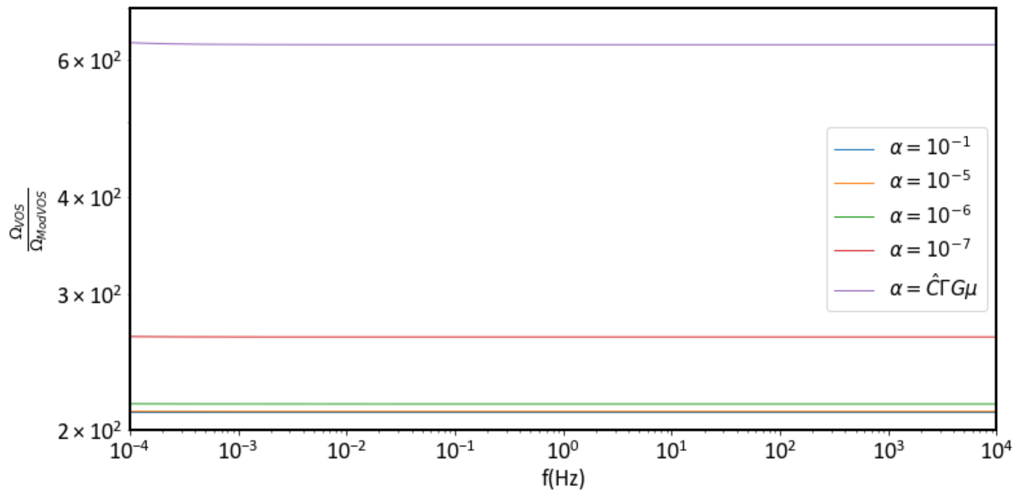

Figure 5.3: Ratio between the radiation era plateau predicted by the VOS Model and the Modified VOS Model, for different values of α. Parameters used: $\Gamma = 50$, $G\mu = 10^{-10}$, and $\hat{C} = 2.5$

behavior in the large loop regime, which matches the results of the previous chapter, where we verified that varying the string tension, had a similar effect on both small and large-loops.

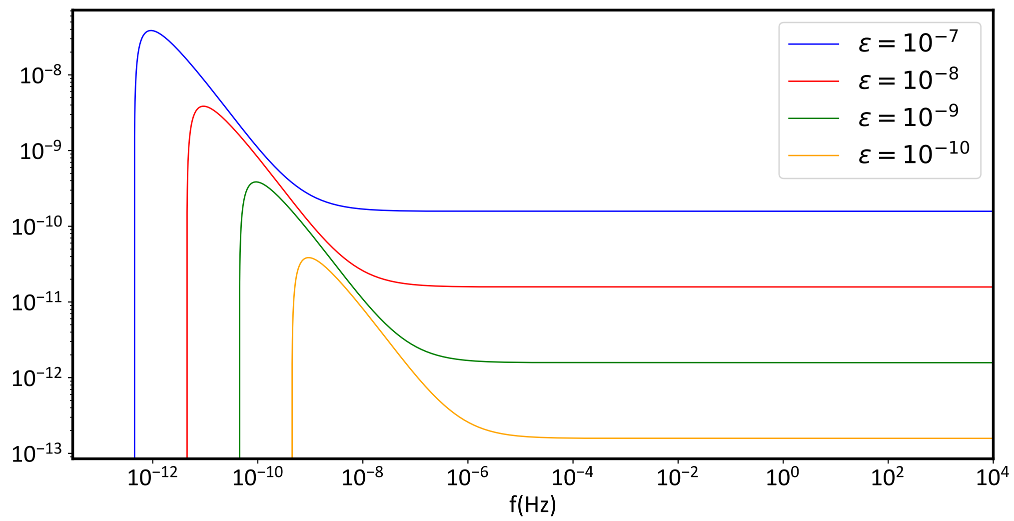

Figure 5.4: SGWB spectrum generated by small-loops for different values of string tension, $\epsilon = G\mu$. Parameters used: $\hat{C} = 5$, $\Gamma = 50$ and $\alpha = \hat{C}\Gamma G\mu$.

Regarding the quality of the analytical approximations, we can see by the plots in Fig. 5.2 that they accurately describe the shape and amplitude of the spectrum originated by loops produced in the radiation dominated era. However, there seems to be a slight underestimation of the contribution of loops in the matter dominated era (which was already reported in the original paper), which is more accentuated for higher values of $\hat{C}$. Our assumption of linear scaling, although realistic in the radiation dominated era, breaks off during the radiation-matter transition, where scaling cannot be maintained, therefore resulting in an underestimation of the number of produced loops [32]. Nevertheless, it accurately describes the SGWB spectrum and can be useful for fast computations of the spectrum, specially in the large-loop regime, where numerical calculations can often be quite slow.

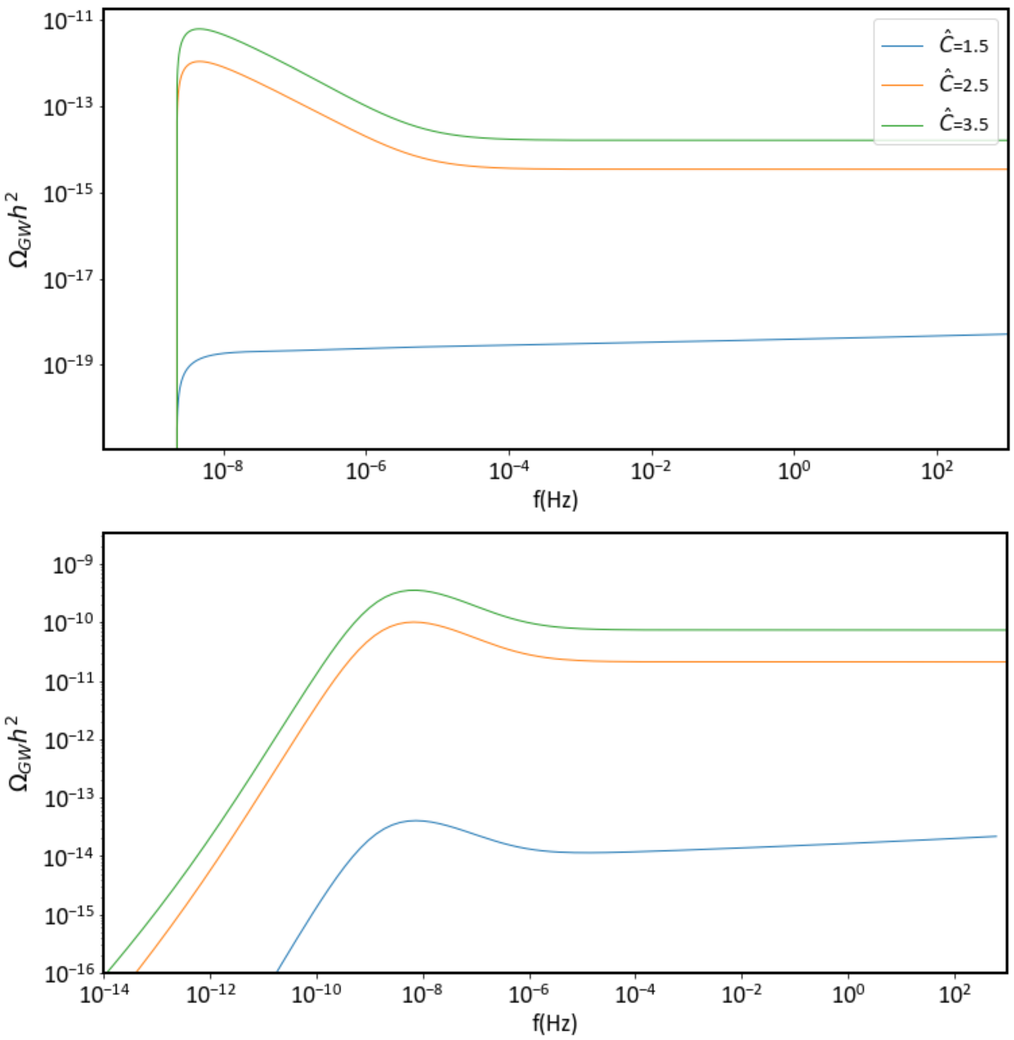

Figure 5.5: SGWB generated by small loops (upper panel) and large loops (lower panel), as predicted by the Modified VOS Model, for different values of the gravitational backreaction efficiency parameter, $\hat{C}$. For $\hat{C} = 1.5$, both $\bar{v}$ and L are out of the linear scaling regime in the radiation and in the matter dominated eras. There is no higher frequencies plateau. For $\hat{C} = 2.5$, $\bar{v}$ and L are in a linear scaling regime in the radiation era (and we recover the high frequency plateau) but are out of scaling in the matter dominated era. For $\hat{C} = 3.5$, the network is in a full linear scaling regime. Parameters used: $\Gamma = 50$, $G\mu = 10^{-10}$ and $\alpha = 0.1$ for the large loop spectrum and $\alpha = \hat{C}\Gamma G\mu$ for the small loop spectrum.

Partial Linear Scaling Regime

Finally, let us assume that K is in a linear scaling regime, but that $\bar{v}$ and L are not. This occurs when $\hat{C} < 2$ in the radiation era, and $\hat{C} < 2.5$ in the matter dominated era. The plots in Fig. 5.5 show the SGWB spectrum, in the small and large loop regime, for three different possible scenarios: the network is in a partial linear scaling regime both in the radiation and matter eras ($\hat{C} = 1.5$); the network is in a partial linear scaling regime only in the matter dominated era ($\hat{C} = 2.5$); the network is in a full linear scaling regime ($\hat{C} = 3.5$). We can observe the absence of the high frequency plateau when the network is not in full scaling in the radiation dominated era, and that the amplitude of the spectrum increases with increasing frequency instead.

5.2. SGWB Generated by Kinks

As it has already been discussed, the presence of small-scale structure on cosmic strings causes them to radiate GWs. Since this radiation is emitted directly by the long strings and, therefore, instantaneous, we will describe this additional contribution to the SGWB in a similar manner to what we did for small-loops in Subsection 5.1.2, with:

$$\left(\frac{d\rho}{dt}\right)_{loops} \longrightarrow \left(\frac{d\rho}{dt}\right)_{kinks}$$
$$p(f) \longrightarrow p_k(f)$$
$$f = \frac{2a}{\ell} \longrightarrow \bar{f} = \frac{2a}{l_k} = 2aK \, ,$$

where, $(d\rho/dt)_{kinks}$ is given by Eq. (4.1), and $p_k(f)$ is a probability distribution function describing the distribution of power radiated by kinks over the different frequencies, and $\bar{f}$ are the average frequencies of the GWs emitted by kinks. The question that now arises, is: *what is* $p_k(f)$*?* We know that, on average, it will be determined by the characteristic lengthscale of small-scale structure, l_k [9]. We also know that there should be a distribution of frequencies. As kinks decay, their sharpness decreases (i.e., their opening angle increases) and their emission becomes less intense. The dominant frequency emitted by kinks with a given sharpness should approximately be determined by the distance between kinks with that sharpness [55]. So, in order to determine $p_k(f)$, we must know the distribution of kinks per sharpness. In [56], the authors propose a distribution function for kink sharpness, but without considering the decay of kinks due to gravitational wave emission. In [55], this decay is included, but only how it impacts the number of existent kinks, and not their opening angle. As a matter of fact, how the sharpness of kinks evolves in their decay or when two kinks (that could have different sharpness) collide is not yet entirely understood. This would require a full treatment of gravitational backreaction, as it plays a crucial role in this process, but this has not yet been possible, even in simpler cases, due to numerical limitations (although analytical approximations have been used to study simple scenarios [57]). Given this, will then only consider the average frequency emitted by kinks, $\bar{f}$, i.e.:

$$p_k(f) = \delta(f - \bar{f}) \ . \tag{5.32}$$

When the network is in a full linear scaling regime, kinks will also generate a plateau in the radiation era. In that case, the shape of the spectrum is completely independent of the probability distribution function, and we can, therefore, obtain an analytical approximation to describe the amplitude of this contribution assuming a Dirac-delta function. During the matter era, there should be a peak, whose shape and slope should highly depend on the unknown $p_k(f)$. Therefore, we will not consider the contribution of kinks that decay during the matter era in our estimation. In [55], the authors calculated the spectrum generated by collisions between kinks, by using an expression to describe the individual burst emitted in these collisions (which depend on the kink sharpness). Their resultant spectrum has a plateau in the radiation dominated era and a peak in the matter era, but since this work does not include the effect of the gravitational backreaction and makes several simplifications, it also has some uncertainty associated with the peak.

With all the above considerations in mind, we can rewrite Eq. (5.15) as:

$$\Omega^k_{GW}(f) = \frac{8\pi(G\mu)^2\Gamma}{3H_0^2} f \int \frac{Ka^3}{L^2 H(a)} \delta(f - 2aK) da \ . \tag{5.33}$$

This integral can be solved using the following property of the Dirac-delta distribution:

$$\int f(x)\delta(g(x))dx = \Sigma \frac{f(x_i)}{|g'(x_i)|} \ , \text{ where } x_i \text{ are the zeros of } g(x) \ , \tag{5.34}$$

obtaining:

$$\Omega^k_{GW}(f) = \frac{4\pi(G\mu)^2\Gamma}{3H_0^2} \frac{a^3 f}{\left| L^2 H(a) \left[1 + \frac{1}{HK}\frac{dK}{dt}\right] \right|} \ , \tag{5.35}$$

where all quantities shall be evaluated at the instant $t = \bar{t}$, i.e., at the instant in time when kinks with frequency $\bar{f} = f$ are created. This equation may be used to obtain an expression for the radiation era plateau of the spectrum in the case where the network is in a complete linear scaling regime, with $\bar{v} = \bar{v}_r$, $L = \xi_r t$ and $K = \zeta_r / t$, assuming that the Friedmann Equation for the radiation era is given by Eq. (5.22). We then find that*:

$$\Omega^k_{\text{plateau}}(f) = \frac{64\pi(G\mu)^2\Gamma\Omega_r\zeta_r}{3\xi_r^2} \ . \tag{5.36}$$

*We can obtain an expression for the kinks that decay in the matter era in the same manner, obtaining $\Omega^k_{peak}(f) = 162\pi(G\mu)^2 H_0^2 \zeta_m^3 \Gamma \Omega_m^2 / (\xi_m^2 f^2)$, but, as discussed, we do not expect for it to be a fairly good estimation.

5.3. SGWB Generated by Cosmic Strings with Small-Scale Structure

Having studied how the presence of small-scale structure affects the SGWB spectrum generated by cosmic strings loops, and the potential contribution of the gravitational radiation resulting from kink decay, we can now estimate the SGWB spectrum generated by a kinky cosmic string network, by adding both these contributions. In this section, we will focus on the cases in which the network is in a full linear scaling regime, since, because the probability distribution function of kinks is not known, it is not possible to estimate their contribution otherwise.

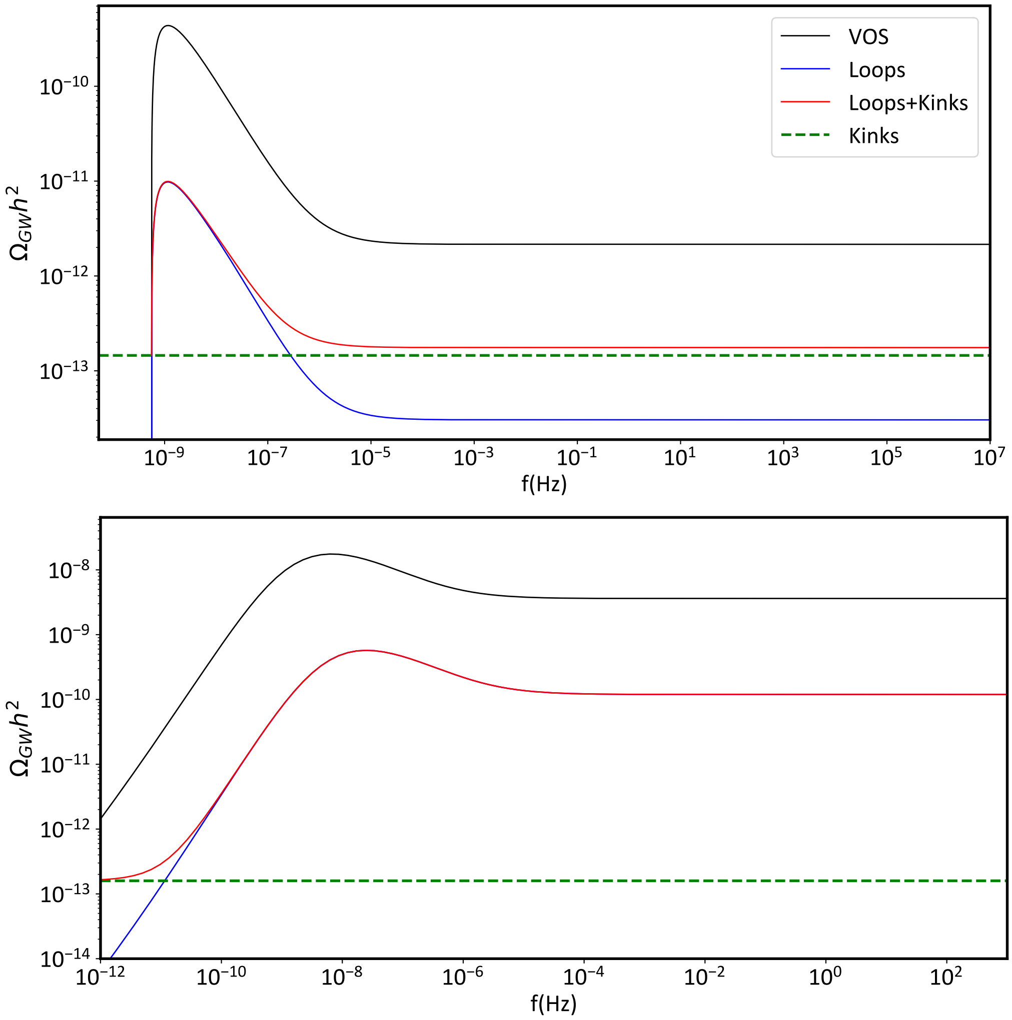

Figure 5.6: SGWB predicted by the VOS Model (black line) and predicted by the Modified VOS Model: blue line represents the contribution of loops, green dashed line represents an estimation of the contribution of kinks to the radiation era plateau, and red line represents an estimation of the total spectrum generated by a cosmic string with small-scale structure. Parameters used: $\hat{C} = 4$, $\Gamma G\mu = 50 \times 10^{-10}$ and $\alpha = \hat{C}\Gamma G\mu$ for the small-loop regime case (top panel) and $\alpha = 0.1$ for the large-loop regime case (bottom panel).

The plots in Fig. 5.6 shows an estimation of the total SGWB spectrum generated by a cosmic string with small-scale structure, in comparison with the spectrum predicted by the

VOS Model. It is important to point out, that our estimation, although fairly good for the radiation dominated era, is quite conservative in the matter era, because, since the peak is higher than the plateau, we are underestimating the contribution of kinks for the lower frequencies. However, it allows us to conclude that the contribution of kinks to the SGWB spectrum is not sufficient to compensate the decrease in the amplitude of the spectrum generated by loops, caused by the presence of small-scale structure. It also seems that, the contribution of kinks to the spectrum is only relevant in the small-loop regime. In fact, by looking at the plot in Fig. 5.7, we can see exactly that. Kinks contribution to the spectrum becomes more relevant as loops get smaller. This behavior was predicted by the authors in [9], although they did not consider what impact could kinks have in loop production: for very large loops, the radiation coming from loop decay dominates, but for loops created with $\alpha \sim \hat{C}\Gamma G\mu$, the contributions from loops and kinks are comparable.

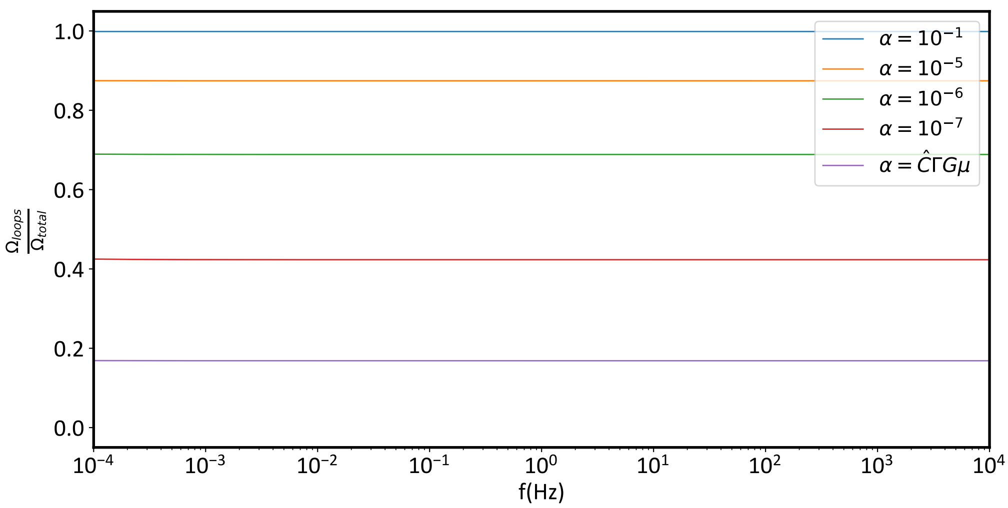

Figure 5.7: Comparison between the radiation era plateau of the SGWB with (Ω_{total} and without (Ω_{loops}) kinks contribution. Parameters used: $\hat{C} = 4$ and $\Gamma G\mu = 50 \times 10^{-10}$.

5.4. Summary

In this final chapter, we accomplished the goal of this dissertation, proposed in Chapter 1 by studying the impact of small-scale structure on the SGWB generated by loops.

We began by reviewing the existent formalism to calculate the SGWB spectrum generated by loops, both in the large and small-loop regime. Making use of the extension to the VOS Model developed in Chapter 4, we computed the spectrum generated by loops, formed in a cosmic string network with small-scale structure. We observed that the presence of kinks causes a decrease in loop production, leading to a decrease in the spectrum's amplitude, comparative to the one predicted by the VOS Model. This difference is more significant in the small-loop regime. The shape of the spectrum, however, is not affected by the presence of kinks.

Additionally, we estimated the contribution of kinks to verify if it could compensate this decrease. Our estimation provides good results in the radiation dominated era, where the amplitude of the spectrum is not dependent on the kink probability distribution function, and shows that, in general, the contribution of kinks is not sufficient to compensate the decrease in the amplitude of the loop's spectrum. In fact, for very large loops, the contribution of kinks to the total spectrum is subdominant, getting more comparable to the contribution of loops as we approach the small-loop regime.

6. Conclusions and Future Work

In this dissertation we have developed a framework to study the cosmological evolution of a cosmic string network with small-scale structure, which enables us to study this structure's impact on the SGWB generated by the GWs emissions of cosmic string loops.

We began by developing, in Chapter 3, an effective model with two lengthscales, by extending the VOS Model, to describe phenomenologically the evolution of small-scale structure and its impact on the evolution of a cosmic string network. This model has fewer undefined parameters than those currently found in the literature, with all of them having a well defined physical interpretation, thus allowing for the study of which physical aspects have a greater impact on the network's evolution. Considering that it is still not possible to include kink decay in simulations, this model is extremely useful to make observational predictions. Not only can it be used to study the spectrum of the SGWB generated by a cosmic string network with small-scale structure, but it can also be useful to study other observational signatures, such as the anisotropies in the CMB generated by cosmic string networks, since it has been shown that kinks may have a significant impact on them [58].

In Chapter 4, we used our extended VOS Model to study the evolution of a kinky cosmic string network. We verified that the presence of small-scale structure causes the network to decelerate and the characteristic lengthscale to increase, i.e., it makes the network less dense, which should have as a consequence, a decrease in the number of strings collisions, and, therefore, a decrease in loop production, which should translate into smaller spectrum amplitudes than the ones currently predicted. However, to proper understand the concrete effect of kink's presence on the network, it would be necessary to know how efficient the gravitational backreaction is and how kinky loops are, i.e., it would be necessary to proper calibrate the parameters $\hat{C}$ and q, which is still not possible, since simulations do not include, as mentioned above, gravitational backreaction.

Finally, in Chapter 5, we verified, that unless gravitational backreaction is very efficient, or loops are extremely kinky, the spectrum may currently be overestimated, as predicted in Chapter 4. Our results contradict current predictions, such as those in [59], where the authors propose that kinks could actually increase the amplitude of the spectrum. This disagreement may be explained by the fact that the model proposed in this paper is motivated by simulations, which, once again, do not take into account the effects of the gravitational backreaction.

We also verified that, in general, kinks contribution to the spectrum is subdominant. However, the SGWB spectrum generated by the emissions of small-scale structure has a peak in the lower frequencies, which might impact the shape and amplitude of the spectrum within that range, leaving a characteristic signature. However, the kink probability function is still unknown, due to the current absence of a proper description of the effects of the gravitational backreaction. We were then only able to provide an estimation of the amplitude of the radiation era plateau, since it is independent of this function. However, our results allow for an estimation of the range of the parameters within which kink contribution may lead to changes in the shape of the spectrum, and so, it is left as future work the study of the form of the kink probability distribution function. We can, however, make some comments about this function: kinks with more sharpness (i.e., kinks with a smaller opening angle), are those created more recently. Since the number of created kinks decreases quickly with time, it is expected that most of the existent kinks have been created at earlier times, therefore having smaller sharpness. The distance between recently created kinks should be larger than the characteristic lengthscale of the small-scale structure, l_k, and so, it is expected for them to emit GWs with frequencies smaller than the average frequency, $\bar{f}$. Therefore, there should be a distribution into lower frequencies. As a consequence, the peak of the spectrum must get lower and wider, thus making the slope at the end of the spectrum less abrupt.

References

[1] A. Einstein, "Cosmological Considerations in the General Theory of Relativity," *Sitzungsber. Preuss. Akad. Wiss. Berlin (Math. Phys.)*, vol. 1917, pp. 142–152, 1917. [Cited on pages 1 and 5.]

[2] E. Hubble, "A relation between distance and radial velocity among extra-galactic nebulae," *The Early Universe: Reprints*, p. 9, 1988. [Cited on page 1.]

[3] E. P. Hubble, "Extragalactic nebulae," *Astrophys. J.*, vol. 64, pp. 321–369, 1926. [Cited on page 1.]

[4] A. A. Penzias and R. W. Wilson, "A measurement of excess antenna temperature at 4080 mhz," in *A Source Book in Astronomy and Astrophysics, 1900–1975*. Harvard University Press, 1979, pp. 873–876. [Cited on page 1.]

[5] D. J. Fixsen, "The temperature of the cosmic microwave background," *The Astrophysical Journal*, vol. 707, no. 2, p. 916–920, Nov. 2009. [Online]. Available: http://dx.doi.org/10.1088/0004-637X/707/2/916 [Cited on page 1.]

[6] A. Einstein, "Näherungsweise integration der feldgleichungen der gravitation," *Sitzungsberichte der Königlich Preußischen Akademie der Wissenschaften*, pp. 688–696, 1916. [Cited on page 1.]

[7] R. Abbott and T. D. Abbott, "Search for lensing signatures in the gravitational-wave observations from the first half of ligo–virgo's third observing run," *The Astrophysical Journal*, vol. 923, no. 1, p. 14, Dec. 2021. [Online]. Available: http://dx.doi.org/10.3847/1538-4357/ac23db [Cited on page 1.]

[8] M. B. Hindmarsh and T. W. B. Kibble, "Cosmic strings," *Rept. Prog. Phys.*, vol. 58, pp. 477–562, 1995. [Cited on page 2.]

[9] A. Vilenkin and E. Shellard, *Cosmic Strings and Other Topological Defects*. Cambridge University Press, 1994. [Cited on pages 2, 12, 13, 66, 76, and 79.]

[10] N. Aghanim *et al.*, "Planck 2018 results. VI. Cosmological parameters," *Astron. Astrophys.*, vol. 641, p. A6, 2020, [Erratum: Astron.Astrophys. 652, C4 (2021)]. [Cited on pages 3, 5, 6, and 7.]

[11] A. G. Riess, A. V. Filippenko, P. Challis, A. Clocchiatti, A. Diercks, P. M. Garnavich, R. L. Gilliland, C. J. Hogan, S. Jha, R. P. Kirshner, B. Leibundgut, M. M. Phillips, D. Reiss, B. P. Schmidt, R. A. Schommer, R. C. Smith, J. Spyromilio, C. Stubbs, N. B. Suntzeff, and J. Tonry, "Observational evidence from supernovae for an accelerating universe and a cosmological constant," *The Astronomical Journal*, vol. 116, no. 3, p. 1009, sep 1998. [Online]. Available: https://dx.doi.org/10.1086/300499 [Cited on page 5.]

[12] E. J. COPELAND, M. SAMI, and S. TSUJIKAWA, "Dynamics of dark energy," *International Journal of Modern Physics D*, vol. 15, no. 11, p. 1753–1935, Nov. 2006. [Online]. Available: http://dx.doi.org/10.1142/S021827180600942X [Cited on page 5.]

[13] B. Ryden, *Introduction to Cosmology*, 2nd ed. Cambridge University Press, 2016. [Cited on page 6.]

[14] B. F. Schutz, *A FIRST COURSE IN GENERAL RELATIVITY*. Cambridge, UK: Cambridge Univ. Pr., 1985. [Cited on pages 8 and 9.]

[15] T. W. B. Kibble, "Topology of Cosmic Domains and Strings," *J. Phys. A*, vol. 9, pp. 1387–1398, 1976. [Cited on pages 9, 12, and 19.]

[16] J. Goldstone, "Field theories with «superconductor» solutions," *Il Nuovo Cimento (1955-1965)*, vol. 19, pp. 154–164, 1961. [Cited on page 10.]

[17] M. Thomson, *Modern Particle Physics*. Cambridge University Press, 2013. [Cited on page 10.]

[18] P. Auclair *et al.*, "Probing the gravitational wave background from cosmic strings with LISA," *JCAP*, vol. 04, p. 034, 2020. [Cited on pages 13 and 65.]

[19] T. W. B. Kibble, "Evolution of a system of cosmic strings," *Nucl. Phys. B*, vol. 252, p. 227, 1985, [Erratum: Nucl.Phys.B 261, 750 (1985)]. [Cited on page 17.]

[20] A. Albrecht and N. Turok, "Evolution of cosmic strings," *Physical Review Letters*, vol. 54, no. 16, p. 1868, 1985. [Cited on page 17.]

[21] D. P. Bennett and F. R. Bouchet, "Evidence for a scaling solution in cosmic-string evolution," *Physical Review Letters*, vol. 60, no. 4, p. 257, 1988. [Cited on page 17.]

[22] B. Allen and R. R. Caldwell, "Small scale structure on a cosmic string network," *Phys. Rev. D*, vol. 43, pp. 3173–3187, 1991. [Cited on pages 17, 25, and 27.]

[23] J. M. Quashnock and T. Piran, "Effects of gravitational back reaction on small scale structure of cosmic strings," *Phys. Rev. D*, vol. 43, pp. R3785–R3788, 1991. [Cited on pages 17, 25, 29, and 49.]

[24] T. W. B. Kibble and E. J. Copeland, "Evolution of small scale structure on cosmic strings," *Phys. Scripta T*, vol. 36, pp. 153–166, 1991. [Cited on page 17.]

[25] B. Allen and E. Shellard, "Cosmic-string evolution: A numerical simulation," *Physical review letters*, vol. 64, no. 2, p. 119, 1990. [Cited on page 17.]

[26] D. Austin, E. J. Copeland, and T. W. B. Kibble, "Evolution of cosmic string configurations," *Phys. Rev. D*, vol. 48, pp. 5594–5627, 1993. [Cited on pages 17, 25, 28, 29, and 60.]

[27] C. J. A. P. Martins and E. P. S. Shellard, "Quantitative string evolution," *Phys. Rev. D*, vol. 54, pp. 2535–2556, 1996. [Cited on pages 17 and 20.]

[28] ——, "Extending the velocity dependent one scale string evolution model," *Phys. Rev. D*, vol. 65, p. 043514, 2002. [Cited on pages 18, 21, and 22.]

[29] A. Vilenkin, "Cosmic string dynamics with friction," *Phys. Rev. D*, vol. 43, pp. 1060–1062, 1991. [Cited on page 21.]

[30] B. Allen and R. Caldwell, "Kinky structure on strings," *Physical Review D*, vol. 43, no. 8, p. R2457, 1991. [Cited on pages 25, 26, 29, 36, and 37.]

[31] T. Kibble and E. Copeland, "Evolution of the small scale structure on cosmic strings," *The Birth and Early Evolution of Our Universe, Proceedings of Nobel Symposium 79*, 1990. [Cited on pages 25, 27, 28, and 29.]

[32] L. Sousa, P. P. Avelino, and G. S. F. Guedes, "Full analytical approximation to the stochastic gravitational wave background generated by cosmic string networks," *Phys. Rev. D*, vol. 101, no. 10, p. 103508, 2020. [Cited on pages 25, 65, 69, 70, 72, and 75.]

[33] J. J. Blanco-Pillado, K. D. Olum, and B. Shlaer, "Number of cosmic string loops," *Physical Review D*, vol. 89, no. 2, Jan. 2014. [Online]. Available: http://dx.doi.org/10.1103/PhysRevD.89.023512 [Cited on page 25.]

[34] L. Sousa and P. P. Avelino, “Stochastic Gravitational Wave Background generated by Cosmic String Networks: Velocity-Dependent One-Scale model versus Scale-Invariant Evolution,” *Phys. Rev. D*, vol. 88, no. 2, p. 023516, 2013. [Cited on page 29.]

[35] P. A. R. Ade, N. Aghanim, C. Armitage-Caplan, Arnaud, and et. al, “Planck2013 results. xxv. searches for cosmic strings and other topological defects,” *Astronomy amp; Astrophysics*, vol. 571, p. A25, Oct. 2014. [Online]. Available: http://dx.doi.org/10.1051/0004-6361/201321621 [Cited on page 38.]

[36] M. Hindmarsh, “Gravitational radiation from kinky infinite strings,” *Phys. Lett. B*, vol. 251, pp. 28–33, 1990. [Cited on page 49.]

[37] M. Sakellariadou, “Gravitational waves emitted from infinite strings,” *Phys. Rev. D*, vol. 42, pp. 354–360, Jul 1990. [Online]. Available: https://link.aps.org/doi/10.1103/PhysRevD.42.354 [Cited on page 49.]

[38] E. J. Copeland, J. Magueijo, and D. A. Steer, “Cosmological parameter dependence in local string theories of structure formation,” *Phys. Rev. D*, vol. 61, p. 063505, 2000. [Cited on pages 60 and 61.]

[39] C. J. A. P. Martins, E. P. S. Shellard, and J. P. P. Vieira, “Models for Small-Scale Structure on Cosmic Strings: Mathematical Formalism,” *Phys. Rev. D*, vol. 90, no. 4, p. 043518, 2014. [Cited on page 61.]

[40] L. Sousa and P. P. Avelino, “Stochastic gravitational wave background generated by cosmic string networks: The small-loop regime,” *Phys. Rev. D*, vol. 89, no. 8, p. 083503, 2014. [Cited on pages 65 and 68.]

[41] J. J. Blanco-Pillado and K. D. Olum, “Stochastic gravitational wave background from smoothed cosmic string loops,” *Physical Review D*, vol. 96, no. 10, p. 104046, 2017. [Cited on page 65.]

[42] T. Vachaspati and A. Vilenkin, “Gravitational Radiation from Cosmic Strings,” *Phys. Rev. D*, vol. 31, p. 3052, 1985.

[43] C. J. Burden, “Gravitational Radiation From a Particular Class of Cosmic Strings,” *Phys. Lett. B*, vol. 164, pp. 277–281, 1985.

[44] B. Allen and E. P. S. Shellard, “Gravitational radiation from cosmic strings,” *Phys. Rev. D*, vol. 45, pp. 1898–1912, 1992. [Cited on page 65.]

[45] L. Sousa and P. P. Avelino, “Probing Cosmic Superstrings with Gravitational Waves,” *Phys. Rev. D*, vol. 94, no. 6, p. 063529, 2016. [Cited on page 66.]

[46] J. J. Blanco-Pillado, K. D. Olum, and B. Shlaer, “Number of cosmic string loops,” *Physical Review D*, vol. 89, no. 2, p. 023512, 2014. [Cited on page 66.]

[47] ——, “Large parallel cosmic string simulations: New results on loop production,” *Physical Review D—Particles, Fields, Gravitation, and Cosmology*, vol. 83, no. 8, p. 083514, 2011. [Cited on page 66.]

[48] T. W. B. Kibble, “Evolution of a system of cosmic strings,” *Nucl. Phys. B*, vol. 252, p. 227, 1985, [Erratum: Nucl.Phys.B 261, 750 (1985)]. [Cited on page 67.]

[49] R. R. Caldwell and B. Allen, “Cosmological constraints on cosmic string gravitational radiation,” *Phys. Rev. D*, vol. 45, pp. 3447–3468, 1992. [Cited on page 67.]

[50] M. R. DePies and C. J. Hogan, “Stochastic Gravitational Wave Background from Light Cosmic Strings,” *Phys. Rev. D*, vol. 75, p. 125006, 2007.

[51] S. A. Sanidas, R. A. Battye, and B. W. Stappers, “Constraints on cosmic string tension imposed by the limit on the stochastic gravitational wave background from the European Pulsar Timing Array,” *Phys. Rev. D*, vol. 85, p. 122003, 2012.

[52] L. Sousa and P. P. Avelino, “Stochastic Gravitational Wave Background generated by Cosmic String Networks: Velocity-Dependent One-Scale model versus Scale-Invariant Evolution,” *Phys. Rev. D*, vol. 88, no. 2, p. 023516, 2013. [Cited on page 67.]

[53] J. J. Blanco-Pillado, K. D. Olum, and B. Shlaer, “The number of cosmic string loops,” *Phys. Rev. D*, vol. 89, no. 2, p. 023512, 2014. [Cited on page 70.]

[54] G. S. F. Guedes, P. P. Avelino, and L. Sousa, “Signature of inflation in the stochastic gravitational wave background generated by cosmic string networks,” *Phys. Rev. D*, vol. 98, no. 12, p. 123505, 2018. [Cited on page 70.]

[55] Y. Matsui and S. Kuroyanagi, “Gravitational wave background from kink-kink collisions on infinite cosmic strings,” *Phys. Rev. D*, vol. 100, no. 12, p. 123515, 2019. [Cited on pages 76 and 77.]

[56] E. J. Copeland and T. W. B. Kibble, “Kinks and small-scale structure on cosmic strings,” *Phys. Rev. D*, vol. 80, p. 123523, 2009. [Cited on page 76.]

[57] J. J. Blanco-Pillado, K. D. Olum, and J. M. Wachter, “Gravitational backreaction simulations of simple cosmic string loops,” *Phys. Rev. D*, vol. 100, no. 2, p. 023535, 2019. [Cited on page 76.]

[58] R. P. Silva, L. Sousa, and I. Y. Rybak, “Cosmic microwave background anisotropies generated by cosmic strings with small-scale structure,” *JCAP*, vol. 07, p. 016, 2023. [Cited on page 81.]

[59] P. G. Auclair, “Impact of the small-scale structure on the Stochastic Background of Gravitational Waves from cosmic strings,” *JCAP*, vol. 11, p. 050, 2020. [Cited on page 81.]